Neuroinflammation in Peripherally Helminth-infected Mice

Report

Exploring mechanisms of behaviour change in a chronic inflammatory model

Sylvia Van Belle

VBLSYL001

Supervisor: Dr Vinogran Naidoo

Co-supervisor: Dr Joseph Raimondo

Presented for BMedSc (Hons) in Physiology

7486 words

October 2017

HUB4088W

Division of Neuroscience

Department of Human Physiology

Faculty of Health Sciences

University of Cape Town

CONTENTS

ABBREVIATIONS AND ACRONYMS

AEC	Animal Ethics Committee
T. crassiceps	*Taenia crassiceps*
T. solium	*Taenia solium*
CNS	Central nervous system
IL	interleukin
fMRI	Functional magnetic resonance imaging
IEG	Immediate early genes
LTP/LTD	Long-term potentiation/depression
SGZ	Subgranular zone
UCT	University of Cape Town
PBS	Phosphate-buffered saline
RIPA	Radioimmunopricipitation assay

RT	Room temperature
AP	Alkaline phosphatase
TH	Tyrosine hydroxylase
DARP-32	dopamine- and cAMP-regulated neuronal phosphoprotein
SDS-PAGE	dodecyl sulphate polyacrylamide gel electrophoresis
DAB	Diaminobenzidine
IHC	immunohistochemistry
HRP	Horse-radishperoxidase
i.p.	intraperitoneal
ELISA	enzyme-linked immunosorbent assay

PLAGIARISM DECLARATION

Name: Sylvia Van Belle

Student Number: VBLSYL001

Course: BSc (Med)(Hons) in Physiology and neuroscience
HUB4088W

I know that plagiarism is wrong. Plagiarism is to use another's work and pretend that it is one's own.

I have used the style of the journal ***Brain, Behaviour, and Immunity*** for citation and referencing. Each contribution to, and quotation in, this ***thesis*** from the work(s) of other people has been attributed, and has been cited and referenced.

This ***thesis*** is my own work.

I have not allowed, and will not allow, anyone to copy my work with the intention of passing it off as his or her own work.

Signature: 

Date 27 October 2017

ABSTRACT

Intraperitoneal *Taenia crassiceps* cysticerci inoculation is a common model of helminth infection in rodents. A previous study found anxiety and memory-related behavioural changes in *T. crassiceps* infected mice, with transcript analysis from that same study revealing altered hippocampal neurotransmitter and cytokine levels. Anxiety and memory changes are often linked to functions of the hippocampus, a neurogenic zone in the brain. While the link between neuroinflammation and behavioural changes has recently produced a wealth of literature, few studies have been conducted on helminth models, which are particularly relevant in the African context, where parasite infections are a significant cause of morbidity and mortality. The present exploratory study sought to characterise the neuroimmunologic mechanisms that allow for communication between peritoneum and brain. Two months after female C57BL/6 mice were intraperitoneally infected with *T. crassiceps* cysticerci, we used immunoblotting, cytokine arrays and immunohistochemistry to investigate relative neuronal activation, synaptic marker expression, catecholaminergic transmission, cytokine levels, the expression of immature and mature markers of neurogenesis, and the inflammatory status of the hippocampus. Our results were inconclusive, with high variability between samples, showing that attempts should be made to reproduce published behavioural data prior to further neurological characterisations being conducted. However, an unknown protein, suspected to be IgG, was highly expressed in *T. crassiceps* hippocampi, believed to be due to blood-brain permeability, although more work is required to understand the significance of this finding. Nonetheless, this work provides a useful framework for investigating neurological mechanisms behind behavioural changes related to memory and anxiety.

248 words

1 BACKGROUND

1.1 Introduction

In 2014, a group of Mexican researchers observed behaviour changes in a cohort of mice infected intraperitoneally with helminth cysticerci, specifically of the *Taenia crassiceps* species (Morales-Montor et al., 2014). With neuroimmunology embracing the concept of systemic inflammation producing neurological changes, we were driven to further examine the mechanisms behind a seemingly innocuous and clinically silent peritoneal infection. We were specifically interested in studying neurological processes that may be altered to effect behavioural changes in these mice. Fig 1 below shows a framework for considering the problem.

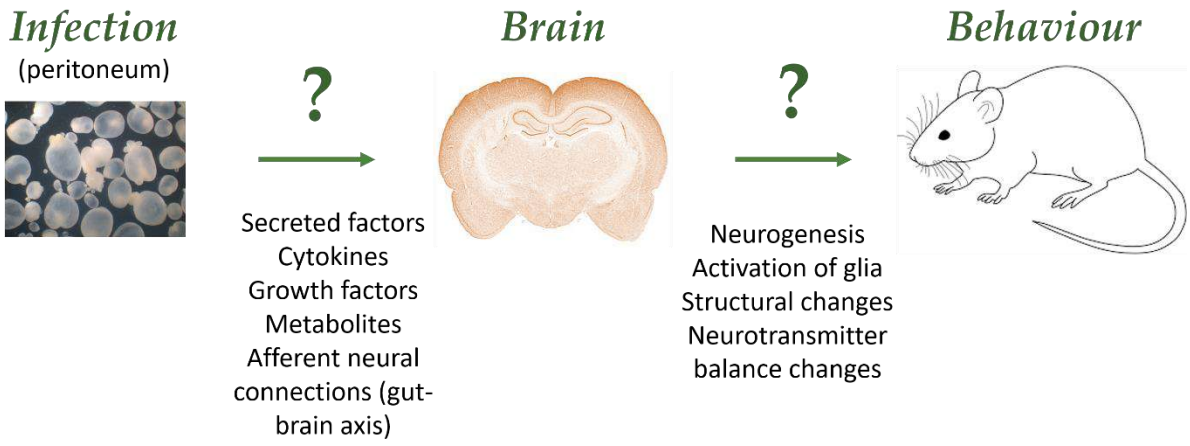

Figure 1: ***A framework for considering how peripheral infection results in behaviour change.*** *This model suggests that two separate systems are considered equally, namely mechanisms of communication between parasite and host brain are and neurological processes that may result in behaviour changes*

The following provides an overview of the study of systemic inflammation on the brain and how the helminth model of intraperitoneal cysticercosis used by Morales-Montor et al. (2014) is relevant to our project. I then describe the various modes through which inflammation could change behaviour, specifically through altered neuronal activation or electrophysiological properties, via increased cell death or alterations to the neurogenic cascade. The importance of glial cells in modifying neuronal circuitry is also discussed. The focus of this introduction is to unify a range of disparate mechanisms through which inflammation could alter behavioural changes, with an emphasis on cytological markers and tools which allow for differentiation of pathological states.

1.2 Immunity and the brain

1.2.1 From the body to the brain

It is well recognised that despite the blood-brain barrier, the central nervous system (CNS) is not "immune privileged", and that not only does the brain have an impact on immune function and health, but immunological status has a profound effect on neurological processes (Irwin, 2008). Perhaps the clearest example of this interaction is "sickness behaviour" – the anhedonia, anorexia, fatigue, difficulty focusing and even impaired memory that occurs in fevered states (Dantzer et al., 2008; Saper et al., 2012). More subtly, mental health disorders are often a significant co-morbidity of chronic diseases characterised by high levels of immune activation such as autoimmune disorders (Silverberg, 2017), type II diabetes (Hajebrahimi et al., 2016), cancer (Irwin, 2008) or age-related disease (Lal and Forster, 1988). Furthermore, immune therapies have been linked to significant psychological side effects (Kovacs et al., 2016).

To explain these phenomena, various inflammatory models have sought to explain how and what signals convey immune status to the brain, and what the subsequent neurological effects are. Prostaglandins have been suggested to play a large role in febrile states and hyperalgia (Saper et al., 2012), while altered metabolic substrates, lipokines and anatomical vascular changes have been implicated in cognitive decline related to metabolic disorders (Toth, 2014). Least understood, perhaps, is the role of peripheral neuronal signals, for example enteric plexus gut-brain signalling in gut disorders (Evrensel and Ceylan, 2015). The role of hormones has also been studied in communicating infection to the brain (Morales-Montor et al., 2004). Although immune effector cells are typically unable to cross the blood-brain barrier, inflammation has been shown to permeabilise this barrier, allowing entry into parenchyma (Chapouly et al., 2015). Most significantly, perhaps, are cytokines, the major signalling molecules of the immune system. Cytokines are able to act directly on neurones through cytokine receptors or modulation of other receptors and channels (Lopez-Griego et al., 2015; Schafers and Sorkin, 2008; Vezzani and Viviani, 2015). Furthermore, they transmit peripheral signals to microglia, which are then able to amplify the signal and recruit and impact local cells.

When studying immune activation and the brain, a classical model involves peripheral or targeted lipopolysaccharide stimulation, a model of bacterial infection, a potent inducer of pro-inflammatory pathways (Ekdahl et al., 2009; Monje et al., 2003; Xie et al., 2003; Zonis et al., 2013). However, this is analogous to acute bacterial infections. Immune responses, however, are multivariate and complex, particularly in chronic, autoimmune, or non-bacterial insults (i.e. viral, fungal, parasitic or neoplastic). Beyond inducing an actual infection or introducing antigen, more specific techniques for studying the

neurological sequelae the immune dysfunction include genetic knock-out of immune-mediators or administration of receptor agonists/antagonists.

1.2.2 A helminth model of inflammation

Although more and more research has focused on chronic inflammatory models of irritable bowel disease, obesity and metabolic disorders (Chesnokova et al., 2016; Hajebrahimi et al., 2016; Zonis et al., 2015), there is a paucity of studies on helminthic infections, beyond the pioneering work by the Morales-Montor group (Arteaga-Silva et al., 2009; Lopez-Griego et al., 2015; Morales-Montor et al., 2004; Morales-Montor et al., 2014; Rodriguez-Dorantes et al., 2007). Not only are helminth infections an important model of chronic inflammation, but parasites are a highly relevant clinical concern as a significant cause of morbidity and mortality, particularly in Sub-Saharan Africa where almost one third of the world's population is estimated to be parasite-infected (Hotez et al., 2008). Although the infections are a significant cause of morbidity from symptoms of anaemia and malnourishment (Anthony et al., 2007), efficient host-parasite coevolution and symbiosis leads to modification and recalibration of the immune system so that stable, chronic infections can exist silently for up to 20 years (Maizels and McSorley, 2016). This may have more subtle negative outcomes that have not yet been fully characterised, such as potential neurological deficits – in keeping with the idea that systemic inflammatory status has neurological implications.

Although studies have shown associations between intestinal helminth infection and cognitive functioning (Ezeamama et al., 2012; Nokes et al., 1992; Watkins and Pollitt, 1997), the extent to which this is generalizable to systemic non-gut infections is questionable, due to confounding and poorly understood role of gut-brain axis and signalling via the enteric nervous system (Daulatzai, 2014; Guernier et al., 2017). Beyond intestinal parasites, behaviour changes in helminth models have also been investigated in CNS-specific infections with organisms such as *Taenia solium* (neurocysticercosis) and *Toxoplasma gondii* (Adamo and Webster, 2013; Bolton and Robertson, 2016).

No evidence could be found of research on psychiatric or behavioural effects of systemic parasitic infections, with the exception of Morales-Montor et al. (2014), who have characterised some of the hormonal, reproductive and behavioural changes in a relatively silent intraperitoneal cysticercosis model, using *Taenia crassiceps* as murine experimental analogue for *T. solium* which infects humans (Arteaga-Silva et al., 2009; Lopez-Griego et al., 2015; Morales-Montor et al., 2004; Morales-Montor et al., 2014; Rodriguez-Dorantes et al., 2007). Fig. 2 shows the complete lifecycles of *T. solium* and *T. crassiceps*.

Recent meta-analysis of human *T. solium* cysticercosis placed circulating antigen seroprevalence in seven African countries studied at 7.3%, with antibody seroprevalence at 17.37% (Coral-Almeida et

al., 2015). As mentioned above, *T. solium* is more typically associated with studies of neurocysticercosis, which is closely linked to epilepsy (Serrano Ocana et al., 2009), however, results have suggested that even a peripheral cysticercosis can have a significant neurological impact. Specifically, Morales-Montor et al. (2014) found that chronic cysticercosis impaired short-term memory, and affected mobility scores and performance in forced swim tests. On a molecular level, hippocampal serotonin and noradrenaline mRNA expression was affected in females and males respectively (sex differences were significant). They found that hippocampal Interleukin-6 (IL-6), IFN-γ and TNF-α mRNA levels were increased in both sexes and IL-4 expression was increased in females and decreased in males.

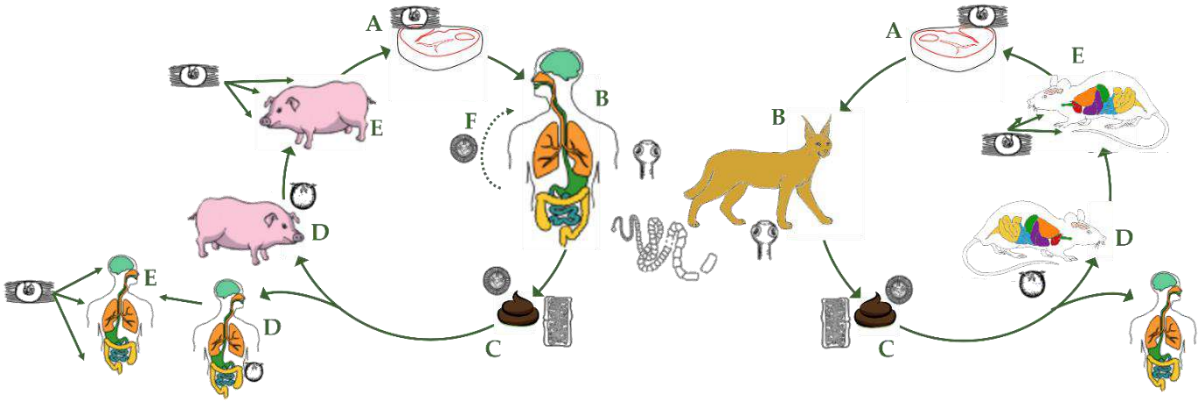

Figure 2: ***The life cycles of cestodes T. solium (left) and T. crassiceps (right)****. Raw or poorly cooked cysticercosis-infected meat is ingested (A). In the definitive host (B), the cysts/larvae hatch in the small intestine and the head/scolex attaches to the mucosal wall and begins developing segments (proglottids). Mature proglottids containing fertile eggs are excreted in faeces (C), which are then ingested by the intermediate host (D). The oncospheres in the eggs hatch due to gastric acid/intestinal fluids, cross the intestinal wall enter the bloodstream and establish an infection in various tissues as cysticerci (E). Autoinfection from within the gastrointestinal tract has been postulated to explain the high rates of cysticercosis in tapeworm carriers (F) (Garcia et al., 2003).*
In T. solium, the definitive host is the human, and while the intermediate host is naturally the pig, humans can also be infected with cysticercosis in a dead-end infection. The definitive hosts of T. crassiceps includes foxes, dogs and felids, while intermediate hosts include small mammals such as mice and rabbits, although very rare intermediate infection of humans has been recorded (Lescano and Zunt, 2013).
In humans, T. solium cysticerci have a predilection for the CNS, the eye, muscle, the heart and subcutaneous tissue, while in pigs the cysts are typically found in muscle, similarly, T. crassiceps cysticerci lodge predominantly in the muscle, peritoneum and pleura of rodents, although it has been seen in the brain of mice and cats(Lescano and Zunt, 2013). Again, in humans, both intestinal worm taeniasis and cysticercosis infections are typically symptomless. The former causes mild inflammation at the site of implantation, possibly accompanied by ome mild diarrhoea and nausea, while cysticercosis only causes major pathology in neurocysticercosis or ophthalmic cysticercosis, due to the mass action, or the inflammation caused by cyst degeneration in the case of epileptic seizures in neurocysticercosis. (Garcia et al., 2003)
Image based off that of the CDC, available at https://www.cdc.gov/dpdx/cysticercosis/index.html

Beyond assessing mRNA levels of cytokines, other methods to assess neuroinflammation include glial activation (microglia and astrocytic responses), activation of inducible nitric oxide synthase (i-NOS) and assessment of MAP kinase pathway activation (Monnet-Tschudi et al., 2011).

Refer to *Section 8.2.1* for details on Helminthic and *T crassiceps* immune phenotypes.

1.2.3 Intrinsic neuronal changes

Once an immune response is characterised, it is then necessary to link specific neurological changes to the immunological changes observed or induced. There are several elements that can be examined, including neuronal activation and modification of electrophysiological properties, cell death, changes to neurogenesis or changes in the environment – particularly through changes in glial function.

1.2.3.1 Neuronal activation

The activation of specific circuits or specific regions provides vital information for explaining behavioural changes or neurological deficits, based on current knowledge of the functions of those regions. Functional magnetic resonance imaging (fMRI) is a well-established technique predominantly used in human subjects, but it does not confer the cellular resolution required for accurate circuit mapping (Kawashima et al., 2014). A popular technique for obtaining higher resolution includes the identification of genes, so-called "immediate early genes" (IEGs), that are activated by neuronal activation, typically due to calcium influx triggering calcium-dependant kinase cascades (Flavell and Greenberg, 2008). These genes, such as the popularly used *c-fos* and *Arc* (activity-regulated cytoskeletal-associated protein), are typically transcription factors that regulate mediators of dendritic outgrowth and synapse maturation (Flavell and Greenberg, 2008; Kawashima et al., 2014). Genome wide analysis of genes acutely expressed in response to membrane depolarisation, neurotransmitter application, LTP and seizure induction has revealed several candidates which could be used as markers for activation, including membrane protein candidate plasticity gene 15 (*Cpg15*), which appears to enhance dendritic outgrowth, presynaptic axonal elaboration and AMPA receptor insertion (Cantallops et al., 2000); serum-inducible kinase (*SNK*) which regulates postsynaptic intracellular pathways resulting in synapse destabilisation; *microRNA-134* which restricts excitatory synapse development and inhibits dendritic growth; MHC class I; *Homer1a* and *BDNF* (whose role is poorly defined due to conflicting studies) (Flavell and Greenberg, 2008). These IEGs, although appearing to have conflicting functions, can be used in proteomic assessment (e.g. immunoblotting) for aggregate activation. Linking genetically encoded inducible fluorescent tags to IEGs allows for "targeted recombination in active populations", that is, long-term labelling at a specific time-point allowing for increased experimental control (Guenthner et al., 2013).

Other mechanisms to visualise neuronal activation involve genetically encoded indicators of synapse function, used in brain slice culture and imaged live during electrophysiological stimulation. These indicators include vesicular release indicators, pH indicators, neurotransmitter indicators, voltage indicators and calcium indicators (Lin and Schnitzer, 2016). Optogenetics also for experimental

manipulation of the activity of specific neurones, permitting causal associations with observed behavioural and biochemical outcomes (Pastrana, 2011). Taken together, these techniques have allowed for identification of differential neuronal activation in inflammation. For example, regions that play a role in sickness behaviour have been examined (Saper et al., 2012), such as the paraventricular nucleus, which has a role in hyperalgesia and nociception (Tarr et al., 2012). IFN-α treatment in cancer patients decreased activity in the dorsal prefrontal cortex and increased activity in the cerebellum and basal ganglia, that correlated with neurovegetative symptoms (Capuron et al., 2007). Peripheral LPS injections prevented activation of several brain regions in response to new stimuli (Stone et al., 2006), while incubation of brain slices in LPS selectively increased excitability in dopamine-2but not dopamine-1 neurones, expressing striatal spinal projection neurones (Winland et al., 2017).

1.2.3.2 Electrophysical characterisation

Electrophysiological studies performed *in vitro* and *in vivo* have allowed for the characterisation of tissue excitability, such as baseline excitability, changes in how neurones change in response to stimulation (i.e. LTP or LTD), or susceptibility to seizure-like activity (Tao et al., 2015). Electrophysiological studies in inflammatory models including exogenous application of LPS or cytokines have shown increased seizure susceptibility (Galic et al., 2012) and LTP potentiation (Wall et al., 2015). Cytokines, such as TNF-α, IL-1β and IL-6, have been shown to modulate voltage-gated channels (Schafers and Sorkin, 2008; Vezzani and Viviani, 2015), to modulate receptor-coupled ion alter ligand-binding (e.g. NMDA receptor). The specific effects of each cytokine on each channel in various models of inflammation are beyond the scope of this introduction.

1.2.3.3 Cell death

Cell death in neurological studies is particularly relevant to altered functioning due to the lack of regenerative capacity. The behavioural and psychological effects of cell death can be clearly demonstrated in neurodegenerative disorders, such as Alzheimer's, Parkinson's and Huntington's disease. While the mechanisms behind cell death are manifold, examples include proteinopathies mediated by the breakdown of protein degradation pathways, membrane damage and mitochondrial dysfunction (Golde et al., 2013); excitotoxicity mediated by calcium dysregulation, dysfunction of ATPases and mitochondrial dysfunction (Connolly and Prehn, 2015); and microglia-induced cytotoxicity, mediated by death receptor signalling in inflammation (Cunningham, 2013). The multiple and complex intracellular pathways that are involved in apoptosis have led to the development of a host of antibody markers, including targets in the Bcl-2/caspase, p53 and death receptor signalling pathways (see section 8.2.2 for detailed diagrams of these pathways). These markers allow for quantification through immunoblotting or IHC. Other hallmarks can be measured such as decreased mitochondrial membrane potential, cytochrome c release, and on imaging a loss of membrane

asymmetry, nuclear condensation, and membrane blebbing can be visualised (Wlodkowic et al., 2011) Various assays are available to assess cell viability/cell activity, cytotoxicity and apoptosis. Synaptic markers are also used as a measure of cell death as synapse degeneration is one of the earliest pathological events in many chronic neurodegenerative diseases (Wlodkowic et al., 2011). However, biochemical assays and neuronal population measurements can be skewed by cell-to-cell variability/heterogeneity, and contributions from non-neuronal cells Connolly and Prehn (2015). In inflammatory models, Semmler et al. (2005) showed increased apoptosis in the cortex, hippocampus, midbrain and cerebellum in LPS-treated mice, while inflammation plays a significant role in neurodegenerative diseases through activation of microglia; whether this inflammation is casual, contributory or consequential has not been elucidated (Chen et al., 2016).

1.2.3.4 Neurogenesis

Another proposed mechanism to account for the altered behaviour seen in models of inflammation models is through modification of adult neurogenesis. Despite the interest the field has attracted, our knowledge surrounding it is still limited and even the basic functions of neurogenesis are still being argued. It has been argued that neurogenesis simply assists the hippocampus in hippocampal tasks, rather than having a specific function attributable to it (Kohman and Rhodes (2013).Emerging theories are focusing on a potential role in pattern separation, recognition, spatial memory, emotional regulation and stress responses, behavioural inhibition, orientation and attention shifting (Cameron and Glover, 2015). These hippocampus-dependant behavioural and cognitive functions are also affected in immune activation dysfunction (Hein et al., 2010; Kranjac et al., 2012; Yirmiya and Goshen, 2011) and, like neurogenesis, have been associated with psychiatric disorders (Dantzer et al., 2008; Deslauriers et al., 2017; Meyer, 2017). Both decreased neurogenesis and increased inflammation have been implicated as mechanisms behind age-related cognitive decline and dementia (Bizon et al., 2004; Liu et al., 2013; Villeda et al., 2011).

Adult neurogenesis has been described in mammals occurring throughout life, with adult neural stem cells identified within the subgranular zone (SGZ) of the dentate gyrus in the hippocampus as well as the subventricular zone of the lateral ventricles (Sierra et al., 2010). These regions are considered neurogenic “niches” containing a microenvironment permissive of proliferation/self-renewal and differentiation of neural stem cells. These cells create a progeny comprising of neurones, oligodendrocytes and astrocytes. The differentiation process is a complex one, affected by not only by the microenvironment, but by local neuronal circuitry, macro-circuitry and humoral signals (Kempermann et al., 2015). The stages of neuron development have been relatively well characterised, and a diagram produced by Encinas et al. (2011) provides a useful framework for

identification of cell maturation stage. (Fig. 3). Sato (2015) postulates that the age of a new-born neuron may define its role in specific forms of memory formation.

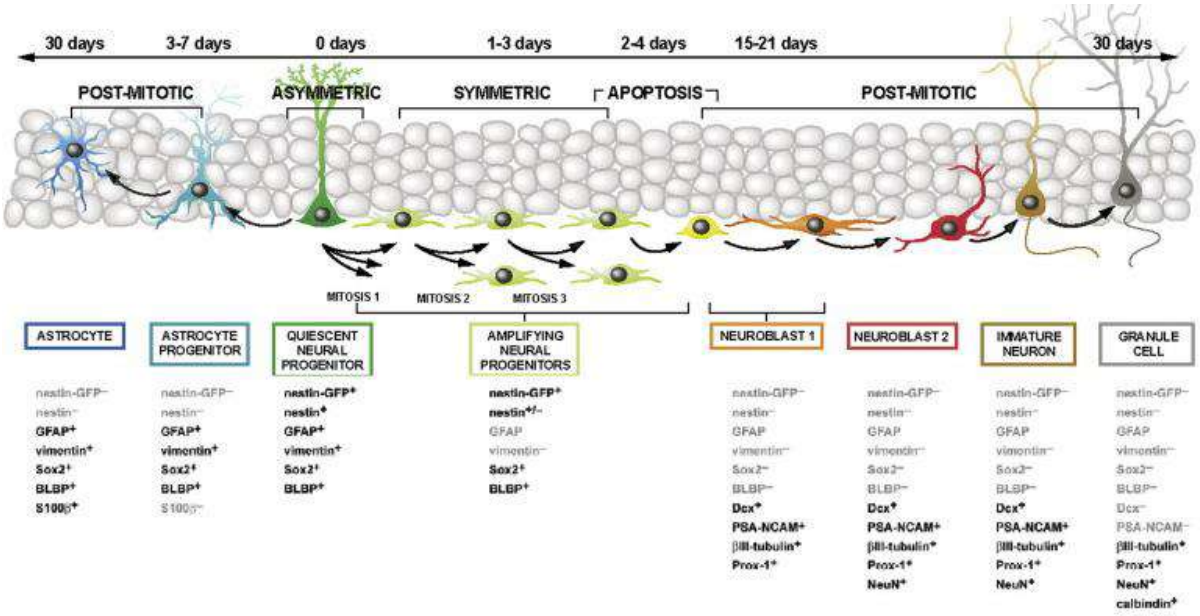

Figure 3: ***Markers of neurogenesis,*** *showing marker expression in across stages of NPC differentiation into astrocytes and granule cells, taken directly from Encinas et al. (2011).*

These maturation pathways have been of interest in studies attempting to explain decreasing neural stem cell populations that correspond to aging, a consistent finding which is thought to play a role in age-related neurodegeneration. Unlike classical stem cells which undergo lifelong cycles of exiting and entering quiescence, neural stem cells appear to exist the quiescent state, undergo several rapid asymmetric divisions to produce neurones before themselves terminally differentiating into astrocytes, effectively leaving the stem cell pool (Encinas et al. (2011). Factors that cause stem cells to activate and leave the quiescent state is another popular area of study, although trauma, seizures and disease has been strongly implicated (Encinas et al., 2011). Furthermore, although differential maturation markers have been well identified, the signalling mechanisms that induce astrocytic rather than neuronal differentiation lacks research is still under active investigation. Preferential differentiation into astrocytes has, however, been observed in several inflammatory models (Keohane et al., 2010; Zonis et al., 2015).

An understanding of neurogenesis is vital if one is to attempt to study how external signals, such as cytokines and other inflammatory mediators, impact neurogenesis (a more comprehensive outline of the mechanisms and stages are described in Section 8.2.3

1.2.4 Glial changes

Glial cells are crucial to nervous system signalling by supporting neuronal functioning. Microglia, cells of monocyte origin, not only play a vital immunological role in infection, but also regulate basal neurological processes in the absence of immune activation (Kohman and Rhodes, 2013). Astrocytes, classically and exceptionally vaguely dubbed "support cells of the CNS", exist in a diverse range of phenotypes, suggesting an equally diverse range of function (Khakh and Sofroniew, 2015). There is minimal information regarding oligodendrocytes, the myelinating cells of the CNS, and their impact on inflammation, as literature has focused on the impact of neuroinflammation on oligodendrocyte function and myelination (Sommer et al., 2017).

At the core of the CNS's immune response, microglia have the potential to act as an "immune transmitter". Far more sensitive to peripheral cytokine signalling than other neural cells, microglia are able to sense and relay or amplify signals through cytokine production to neighbouring astrocytes and neurones (Kettenmann et al., 2011). Microglia have been broadly classified into two phenotypes when activated, the supposedly neurodegenerative M1 and neuroprotective M2 phenotypes (Kohman and Rhodes, 2013), although Sato (2015) warns against arbitrary subtyping. Even resting microglia have been shown to have an important role in the survival phase of neurogenesis by phagocytosing apoptotic cells (Sierra et al., 2010). Kettenmann et al. (2011) thus challenges the label "resting", noting that they also participate in active environmental surveillance.

1.3 A new paradigm

This project hopes to clarify cellular mechanisms behind the behaviour changes manifested by *T. crassiceps*-infected mice by characterising inflammation in the brain and assessing how this correlates to neurological processes such as neuronal activation, cell death, neurogenesis and glial changes, thus providing a framework to approach investigations into behavioural outcomes. This study hopes to bring systemic helminth infection into the discourse on chronic inflammatory models of behaviour change, which is relevant not only because of the high burden of disease, but also because the distinct immune phenotype of these organisms mean that classic models may not be applicable.

2 Research plan & Methodology

2.1 Aims and objectives

The overall aim of this study was to explore the neurological impact of systemic chronic helminth in female mice in an attempt to explain observed behavioural changes in *T. crassiceps* cysticercosis. This goal was addressed through the following specific aims:

1. To characterise relative levels of neuronal activation, using immediate early gene markers.
2. To characterise relative levels of cell death, by evaluating synaptic integrity and p21/p53-mediated neural apoptosis.
3. To characterise markers of neurogenesis as an indication of preferential differentiation.
4. To examine differential cytokine levels and microglial activation in the hippocampus as putative indicators of neurological inflammation

2.2 Experimental procedures

2.2.1 Ethical statement

Ethical approval for using live animals was obtained from the University of Cape Town's Animal Ethics Committee (AEC) by co-supervisor Joseph Raimondo on 28 April 2015 for the period of 1 June 2015 until 31 May 2018 (Ethics approval 014/035).

2.2.2 Animals, experimental infections and tissue harvesting

Female age-matched C57BL/6 (B6) inbred mice were used, and animals were housed in the animal care facilities at the Faculty of Health Sciences at the University of Cape Town (UCT), under controlled temperature conditions and a 12-hour dark-light cycle. Control mice were housed in a separate cage in the same facility, while infected mice were housed in two cages of seven animals each. Maintenance of a controlled environment between test groups is vital, as environmental factors have been shown to have a significant factor on neurogenesis (Zhao et al., 2008).

As shown in Fig 5, *T. crassiceps* larvae were harvested from 3-month old donor mice had been infected at approximately postnatal day 30, the cysts were serially washed with phosphate-buffered saline PBS (Sigma-Aldrich, MO, USA), pH 7.5, and assessed for viability. Twenty non-budding cysts were selected and injected intraperitoneally into the host mouse at approximately postnatal day 30, while control mice were injected with PBS, pH 7.5, in accordance with the model described by Morales-Montor et al. (2014).

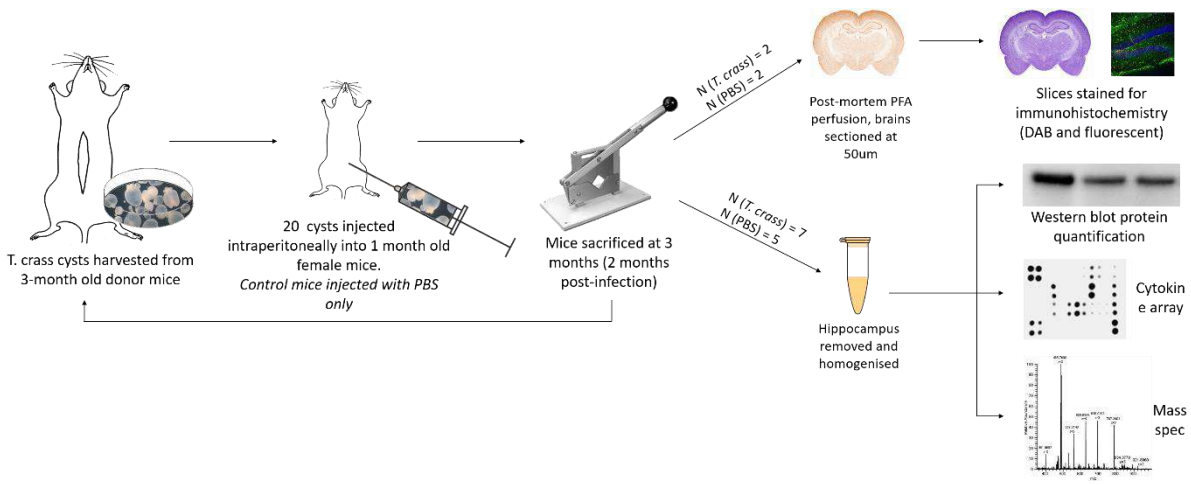

Figure 4: ***Summary of work flow and different methods applied.***

2.2.3 Western blots

Thirteen mice (*T. crassiceps* = 8, PBS = 5) were euthanised by halothane, death was confirmed by cervical dislocation, the skull was opened and the hippocampus dissected out, snap frozen and stored in liquid nitrogen.

Samples were sonicated in RIPA buffer (Merk, Damstadt, Germany), pH 8.0, and Halt™ protease inhibitor cocktail (Thermo Scientific, Massachusetts, USA) on ice for 30 min, and then centrifuged at 17,200 g at 4°C for 30 min. The supernatant was recovered and the protein concentration determined by the Bicinchoninic acid (BCA) method (Thermo Scientific). Identical amounts (between 20 and 35) µg of protein were subjected to SDS-PAGE and then blotted onto nitrocellulose membranes (Amersham, GE Healthcare Life Sciences, Little Chalfont, United Kingdom). Membranes were blocked with 5% fat-free milk for 1 hr at room temperature (RT) and incubated with primary antibodies at 4°C overnight, incubated with secondary antibodies for 1 hr at RT and incubated with Alkaline Phosphatase (AP)-conjugated secondary antibodies for 2 hrs at RT. Finally, the bands were visualized with a 5-bromo-4-clhoro-3-indolyl phosphate/nitro-blue tetrazolium (BCIP/NBT) reagent in a 1mM $MgCl_2$ (Merk) /0.1M $NHCO_3$ (Merk) buffer, pH 9.8.

Gel loading was controlled for with β-actin (1: 5000, Abcam ab8226) or α-tubulin (1:6000, Sigma-Aldrich, Missouri, USA, T5168), depending on relative molecular weights. Primary antibodies used were mouse anti-c-fos (1:750, Calbiochem, San Diago, USA, OP17); mouse anti-synaptophysin (1:5000, Abcam, Cambridge, UK, ab18008), mouse anti-tyrosine hydroxylase (TH) (1:3000, Sigma-Aldrich, T2928), mouse anti-DARP-32 (1:400, Santa Cruz, Dallas, USA, sc-135877), rabbit anti-NeuN (1:5000, Abcam, ab177487) goat anti-IgG (1:200 Abcam, ab6668), mouse anti-p53 1:750 (1:750, Santa Cruz, sc-393031), goat anti-Iba-1 (1:200 Abcam, ab10715), rabbit anti-S100B (1:500 Dako, GLostrup, Denmark, Z0311) and goat anti-doublecortin (DCX) (1:200, Santa Cruz sc-8066). Secondary antibodies used were

donkey anti-mouse-AP conjugate (1:2000, Novex, Frederick, USA, A16014), donkey anti-goat-AP conjugate (1:2000, Novex, A16002), donkey-anti-rabbit-AP conjugate (1:2000, Novex, A16026). Blots were scanned and mean pixel density was determined using Un-Scan-It v6.1 (Silk Scientific, Orem, USA).

2.2.4 Cytokine Array

Homogenate from two PBS and two *T. crassiceps* samples described in section 0 were used in a mouse Cytokine Array (RayBiotech, Norcross, USA, AAM-CYT-3-4). Different protein concentrations were used in attempts to optimise the technique using four available arrays. Protein (160 µg or 220 µg/array) for one PBS and one *T. crassiceps* sample. The manufacturer's protocol (RayBiotech) was followed, with chromogenic detection using an AP-streptavidin conjugate (1:1000, R&D Systems, Minneapolis, USA) diluted in 1.5% milk-tris-buffered saline (Merk), pH 7.5. The arrays were scanned and analysed by densitometry in ImageJ (NIH, Rochville, USA, v1.51) using Gilles Carpentier's Dot-Blot-Analyzer macro (written by Gilles Carpentier, 2008).[1] Arrays were normalised according to the protocol provided[2] (Carpentier, 2010; Rahimi et al., 2009).[3]

2.2.5 Mass spectrophotometry

In the western blots, an unknown band at approximately 30kDa consistently developed in several of the blots non-specific to the antibodies used, showing a considerable effect between test and control groups. In order to identify this band, an SDS-PAGE electrophoresis gel was run with a *T. crass* and control sample, stained with 0.1% Coomassie Blue R250 (B&M Scientific, Cape Town, South Africa)/10% acetic acid (Merk)/50% methanol (Merk). Bands at approximately 30 kDa were excised and sent to the Centre for Proteomic and Genomic Research (CPGR), Cape Town, for mass spectrometric analysis.

Section 8.3 describes the parameters used.

2.2.6 Imaging and immunohistochemistry

Four mice (two *T. crassiceps* and two control were euthanised with halothane delivered by inhalation, death was confirmed by cervical dislocation, and transcardially perfused with 4% paraformaldehyde (PFA) (Merk), before brains were removed from the skull and placed into PFA for full fixation. After 24 hours, PFA was replaced by 30% sucrose (Sigma)/0.1M PO_4 (Merk) pH7.4 buffer for cryoprotection until the brains sank (showing full perfusion of tissue). Brains were sagittally-

[1] Available at http://rsb.info.nih.gov/ij/macros/toolsets/Dot%20Blot%20Analyzer.txt
[2] Available at http://image.bio.methods.free.fr/ImageJ/?Protein-Array-Analyzer-for-ImageJ.html
[3] Reference for method: http://journals.plos.org/plosone/article?id=10.1371/journal.pone.0007694 - pone.0007694-Abramoff1.

sectioned (40 µm) with a cryostat (Leica CM1850). To examine overall morphological and cellular integrity, sections were mounted on Superfrost® Plus (Thermo Scientific) slides and stained with 0.1% cresyl violet solution. Sections were dehydrated and coverslipped with Entellan® (Merck) mounting medium

For 3,3'-Diaminobenzidine (DAB) staining, sections were incubated with 0.6% H_2O_2 for 30 min to reduce background, before blocking in 3% donkey serum for an hour and incubating overnight in 4 ^oC with the appropriate primary antibodies. Following incubation with secondary antibody for 2 hours at RT the following day, sections were incubated in avidin–biotin solution (Vectastain Elite ABC kit, Vector Laboratories, Burlingame, USA) for 1 hour at RT to enhance staining. Following washing, sections were transferred to plate wells containing 1% DAB (Sigma)/0.03% H_2O_2 (Merk)/0.5% $NiCl_2$ (Sigma) made up in distilled H_2O until well-stained. Tissues were then quenched in H_2O, mounted on Superfrost® Plus (Thermo Scientific) slides, dehydrated and coverslipped with Entellan® (Merck) mounting medium.

Primary antibodies used for DAB staining were mouse anti-c-fos (1:150, Calbiochem, OP17); goat anti-CD11b/c (1:200, Abcam, ab1211) and mouse anti-GFAP (1:1000, Acris Laboratories, Herford, Germany, AM20989PU-N) Secondary antibodies used were biotin-SP-conjugated donkey anti-mouse (1:1000, Jackson Laboratories, Bar Harbour, USA, 715-065-151) and donkey anti-goat (1:1000, Jackson Laboratories 705-065-147) The donkey anti-mouse secondary was also used without a primary antibody to examine non-specific binding .

For immunofluorescence staining, sections were blocked in 3% donkey serum for an hour and incubated overnight at 4^{O}Cwith primary antibodies. Rabbit anti-NeuN (1:5000, Abcam, ab177487) and goat anti-doublecortin (DCX) (Santa Cruz, sc-8066) were colocalised using anti-rabbit Alexa 488 (1:1000, Jackson Laboratories 711-546-152) and anti-goat Cy3 (1:1000 Jackson Laboratories 705-166-147) secondary antibodies. Rat anti-CD86 (1:200, Thermo Scientific 50-127-36) and goat anti-CD206 (1:200, R&D Systems AF2535) were colocalised using anti-rat Alexa 488 (1:1000, Jackson Laboratories 712-546-153) and anti-goat Cy3 secondary antibodies (1:1000 Jackson Laboratories, 712-545-150). Both sets were stained with Hoechst 33342 (1:1000 Thermo Scientific H1399,) nuclear stain. After secondary incubation for 2 hours in the dark, sections were stained with a nuclear counterstain (Hoechst 33342, 1:1000) (Thermo Scientific, H1399) for 15 min at RT. Sections with mounted on Superfrost® Plus (Thermo Scientific) slides using Mowiol® 4-88 (Sigma) mounting medium.

Slides were imaged using a brightfield Zeiss Axioskop M microscope and confocal Zeiss LSM 880 at the UCT Confocal and Light Microscope Imaging Facility, Cape Town. Due to time restrictions and a paucity of sample for appropriate optimisation, no formal quantification was conducted on acquired images.

2.3 Statistical analysis

GraphPad Prism 6 (San Diego, CA, USA) was used for all statistical analyses. Due to the small sample size, non-parametric Mann-Whitney *t*-tests were used to determine significance between *T. crassiceps* and control groups. Unless otherwise specified, the median and interquartile range are used for graphs, as is compatible with data that are not normally distributed. Significance was considered when $p < 0.05$.

3 RESULTS

3.1 Neuronal activation, cell death and synaptic transmission

To assess neuronal function, hippocampal homogenates were used to immunoblot for markers of neuronal activity (c-fos), cell death (p21 and p53), synaptic integrity (synaptophysin) and catecholaminergic transmission (TH and DARP-32). *T. crassiceps* mice showed increased levels of c-fos compared to sham PBS inoculated controls (Fig. 5A). This finding was confirmed with immunohistochemical data showing no obvious differences (Fig. 6) between staining levels in *T. crassiceps* and control sections (Fig 6). Attempts to characterise p21 and p53 protein expression failed due to technical problems with those primary antibodies. No differences in levels of synaptic marker synaptophysin were detected (Fig.5B) suggesting no general loss of synaptic function in the hippocampi from control versus *T. crassiceps*-infected mice. Cresyl violet staining showed no identifiable cell death as there was an absence of pyknotic (Fig 6).

Synapses were further characterised according to specific neurotransmitters, using markers for tyrosine hydroxylase (TH) and cyclic AMP-regulated phosphoprotein-32 (DARP-32). There was significant ($p = 0.382$) variation in TH levels (Fig 5C) making interpretation difficult. DARP-32 levels in *T. crassiceps* are increased compared to sham PBS inoculated controls but this difference is not statistically significant.

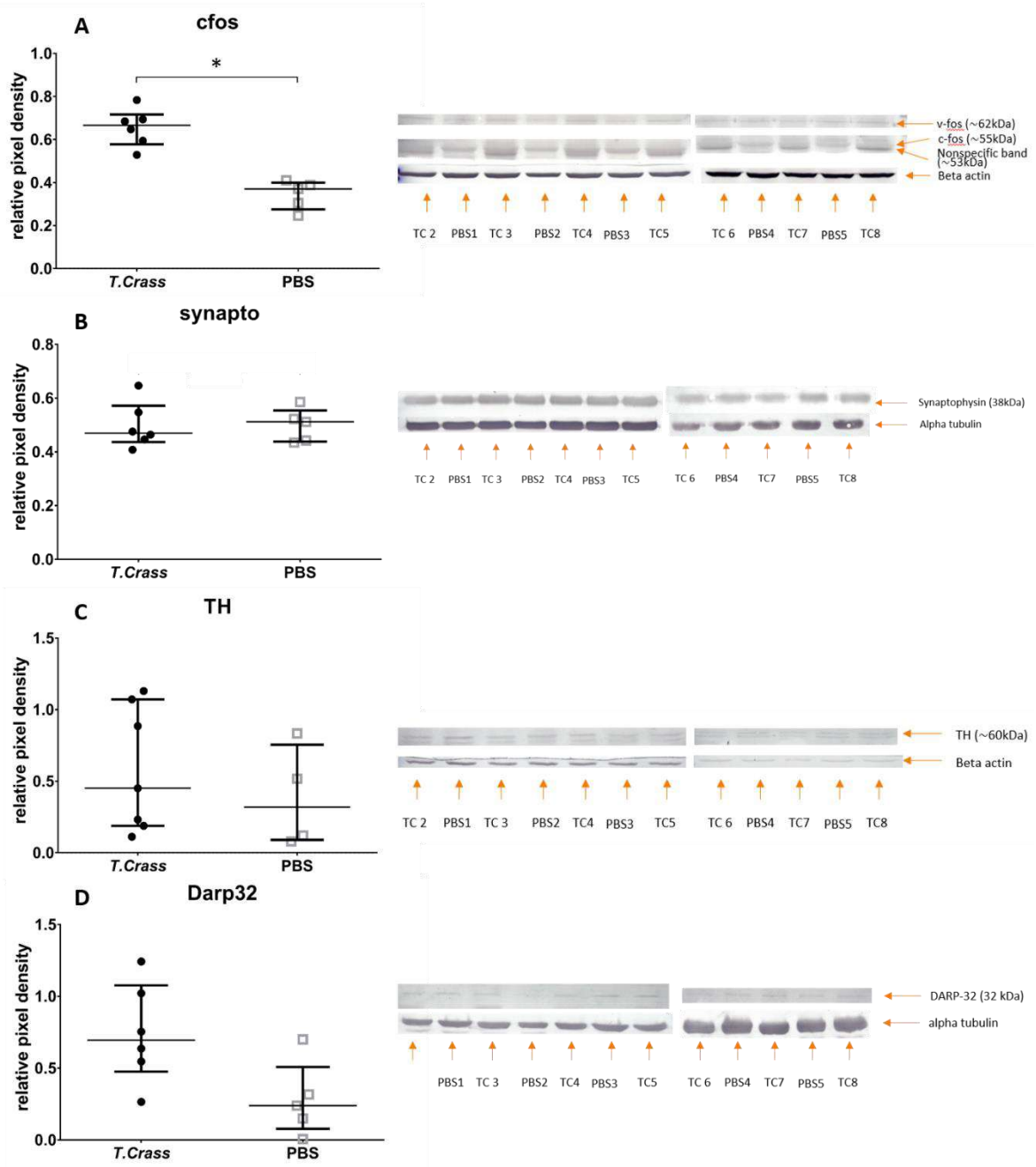

Figure 5: ***Western blot analyses of cellular markers****. Quantification of westernblots performed of hippocampal homogenate from T. crassiceps and sham inoculated samples of show a significant difference in c-fos levels, p=0.004 (**A**),no difference in levels of synaptophysin, p>0.999 (**B**), an a non-significant difference in TH, p = 0.382 (**C**) and DARP-32, p=0.052 (**D**) levels.*

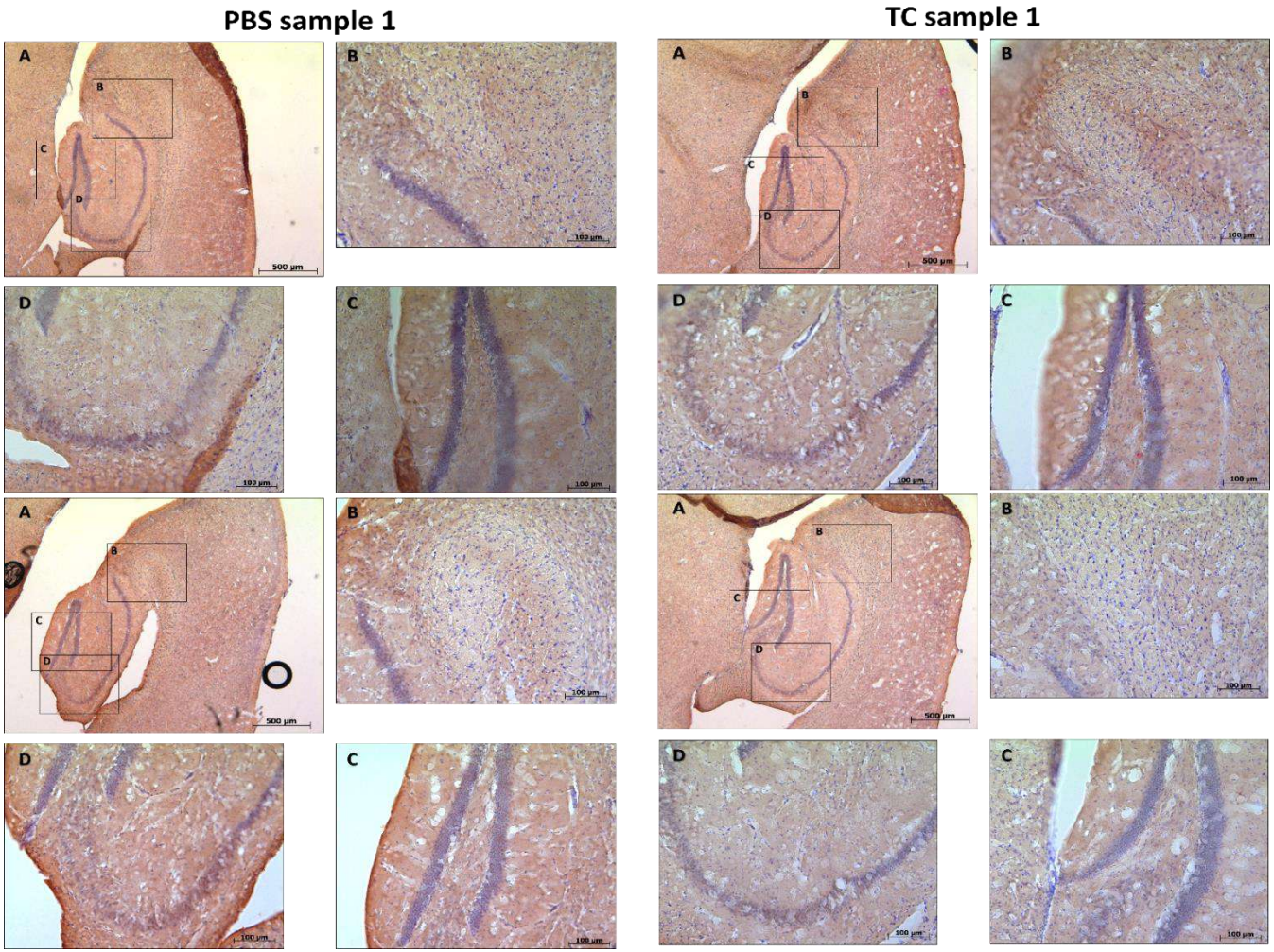

Figure 6: ***Effect of T. crassiceps inoculation on neuronal activation.*** *Sagittal sections of perfusion fixed brains from T. crassiceps and sham PBS inoculated mice, labelled with anti-cfos DAB IHC, counterstained with cresyl violet. c-fos positive staining should appear as dark brown spot, however, only faint staining on sporadic sections could be seen. Images show a low magnification overview (A), a region of the ventral subiculum for staining control (B), the dentate gyrus (C) and CA1-CA3 hippocampal regions(D). There are two sections from each sample (top and bottom sets of images)*

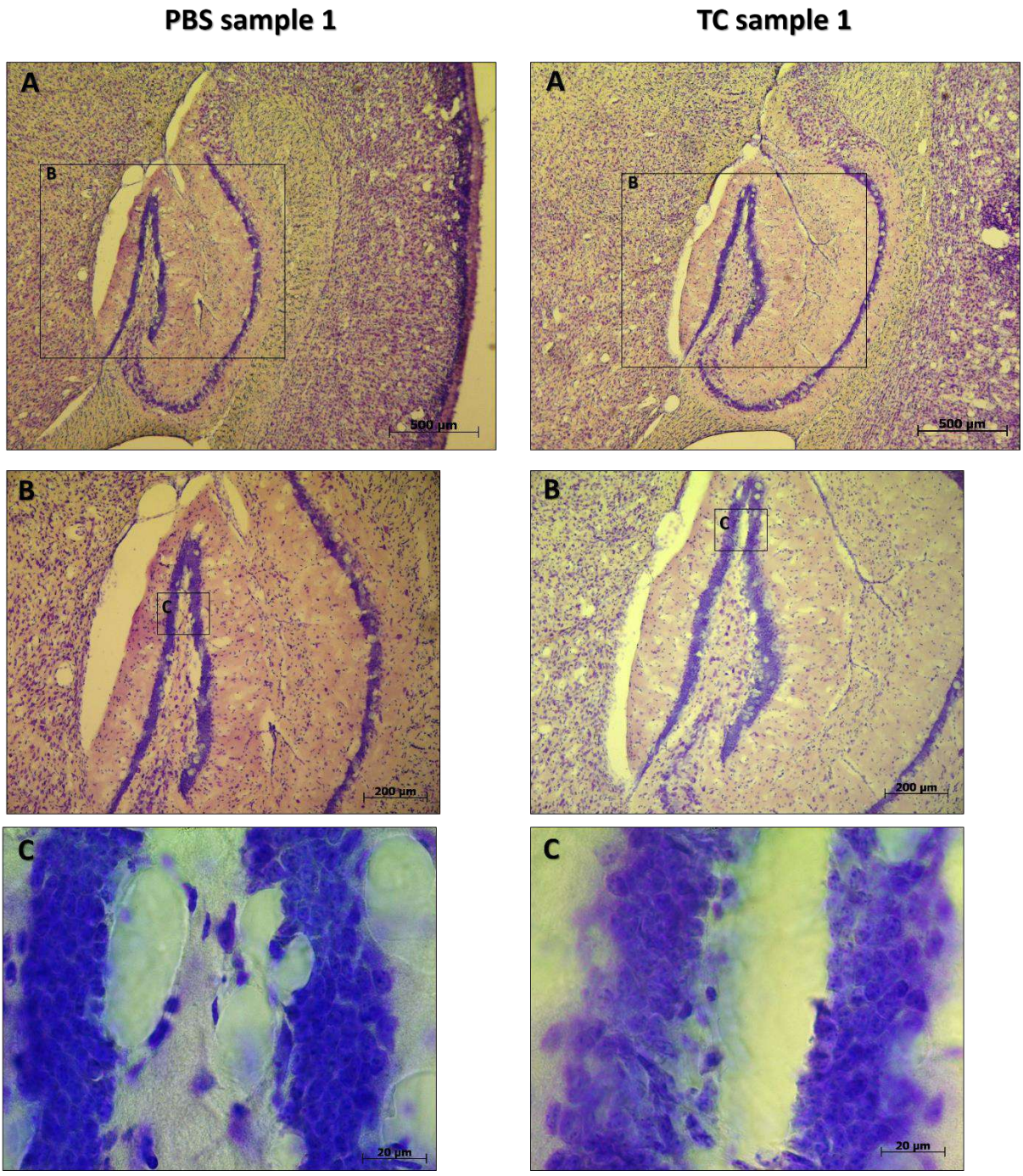

Figure 7 ***Effect of T. crassiceps inoculation on neuronal activation on hippocampal morphology and cell death.*** *Sagittal sections of perfusion fixed brains from T. crassiceps and sham PBS inoculated mice stained with cresyl violet, shown at progressive magnifications (**A**: 5x, **B**: 10x and **C**: 100x) of the dentate gyrus, showing no pyknotic nuclei.*

3.2 Neurogenic cascade

One of the original goals of this project was to immunoblot for neurogenesis markers including NeuN, which labels mature neurones; DCX, which labels immature neurones; S100B, which labels mature astrocytes; and nestin, which labels quiescent neural progenitor cells. However, due to failure of primary antibodies to recognise the target proteins in western blots, and a limited number of sections available for IHC meant that only DCX-positive (+) and NeuN-positive (+) neurones could be examined before the tissue was exhausted. There was significant variation within different sections from the same sample (e.g. sections A and B from sham inoculated PBS sample in Fig. 8), thus stereology is required to number immature neurones. DCX-positive cells can be seen at the subgranular zone, with cellular processes running across the granular zone (Fig. 8E-H).

3.3 Glial activation

Once again, primary antibodies for glial markers were unreactive in western blots. Immunoreactivity for GFAP, an astrocyte and neural progenitor cell marker, revealed similar morphologies and staining intensity (Fig 9), rather than displaying changes associated with "astrogliosis" such as hypertrophy of cellular processes. Iba-1-immunoreactive neurons were visible in the hippocampus, but quality of the staining did not allow for differentiation of resting "ramified" microglia and "amoeboid" inflammatory microglia (Fig 10).

PBS sample 1

TC sample 1

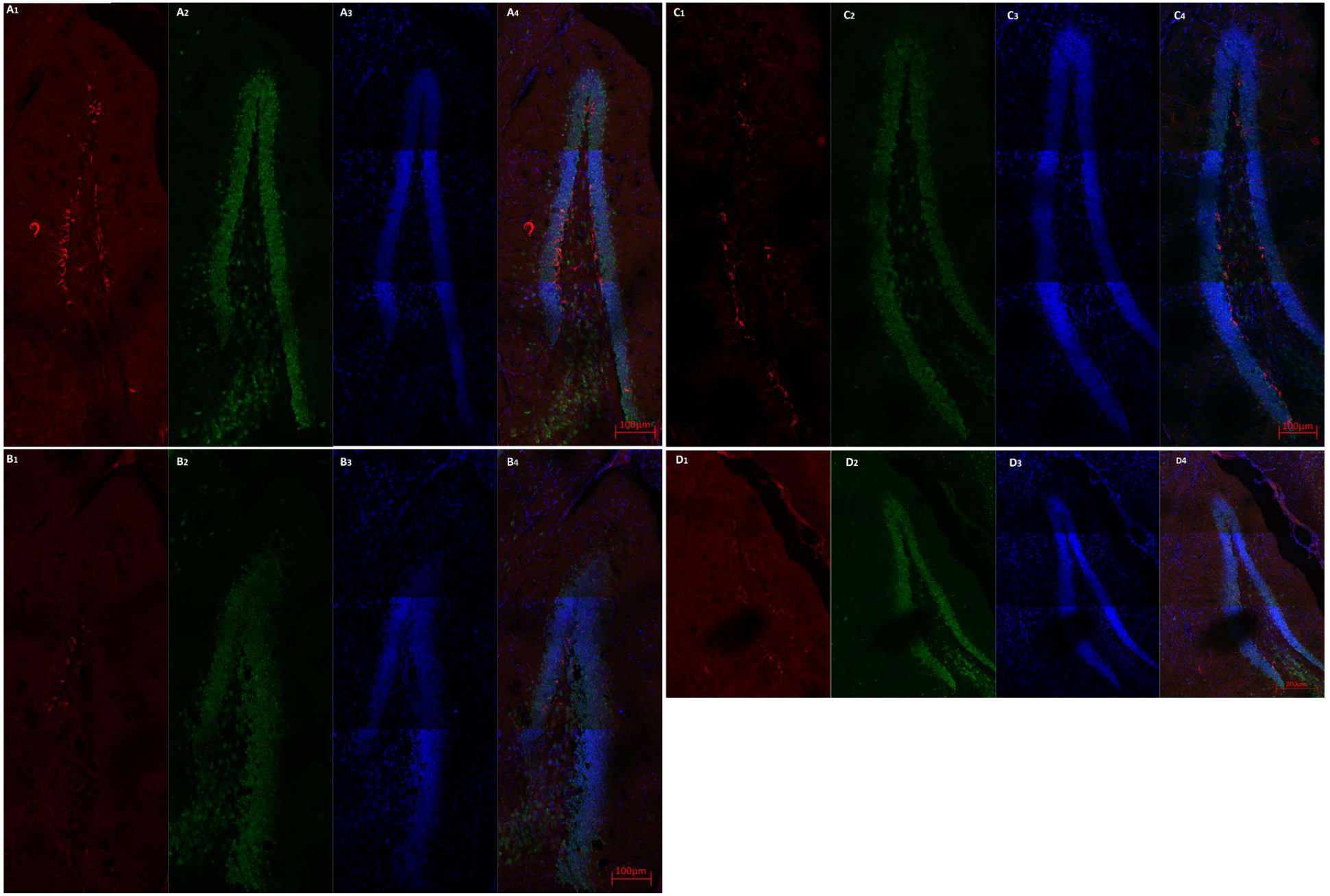

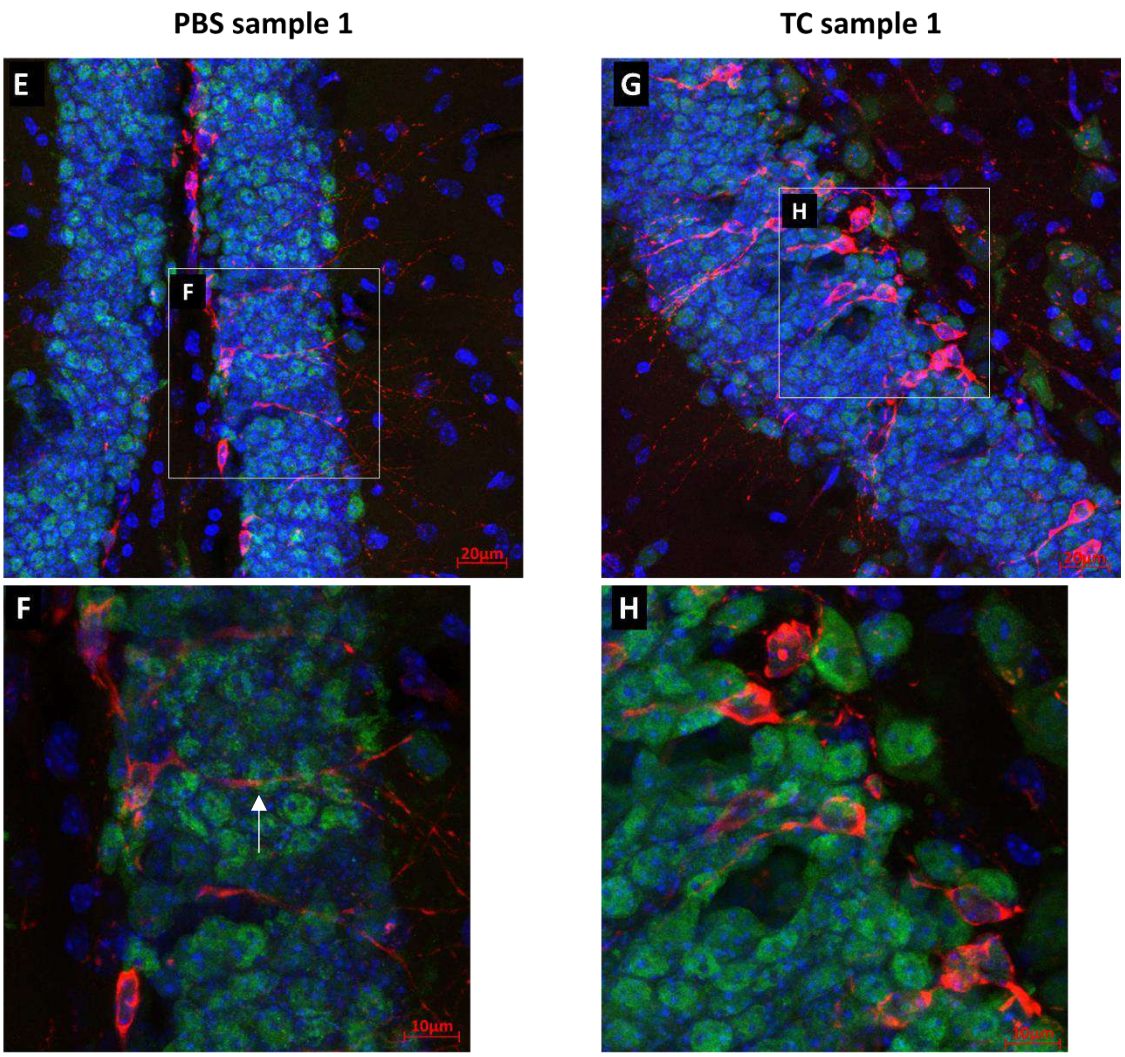

Figure 8: ***Effect of T. crassiceps inoculation on neurogenesis.*** *Sagittal sections of perfusion fixed brains from T. crassiceps and sham PBS inoculated mice labelled with anti-DCX (red), anti-NeuN (green) and Hoescht nuclear stains.* ***A-D*** *show two sections from a PBS (****A*** *and* ***B****) and a T. crassiceps (****C*** *and* ***D****) sample at 20x magnification. DCX localises to cell bodies and processes, while NeuN localises to the nucleus. Hoechst s a nuclear stain.****E-H*** *show the morphology of DCX- and NeuN-positive cells at 40x (****A****) and 63x(****B****) magnifications. NeuN colocalises with the nucleus) but not with DCX, showing that the two markers differentiate neurones. Note the morphology of the DCX positive cells with radiating processes across the granular zone (arrow).*

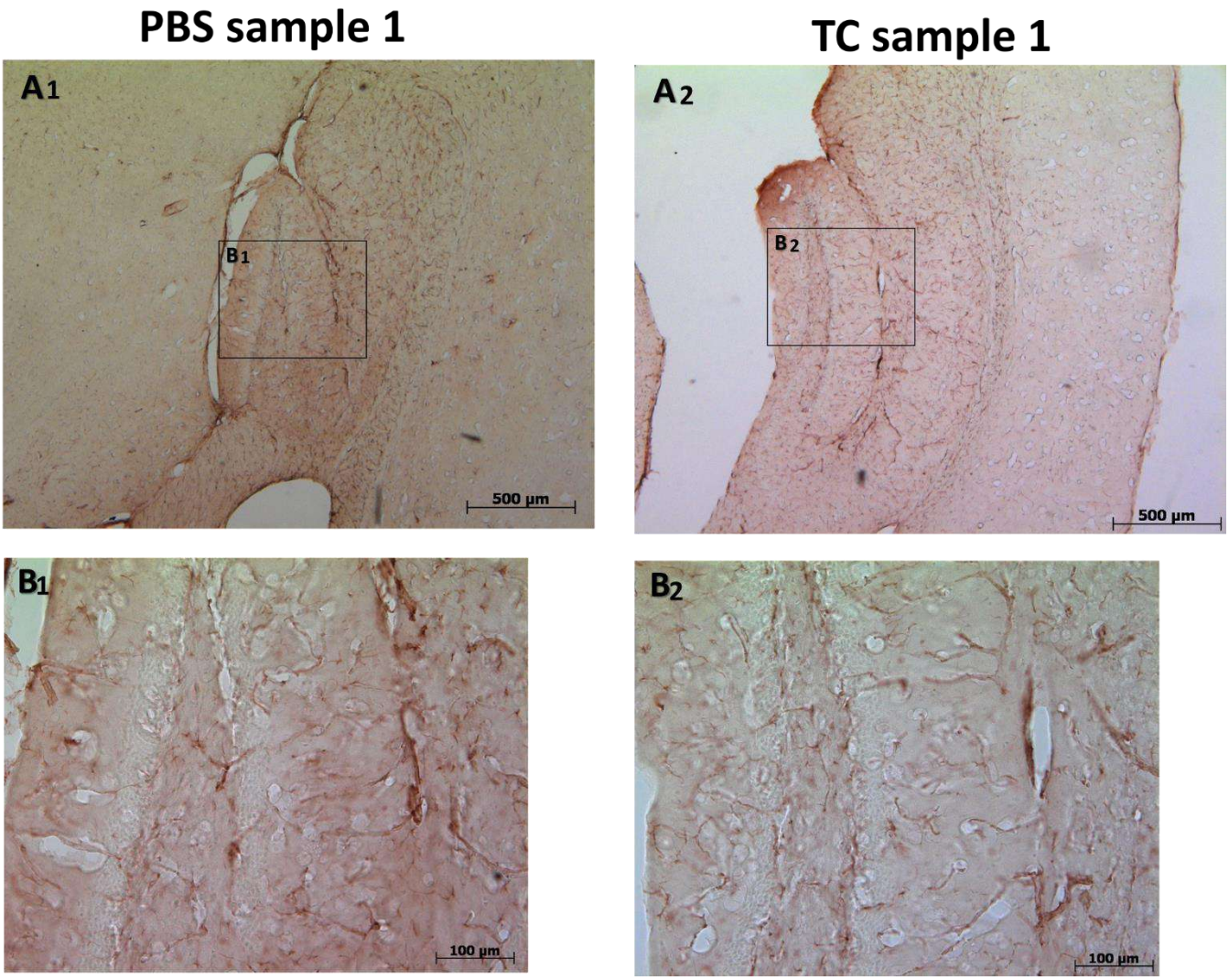

Figure 9 ***Effect of T. crassiceps inoculation on astrocyte morphology.*** *Sagittal sections of perfusion fixed brains from T. crassiceps and sham PBS inoculated mice, labelled with anti-GFAP DAB IHC. A provides overview of the hippocampus at 5x magnification (A), and an image at 20x magification shows astrocytpe morphology (B). One section from each sample is shown.*

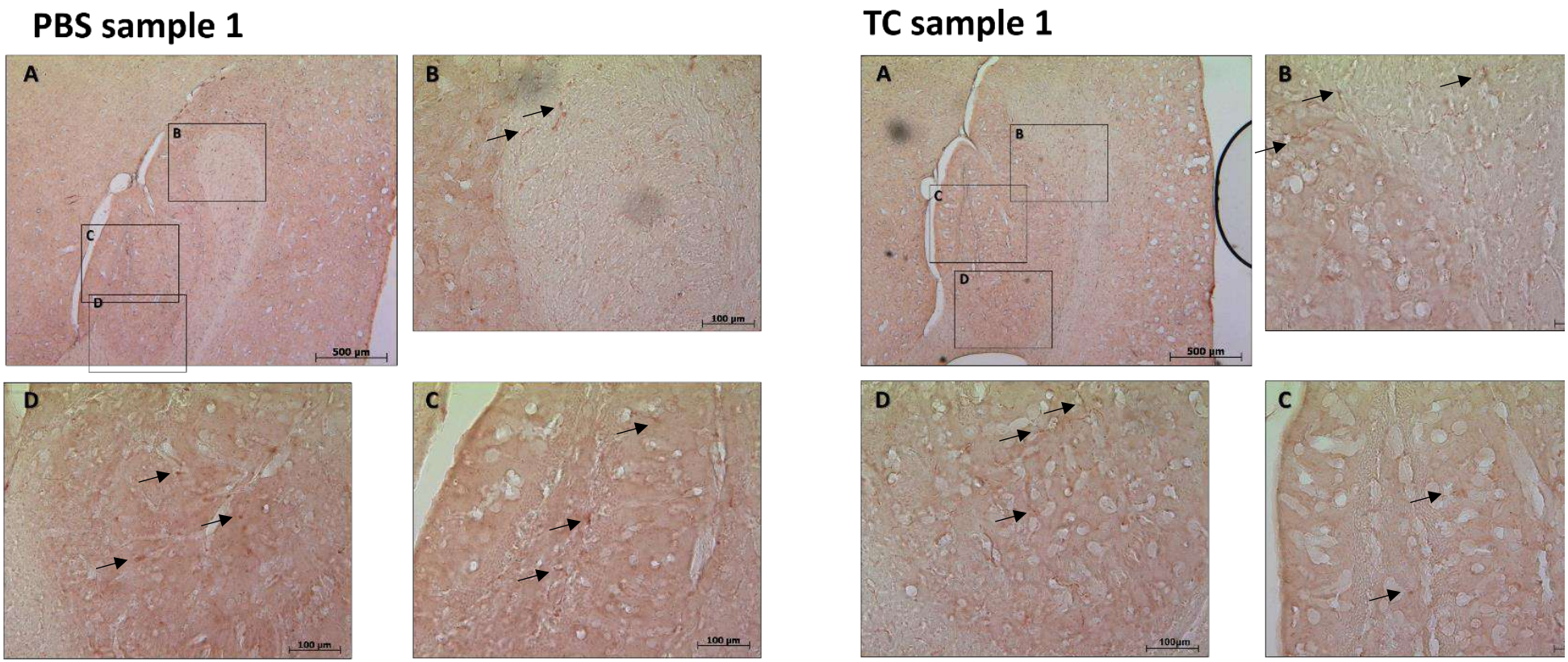

Figure 10: ***Effect of T. crassiceps inoculation on microglial morphology.*** *Sagittal sections of perfusion fixed brains from T. crassiceps and sham PBS inoculated mice, labelled with anti-Iba-1 DAB IHC. Images show a low power overview at 20x magnification (**A**), a region of a region of the ventral subiculum for staining control (**B**), the dentate gyrus (**C**) and CA1-CA3 hippocampal regions(**D**).*

3.4 Immune Activation

3.4.1 Cytokine array

Cytokine arrays conducted on two PBS and two *T. crassiceps* samples showed high levels of variability for many of the cytokines. Fig. 11 shows select cytokines where variability within groups was low and the effect size was relatively large. Section 8.4.2 contains a list of the functions of these proteins., as well as the complete results of all 62 cytokines tested.

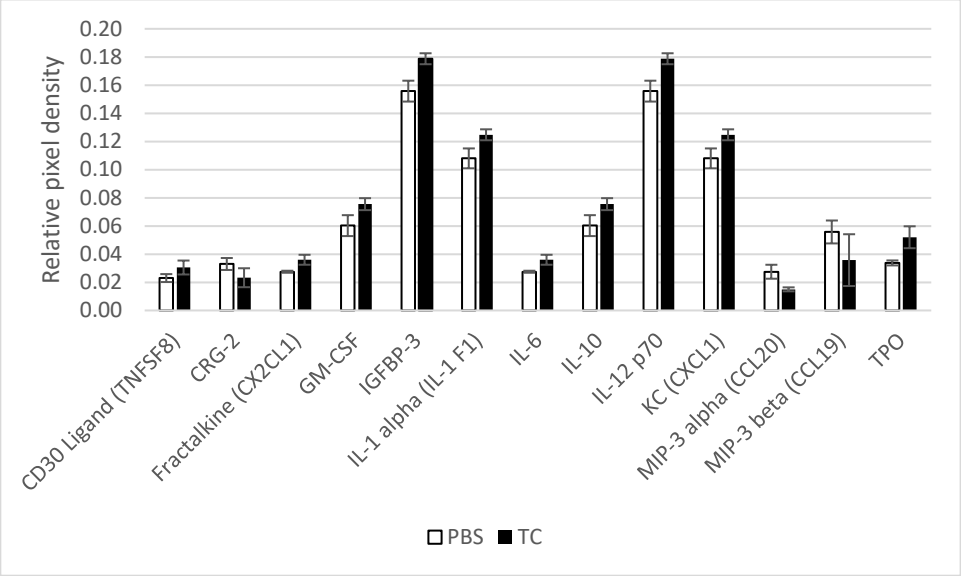

Figure 11: ***Differential expression of cytokines due to T. crassiceps inoculation.*** *Select cytokines from the cytokine arrays performed on hippocampal homogenate from T. crassiceps (n=2) and sham PBS inoculated (n=2) samples. Cytokines selected show promising effect sizes (p<0.25). Error bars show 95% confidence intervals.*

3.5 Unknown western blot band

During the western blot experiments described above, unknown bands appeared consistently at a molecular weight (at approx. 28 and 52 kDa) unrelated to the primary antibodies used in the experiment. Intriguingly, these bands showed a significant effect between *T. crass* and sham PBS pH inoculated groups, warranting further investigation (Fig. 12). The bands appeared only in experiments using primary antibodies and it transpired that the bands were specific for anti-mouse secondary antibodies, and also reacted to goat anti-IgG, which suggests the identity of the band. Immunohistochemistry with donkey-anti-mouse secondary showed a suggestive increase in staining (Fig 13).

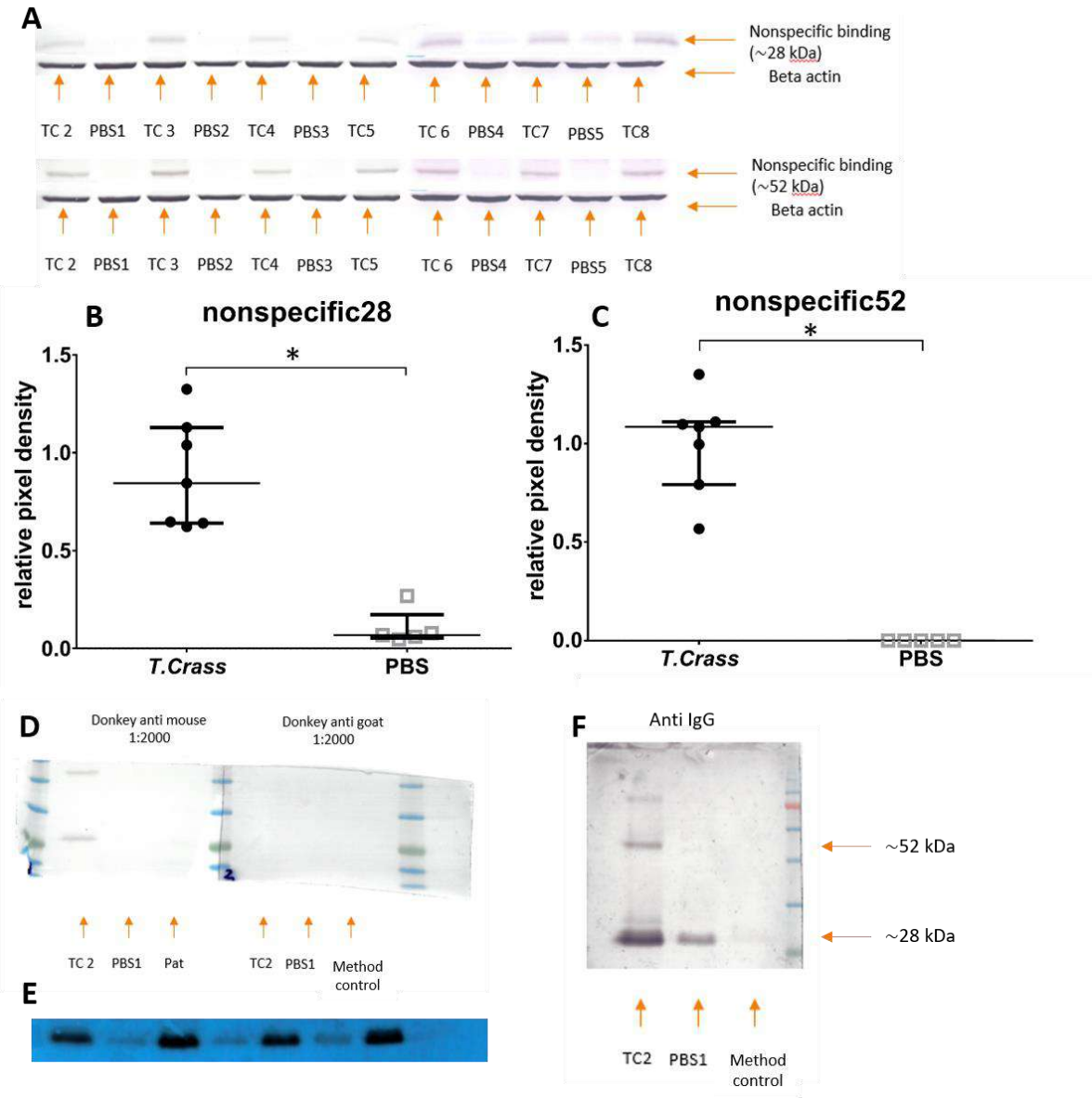

Figure 12: ***Investigation of "mystery" western blot band showing a large effect between T. crassiceps and sham inoculated mice.*** *Unknown bands appeared on western blots of hippocampal homogenate from T. crassiceps and sham inoculated samples using various primary antibodies raised in mouse (**A**; mouse anti-p53 primary). **B** and **C** show quantification of these bands with a significant (p=0.003) difference between T. crass and sham PBS inoculated samples. Blots were then incubated with secondary antibodies only, raised against mouse and goat, indicating that the band is specific to anti-mouse secondary antibodies (**D**). **E** shows a blot incubated with an HRP-conjugated anti-mouse secondary (anti-c-fos primary), showing that the bands are not specific to the AP-conjugate secondary used in previous blots. Similar bands appeared when incubated with a goat anti-IgG primary antibody and anti-goat secondary (**F**), suggesting the identity of the band. "Method control" refers to a negative control from rat hippocampal homogenate from an unrelated project.*

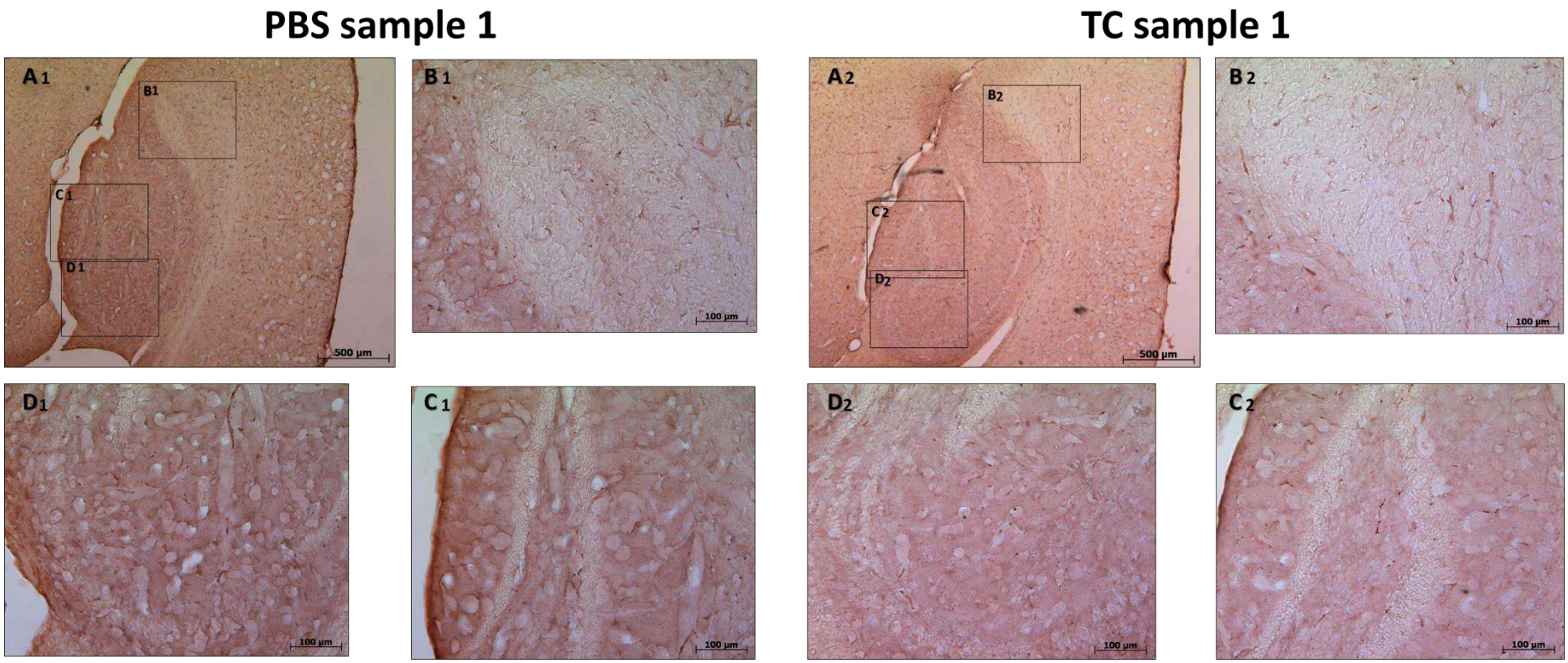

Figure 13 ***Effect of T. crassiceps inoculation on anti-mouse secondary only labelling.*** *Sagittal sections of perfusion fixed brains from T. crassiceps and sham PBS inoculated mice, labelled with donkey-anti-mouse secondary antibodies using DAB IHC. Images show a low power overview at 20x magnification (**A**), a region of a region of the ventral subiculum for staining control (**B**), the dentate gyrus (**C**) and CA1-CA3 hippocampal regions(**D**).*

Mass spectrophotometry was run on a band from a single *T. crassiceps* and sham PBS inoculated sample. No immunoglobulins were isolated in the sample; however, Fig. 14 shows select proteins that were differentially represented. Most prominent of these was 14-3-3 protein zeta/delta which showed over a thousand-fold increase.

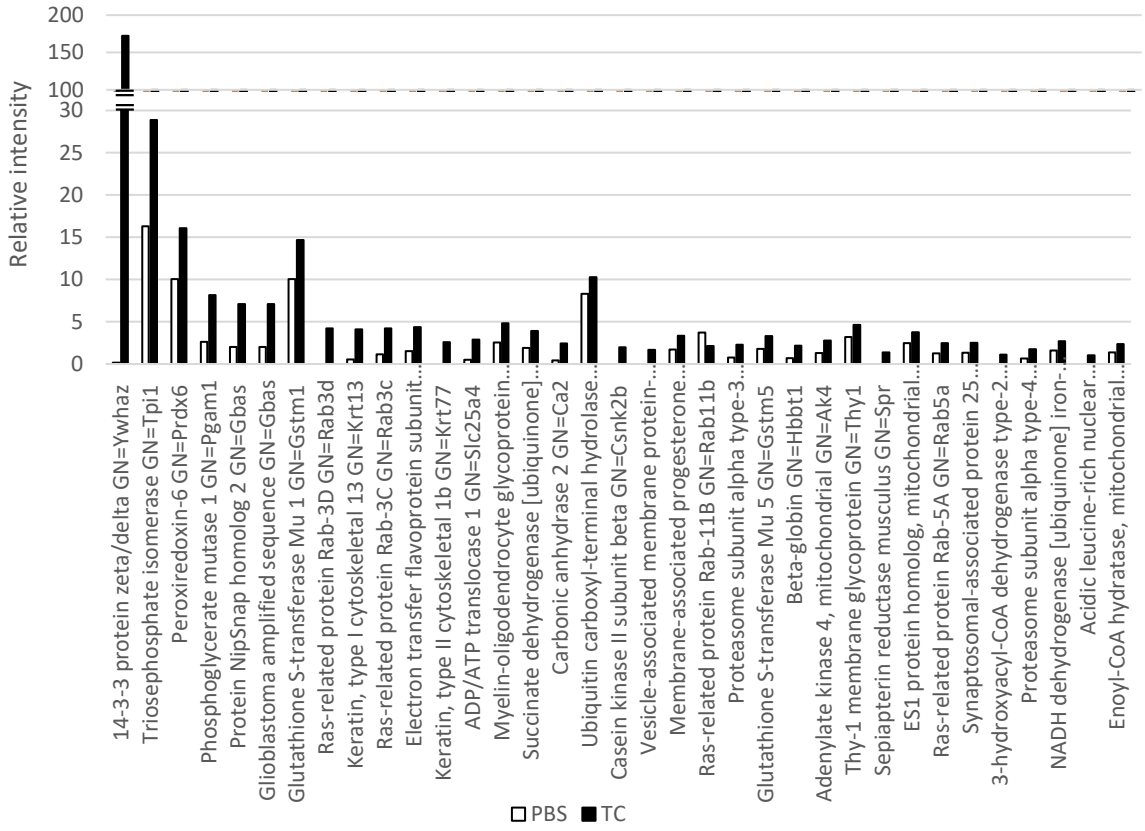

Figure 14. ***Mass spectrophotometric results for mystery western blot band:*** *showing proteins selected (and ordered) by their differential expression in sham PBS inoculated versus T. crassiceps sample. n=1Results*

4 Discussion

As part of their ground-breaking work on the neuroendocrinology of helminth infections, Morales-Montor et al. (2014) discovered behavioural changes in their i.p. *T. crassiceps* inoculated mice. The present study is an exploratory investigation that builds on this finding, aiming to get insight into the neurological mechanisms behind these behavioural changes. It is hoped that a greater understanding of the neuroinflammatory response to this helminth will not only inform on the neuro-behavioural effects of related organism *T. solium*, which infects humans, but will also provide generalisable insight about the effects of other peripheral parasitic infections. Thus far, neuroimmunological studies in parasite models have been reserved for infections localised in the CNS and intestinal helminths

(Ezeamama et al., 2012; Nokes et al., 1992; Watkins and Pollitt, 1997), but have not been conducted in systemic infections.

To fill this gap, our approach was to characterise various neurophysiological systems and note any changes in the *T. crassiceps* infected mice. The systems identified as relevant included neuronal activation, cell death, the neurogenetic cascade, microglial activation and immune activation, however, due to methodological and time limitations, all areas of interest could not be examined sufficiently. Methods used included western blots, cytokine arrays and mass spectrophotometry on hippocampal supernatant and immunohistochemistry on perfusion-fixed sagittal whole-brain sections. A number of primary antibodies failed to react in both western blots which limited the quantitative power of the study, potentially due to loss of antibody reactivity or poor transfer with high/low molecular weight proteins, however many of these, such as NeuN and DCX, were successful in IHC.

Using these methods, major findings included upregulation of *c-fos*, an immediate early expression gene in neuronal activation, and a suggestive increase of dopamine-related protein DARP-32. There was no evidence of cell death as pyknotic nuclei or decreased expression of synaptic marker synpatophysin, contrary to what was seen by Zepeda et al. (2017). Certain cytokines identified by the cytokine array were differentially expressed, as were a number of proteins identified by mass spectrophotometry, however, as discussed below, no firm trends could be identified. Most significantly, perhaps, was the effect seen between *T. crassiceps* and sham (PBS)-inoculated groups in the non-specific band mentioned in section 3.5. An immunoblot using an anti-IgG primary antibody suggested that this band was due to non-specific binding of anti-mouse secondary antibodies to an antibody. Parenchymal IgG is typically only seen in blood brain barrier permeabilization and has been noted in pathology models of seizures, amyotrophic lateral sclerosis and Alzheimer's (Drummond et al., 2013; Marchi et al., 2010; Nicaise et al., 2009; Seitz et al., 1985), and serum T. solium-specific IgG has been suggested as a biomarker in neurocysticercosis (Soba et al., 2014). However, when the Western blot band in question was excised and sent for mass spectrophotometry there was no evidence of antibody fragments, leaving the question of the identity of this band unanswered. A *T. crass* specific ELISA could confirm the IgG hypothesis and may suggest the presence of antigens in the CNS.

Similarly antithetical, the cytokine array produced conflicting results, showing downregulation of certain chemotactic factors, such as CRG-2, MIP-2 alpha and MIP-2 beta, and upregulation of other chemotactic factors such as fractalkine. Cytokines that were more highly expressed that are indicative of a Th1-type response in the *T. crassiceps* mice include IL-1α and CD30 ligand, but IFN-γ and TNF-α,

key mediators of this response (Cavaillon, 2001), showed no significant changes. On the other hand, IL-6, a "neuropoeitin"(Erta et al., 2012) and IL-10, a negative modulator of neuroinflammation (Garcia et al., 2017) were elevated, consistent with a Th2-type response, however, key cytokines IL-4, IL-5 and IL-13 associated with this response (Peon et al., 2013) showed no significant changes. Another inconsistency was the higher expression of both IL-10 and granulocyte-macrophage colony-stimulating factor (GM-CSF) as the former supposedly inhibits the synthesis of GM-CSF (de Waal Malefyt et al., 1991). Proliferation regulators keratinocyte chemoattractant (KC) and thrombopoietin (TPO), which promote angiogenesis and tumorigenesis and proliferation of megakaryocytes (responsible for platelet generation) respectively, were also upregulated in the *T crass* mice. Although the significance of this is debatable, cytokines that were relatively highly expressed within the sample include Axl, an intracellular signal transducer involved in cellular proliferation with a putative role in hippocampal neurogenesis (Ji et al., 2015), VCAM-1, which plays a role in permeabilising the blood brain barrier (Haarmann et al., 2015), CTACK, IL-1α, IL12p70, KC, M-CSF, MIP-2, PF-4 and P-Selectin.

Of the cytokines that Morales-Montor et al. (2014) found that were elevated, including IL-4, IL-6 and TNF-α, only IL-6 in our study, mirrored their findings. Lopez-Griego et al. (2015), however, found that IL-6 was downregulated in *T. crassiceps* infected mouse hippocampi. Differences in findings may be due to the above studies measuring RNA, rather than directly measuring protein levels, and differences between mice strains (Balb/c AnN mice as used by Morales-Montor et al. (2014), rather than C57BL/6). Furthermore, only female mice were used in the present study, and Morales-Montor et al. (2014) found that there were differential responses between the sexes. The small sample size of this study may be the source of inconsistencies, and with several cytokines there was high variability between the two samples in the two treatment groups.

Beyond the cytokines listed above, certain proteins that were highlighted by mass spectrophotometry as differentially expressed include, amongst others, 14-3-3 protein zeta/delta,[4] an adaptor protein involved in general and specialised signalling pathways including Golgi reassembly, protein targeting and regulation of cell death, triosephosphate isomerase,[5] an enzyme involved in gluconeogenesis which has been found to be required for synaptic vesicle function(Roland et al., 2016), and peroxiredoxin-6[6], a peroxidase protective against oxidative stress and associated with Alzheimer's (Power et al., 2008). These proteins and cytokines may be of further interest as a focus for future studies. However, as with the cytokine array, the mass spectrophotometry data had a very limited sample size (*n*=1), which proved to be one of the main limitations of the study. Several western

[4]UniProt accession no: P63101
[5] UniProt accession no: P17751
[6] UniProt accession no: O08709

blots (TH and DARP-32, for example) and cytokine levels between samples of the same group showed high variability, indicating that more samples are required before any conclusions can be drawn.

Limitations inherent in the techniques include, for western blots, a lack of cellular detail due to homogenisation of the entire hippocampus, and although IHC allows for localisation that western blots do not, effective quantification requires stereology which takes into account the three-dimensional aspect of the tissue. It can be seen in our IHC results in attempts to classify neurogenic and glial phenotypes that simple sectioning and staining is insufficient to provide workable data, and attempts to colocalise CD86 and CD206 to assess differential microglial activation were unsuccessful. Primary recommendations for a follow-on study would thus be to increase the sample size for each of the experiments, which would allow for better optimisation of techniques such as IHC stereology, and improve the generalisability of the results, particularly for the cytokine array. Other techniques that could be considered include cell death assays and electrophysiological studies. Mass spectrophotometry of entire samples would provide a far more specific and sensitive picture of differences between samples than western blots, although it would still be limited to providing only averaged values for the entire area sampled, without providing cellular detail. Other applications of the model could include examining other areas of the brain, such as the amygdala, and this may also provide valuable insight, measuring systemic inflammation and local peritoneal inflammation, while also considering the role of the gut-brain axis. However, before more expensive and labour-intensive studies are conducted, it would be prudent to attempt to reproduce the behavioural changes observed by Morales-Montor et al. (2014), as, in addition to the possible presence of IgG in the brains of *T. crassiceps* infected mice, our study has provided minimal evidence of tangible differences between test and control groups.

By briefly touching on elements of cell death, neurotransmitter levels, inflammatory mediators, glial cell morphology and neurogenesis, this study has attempted to find differences between *T. crassiceps* infected and sham PBS inoculated mice. It remains to be determined whether findings in the *T. crassiceps* model can be generalised to *T. solium* in humans and even other parasitic infections, as this would bear impact on the question of whether the billions of people living with various helminth infections are suffering from neurological sequelae.

5 Conclusion

The aim of this study is to explore the neurological impact of systemic chronic helminth in an attempt to explain observed behaviour changes in *T. crassiceps* cysticercosis.

Results were inconclusive, with high variability between samples and experimental failure and small sample size leading to a paucity of data. Although activation marker c-fos and an unknown western blot band (potentially IgG) showed significant effects between groups, the data does not conclusively suggest the presence of neurological differences. Attempts should be made to reproduce the behaviour changes observed by Morales-Montor et al. (2014) before further neurological characterisation is conducted. However, this work provides a useful framework for investigating neurological mechanisms behind behaviour change – namely to systematically examine neuronal activation, cell death, cytokine and immune activation, glial changes and neurogenesis.

Furthermore, this work adds to an understudied field – parasitic infections are a significant cause of morbidity and mortality, and the psychiatric/neurological burden of the pandemic remains as yet unquantified.

6 ACKNOWLEDGEMENTS

I would like to acknowledge my supervisor and co-supervisor Drs Vinogran Naidoo and Joseph Raimondo for all their input and support.

I would like to thank PhD candidates Patricia Swart and Hayley Tomes, the former for being the most amazing Western Blot magician anyone could wish for and for being an absolutely awesome (and very forbearing) labmate, and the latter for always being ready to provide a shoulder to cry on. Thanks to the Raimondo lab in general for their openness, acceptance and willingness to eat my desserts, even when they looked like brains.

To Prof Asfree Gwanyana, heartfelt thanks for his amazing generosity, which averted several crises.

To Prof Dirk Lang and his assistant Carla van Niekerk from the Confocal and Microscopy Unit, thanks for helping me at the 11th hour.

Finally, I would like to thank Prof Arieh Katz, without whom I would not have had the opportunity to do this Honours course.

I would like to acknowledge the Marcus Rubin Scholarship and UCT Clinician Scientist Scholarship (funded by the South African Medical Research Council), as well as my father, for supporting me financially this year.

7 REFERENCES

Adamo, S.A., Webster, J.P., 2013. Neural parasitology: how parasites manipulate host behaviour. J Exp Biol 216, 1-2.

Altman, J., Das, G.D., 1965. Autoradiographic and histological evidence of postnatal hippocampal neurogenesis in rats. J Comp Neurol 124, 319-335.

Anthony, R.M., Rutitzky, L.I., Urban, J.F., Jr., Stadecker, M.J., Gause, W.C., 2007. Protective immune mechanisms in helminth infection. Nat Rev Immunol 7, 975-987.

Apple, D.M., Fonseca, R.S., Kokovay, E., 2017. The role of adult neurogenesis in psychiatric and cognitive disorders. Brain Res 1655, 270-276.

Arteaga-Silva, M., Vargas-Villavicencio, J.A., Vigueras-Villasenor, R.M., Rodriguez-Dorantes, M., Morales-Montor, J., 2009. Taenia crassiceps infection disrupts estrous cycle and reproductive behavior in BALB/c female mice. Acta Trop 109, 141-145.

Bizon, J.L., Lee, H.J., Gallagher, M., 2004. Neurogenesis in a rat model of age-related cognitive decline. Aging Cell 3, 227-234.

Bjornsson, C.S., Apostolopoulou, M., Tian, Y., Temple, S., 2015. It takes a village: constructing the neurogenic niche. Dev Cell 32, 435-446.

Bolton, D.J., Robertson, L.J., 2016. Mental Health Disorders Associated with Foodborne Pathogens. J Food Prot 79, 2005-2017.

Bonaguidi, M.A., Song, J., Ming, G.L., Song, H., 2012. A unifying hypothesis on mammalian neural stem cell properties in the adult hippocampus. Curr Opin Neurobiol 22, 754-761.

Bowen, K.K., Dempsey, R.J., Vemuganti, R., 2011. Adult interleukin-6 knockout mice show compromised neurogenesis. Neuroreport 22, 126-130.

Cameron, H.A., Glover, L.R., 2015. Adult neurogenesis: beyond learning and memory. Annu Rev Psychol 66, 53-81.

Cantallops, I., Haas, K., Cline, H.T., 2000. Postsynaptic CPG15 promotes synaptic maturation and presynaptic axon arbor elaboration in vivo. Nat Neurosci 3, 1004-1011.

Capuron, L., Pagnoni, G., Demetrashvili, M.F., Lawson, D.H., Fornwalt, F.B., Woolwine, B., Berns, G.S., Nemeroff, C.B., Miller, A.H., 2007. Basal ganglia hypermetabolism and symptoms of fatigue during interferon-alpha therapy. Neuropsychopharmacology 32, 2384-2392.

Carpentier, G.H., Emilie, 2010. Protein Array Analyzer for ImageJ. In: Tudor, H. (Ed.), ImageJ User and Developer Conference, Centre de Recherche Public, pp. 238-240.

Cavaillon, J.M., 2001. Pro- versus anti-inflammatory cytokines: myth or reality. Cellular and molecular biology (Noisy-le-Grand, France) 47, 695-702.

Chapouly, C., Tadesse Argaw, A., Horng, S., Castro, K., Zhang, J., Asp, L., Loo, H., Laitman, B.M., Mariani, J.N., Straus Farber, R., Zaslavsky, E., Nudelman, G., Raine, C.S., John, G.R., 2015. Astrocytic TYMP and VEGFA drive blood-brain barrier opening in inflammatory central nervous system lesions. Brain 138, 1548-1567.

Chen, W.W., Zhang, X., Huang, W.J., 2016. Role of neuroinflammation in neurodegenerative diseases (Review). Mol Med Rep 13, 3391-3396.

Cheong, C.U., Chang, C.P., Chao, C.M., Cheng, B.C., Yang, C.Z., Chio, C.C., 2013. Etanercept attenuates traumatic brain injury in rats by reducing brain TNF- alpha contents and by stimulating newly formed neurogenesis. Mediators Inflamm 2013, 620837.

Chesnokova, V., Pechnick, R.N., Wawrowsky, K., 2016. Chronic peripheral inflammation, hippocampal neurogenesis, and behavior. Brain Behav Immun 58, 1-8.

Connolly, N.M., Prehn, J.H., 2015. The metabolic response to excitotoxicity - lessons from single-cell imaging. J Bioenerg Biomembr 47, 75-88.

Coral-Almeida, M., Gabriel, S., Abatih, E.N., Praet, N., Benitez, W., Dorny, P., 2015. Taenia solium Human Cysticercosis: A Systematic Review of Sero-epidemiological Data from Endemic Zones around the World. PLoS neglected tropical diseases 9, e0003919.

Crowther, A.J., Song, J., 2014. Activity-dependent signaling mechanisms regulating adult hippocampal neural stem cells and their progeny. Neurosci Bull 30, 542-556.

Cunningham, C., 2013. Microglia and neurodegeneration: the role of systemic inflammation. Glia 61, 71-90.

Dantzer, R., O'Connor, J.C., Freund, G.G., Johnson, R.W., Kelley, K.W., 2008. From inflammation to sickness and depression: when the immune system subjugates the brain. Nat Rev Neurosci 9, 46-56.

Daulatzai, M.A., 2014. Chronic functional bowel syndrome enhances gut-brain axis dysfunction, neuroinflammation, cognitive impairment, and vulnerability to dementia. Neurochem Res 39, 624-644.

de Waal Malefyt, R., Abrams, J., Bennett, B., Figdor, C.G., de Vries, J.E., 1991. Interleukin 10(IL-10) inhibits cytokine synthesis by human monocytes: an autoregulatory role of IL-10 produced by monocytes. J Exp Med 174, 1209-1220.

Dellarole, A., Morton, P., Brambilla, R., Walters, W., Summers, S., Bernardes, D., Grilli, M., Bethea, J.R., 2014. Neuropathic pain-induced depressive-like behavior and hippocampal neurogenesis and plasticity are dependent on TNFR1 signaling. Brain Behav Immun 41, 65-81.

Deslauriers, J., Powell, S., Risbrough, V.B., 2017. Immune signaling mechanisms of PTSD risk and symptom development: insights from animal models. Curr Opin Behav Sci 14, 123-132.

Drummond, E.S., Muhling, J., Martins, R.N., Wijaya, L.K., Ehlert, E.M., Harvey, A.R., 2013. Pathology associated with AAV mediated expression of beta amyloid or C100 in adult mouse hippocampus and cerebellum. PLoS One 8, e59166.

Ekdahl, C.T., Kokaia, Z., Lindvall, O., 2009. Brain inflammation and adult neurogenesis: the dual role of microglia. Neuroscience 158, 1021-1029.

Encinas, J.M., Michurina, T.V., Peunova, N., Park, J.H., Tordo, J., Peterson, D.A., Fishell, G., Koulakov, A., Enikolopov, G., 2011. Division-coupled astrocytic differentiation and age-related depletion of neural stem cells in the adult hippocampus. Cell Stem Cell 8, 566-579.

Ernst, A., Alkass, K., Bernard, S., Salehpour, M., Perl, S., Tisdale, J., Possnert, G., Druid, H., Frisen, J., 2014. Neurogenesis in the striatum of the adult human brain. Cell 156, 1072-1083.

Erta, M., Quintana, A., Hidalgo, J., 2012. Interleukin-6, a major cytokine in the central nervous system. Int J Biol Sci 8, 1254-1266.

Evrensel, A., Ceylan, M.E., 2015. The Gut-Brain Axis: The Missing Link in Depression. Clin Psychopharmacol Neurosci 13, 239-244.

Ezeamama, A.E., McGarvey, S.T., Hogan, J., Lapane, K.L., Bellinger, D.C., Acosta, L.P., Leenstra, T., Olveda, R.M., Kurtis, J.D., Friedman, J.F., 2012. Treatment for Schistosoma japonicum, reduction of intestinal parasite load, and cognitive test score improvements in school-aged children. PLoS neglected tropical diseases 6, e1634.

Flavell, S.W., Greenberg, M.E., 2008. Signaling mechanisms linking neuronal activity to gene expression and plasticity of the nervous system. Annu Rev Neurosci 31, 563-590.

Galic, M.A., Riazi, K., Pittman, Q.J., 2012. Cytokines and brain excitability. Front Neuroendocrinol 33, 116-125.

Garcia, H.H., Gonzalez, A.E., Evans, C.A., Gilman, R.H., Cysticercosis Working Group in, P., 2003. Taenia solium cysticercosis. Lancet 362, 547-556.

Garcia, J.M., Stillings, S.A., Leclerc, J.L., Phillips, H., Edwards, N.J., Robicsek, S.A., Hoh, B.L., Blackburn, S., Dore, S., 2017. Role of Interleukin-10 in Acute Brain Injuries. Front Neurol 8, 244.

Gause, W.C., Urban, J.F., Jr., Stadecker, M.J., 2003. The immune response to parasitic helminths: insights from murine models. Trends Immunol 24, 269-277.

Golde, T.E., Borchelt, D.R., Giasson, B.I., Lewis, J., 2013. Thinking laterally about neurodegenerative proteinopathies. J Clin Invest 123, 1847-1855.

Guenthner, C.J., Miyamichi, K., Yang, H.H., Heller, H.C., Luo, L., 2013. Permanent genetic access to transiently active neurons via TRAP: targeted recombination in active populations. Neuron 78, 773-784.

Guernier, V., Brennan, B., Yakob, L., Milinovich, G., Clements, A.C., Soares Magalhaes, R.J., 2017. Gut microbiota disturbance during helminth infection: can it affect cognition and behaviour of children? BMC infectious diseases 17, 58.

Haarmann, A., Nowak, E., Deiss, A., van der Pol, S., Monoranu, C.M., Kooij, G., Muller, N., van der Valk, P., Stoll, G., de Vries, H.E., Berberich-Siebelt, F., Buttmann, M., 2015. Soluble VCAM-1 impairs human brain endothelial barrier integrity via integrin alpha-4-transduced outside-in signalling. Acta Neuropathol 129, 639-652.

Hajebrahimi, B., Kiamanesh, A., Asgharnejad Farid, A.A., Asadikaram, G., 2016. Type 2 diabetes and mental disorders; a plausible link with inflammation. Cellular and molecular biology (Noisy-le-Grand, France) 62, 71-77.

Hein, A.M., Stasko, M.R., Matousek, S.B., Scott-McKean, J.J., Maier, S.F., Olschowka, J.A., Costa, A.C., O'Banion, M.K., 2010. Sustained hippocampal IL-1beta overexpression impairs contextual and spatial memory in transgenic mice. Brain Behav Immun 24, 243-253.

Hotez, P.J., Brindley, P.J., Bethony, J.M., King, C.H., Pearce, E.J., Jacobson, J., 2008. Helminth infections: the great neglected tropical diseases. J Clin Invest 118, 1311-1321.

Iosif, R.E., Ekdahl, C.T., Ahlenius, H., Pronk, C.J., Bonde, S., Kokaia, Z., Jacobsen, S.E., Lindvall, O., 2006. Tumor necrosis factor receptor 1 is a negative regulator of progenitor proliferation in adult hippocampal neurogenesis. J Neurosci 26, 9703-9712.

Irwin, M.R., 2008. Human psychoneuroimmunology: 20 years of discovery. Brain Behav Immun 22, 129-139.

Ji, R., Meng, L., Li, Q., Lu, Q., 2015. TAM receptor deficiency affects adult hippocampal neurogenesis. Metab Brain Dis 30, 633-644.

Kao, H.T., Li, P., Chao, H.M., Janoschka, S., Pham, K., Feng, J., McEwen, B.S., Greengard, P., Pieribone, V.A., Porton, B., 2008. Early involvement of synapsin III in neural progenitor cell development in the adult hippocampus. J Comp Neurol 507, 1860-1870.

Kawashima, T., Okuno, H., Bito, H., 2014. A new era for functional labeling of neurons: activity-dependent promoters have come of age. Front Neural Circuits 8, 37.

Kempermann, G., Song, H., Gage, F.H., 2015. Neurogenesis in the Adult Hippocampus. Cold Spring Harbor perspectives in biology 7, a018812.

Kempermann, G., Wiskott, L., Gage, F.H., 2004. Functional significance of adult neurogenesis. Curr Opin Neurobiol 14, 186-191.

Keohane, A., Ryan, S., Maloney, E., Sullivan, A.M., Nolan, Y.M., 2010. Tumour necrosis factor-alpha impairs neuronal differentiation but not proliferation of hippocampal neural precursor cells: Role of Hes1. Mol Cell Neurosci 43, 127-135.

Kettenmann, H., Hanisch, U.K., Noda, M., Verkhratsky, A., 2011. Physiology of microglia. Physiol Rev 91, 461-553.

Khakh, B.S., Sofroniew, M.V., 2015. Diversity of astrocyte functions and phenotypes in neural circuits. Nat Neurosci 18, 942-952.

Kohman, R.A., Rhodes, J.S., 2013. Neurogenesis, inflammation and behavior. Brain Behav Immun 27, 22-32.

Kovacs, D., Kovacs, P., Eszlari, N., Gonda, X., Juhasz, G., 2016. Psychological side effects of immune therapies: symptoms and pathomechanism. Curr Opin Pharmacol 29, 97-103.

Kranjac, D., McLinden, K.A., Deodati, L.E., Papini, M.R., Chumley, M.J., Boehm, G.W., 2012. Peripheral bacterial endotoxin administration triggers both memory consolidation and reconsolidation deficits in mice. Brain Behav Immun 26, 109-121.

Lai, K., Kaspar, B.K., Gage, F.H., Schaffer, D.V., 2003. Sonic hedgehog regulates adult neural progenitor proliferation in vitro and in vivo. Nat Neurosci 6, 21-27.

Lal, H., Forster, M.J., 1988. Autoimmunity and age-associated cognitive decline. Neurobiology of aging 9, 733-742.

Lee, J., Duan, W., Mattson, M.P., 2002. Evidence that brain-derived neurotrophic factor is required for basal neurogenesis and mediates, in part, the enhancement of neurogenesis by dietary restriction in the hippocampus of adult mice. J Neurochem 82, 1367-1375.

Lee, Y., Morrison, B.M., Li, Y., Lengacher, S., Farah, M.H., Hoffman, P.N., Liu, Y., Tsingalia, A., Jin, L., Zhang, P.W., Pellerin, L., Magistretti, P.J., Rothstein, J.D., 2012. Oligodendroglia metabolically support axons and contribute to neurodegeneration. Nature 487, 443-448.

Lescano, A.G., Zunt, J., 2013. Other cestodes: sparganosis, coenurosis and Taenia crassiceps cysticercosis. Handb Clin Neurol 114, 335-345.

Liebmann, M., Stahr, A., Guenther, M., Witte, O.W., Frahm, C., 2013. Astrocytic Cx43 and Cx30 differentially modulate adult neurogenesis in mice. Neurosci Lett 545, 40-45.

Lin, M.Z., Schnitzer, M.J., 2016. Genetically encoded indicators of neuronal activity. Nat Neurosci 19, 1142-1153.

Liu, Y.H., Zeng, F., Wang, Y.R., Zhou, H.D., Giunta, B., Tan, J., Wang, Y.J., 2013. Immunity and Alzheimer's disease: immunological perspectives on the development of novel therapies. Drug Discov Today 18, 1212-1220.

Lopez-Griego, L., Nava-Castro, K.E., Lopez-Salazar, V., Hernandez-Cervantes, R., Tiempos Guzman, N., Muniz-Hernandez, S., Hernandez-Bello, R., Besedovsky, H.O., Pavon, L., Becerril Villanueva, L.E., Morales-Montor, J., 2015. Gender-associated differential expression of cytokines in specific areas of the brain during helminth infection. J Interferon Cytokine Res 35, 116-125.

Maizels, R.M., McSorley, H.J., 2016. Regulation of the host immune system by helminth parasites. J Allergy Clin Immunol 138, 666-675.

Marchi, N., Teng, Q., Ghosh, C., Fan, Q., Nguyen, M.T., Desai, N.K., Bawa, H., Rasmussen, P., Masaryk, T.K., Janigro, D., 2010. Blood-brain barrier damage, but not parenchymal white blood cells, is a hallmark of seizure activity. Brain Res 1353, 176-186.

Matsuda, T., Murao, N., Katano, Y., Juliandi, B., Kohyama, J., Akira, S., Kawai, T., Nakashima, K., 2015. TLR9 signalling in microglia attenuates seizure-induced aberrant neurogenesis in the adult hippocampus. Nat Commun 6, 6514.

Meyer, J.H., 2017. Neuroprogression and Immune Activation in Major Depressive Disorder. Mod Trends Pharmacopsychiatry 31, 27-36.

Monje, M.L., Toda, H., Palmer, T.D., 2003. Inflammatory blockade restores adult hippocampal neurogenesis. Science (New York, N.Y.) 302, 1760-1765.

Monnet-Tschudi, F., Defaux, A., Braissant, O., Cagnon, L., Zurich, M.G., 2011. Methods to assess neuroinflammation. Curr Protoc Toxicol Chapter 12, Unit12 19.

Morales-Montor, J., Arrieta, I., Del Castillo, L.I., Rodriguez-Dorantes, M., Cerbon, M.A., Larralde, C., 2004. Remote sensing of intraperitoneal parasitism by the host's brain: regional changes of c-fos gene expression in the brain of feminized cysticercotic male mice. Parasitology 128, 343-351.

Morales-Montor, J., Picazo, O., Besedovsky, H., Hernandez-Bello, R., Lopez-Griego, L., Becerril-Villanueva, E., Moreno, J., Pavon, L., Nava-Castro, K., Camacho-Arroyo, I., 2014. Helminth infection alters mood and short-term memory as well as levels of neurotransmitters and cytokines in the mouse hippocampus. Neuroimmunomodulation 21, 195-205.

Moriyama, M., Fukuhara, T., Britschgi, M., He, Y., Narasimhan, R., Villeda, S., Molina, H., Huber, B.T., Holers, M., Wyss-Coray, T., 2011. Complement receptor 2 is expressed in neural progenitor cells and regulates adult hippocampal neurogenesis. J Neurosci 31, 3981-3989.

Nicaise, C., Mitrecic, D., Demetter, P., De Decker, R., Authelet, M., Boom, A., Pochet, R., 2009. Impaired blood-brain and blood-

spinal cord barriers in mutant SOD1-linked ALS rat. Brain Res 1301, 152-162.

Nokes, C., Grantham-McGregor, S.M., Sawyer, A.W., Cooper, E.S., Robinson, B.A., Bundy, D.A., 1992. Moderate to heavy infections of Trichuris trichiura affect cognitive function in Jamaican school children. Parasitology 104 (Pt 3), 539-547.

Ohgidani, M., Kato, T.A., Sagata, N., Hayakawa, K., Shimokawa, N., Sato-Kasai, M., Kanba, S., 2016. TNF-alpha from hippocampal microglia induces working memory deficits by acute stress in mice. Brain Behav Immun 55, 17-24.

Palmer, T.D., Willhoite, A.R., Gage, F.H., 2000. Vascular niche for adult hippocampal neurogenesis. J Comp Neurol 425, 479-494.

Pastrana, E., 2011. Optogenetics: controlling cell function with light. Nat Meth 8, 24-25.

Pechnick, R.N., Zonis, S., Wawrowsky, K., Cosgayon, R., Farrokhi, C., Lacayo, L., Chesnokova, V., 2011. Antidepressants stimulate hippocampal neurogenesis by inhibiting p21 expression in the subgranular zone of the hipppocampus. PLoS One 6, e27290.

Peon, A.N., Espinoza-Jimenez, A., Terrazas, L.I., 2013. Immunoregulation by Taenia crassiceps and its antigens. Biomed Res Int 2013, 498583.

Power, J.H., Asad, S., Chataway, T.K., Chegini, F., Manavis, J., Temlett, J.A., Jensen, P.H., Blumbergs, P.C., Gai, W.P., 2008. Peroxiredoxin 6 in human brain: molecular forms, cellular distribution and association with Alzheimer's disease pathology. Acta Neuropathol 115, 611-622.

Pozniak, P.D., Darbinyan, A., Khalili, K., 2016. TNF-alpha/TNFR2 Regulatory Axis Stimulates EphB2-Mediated Neuroregeneration Via Activation of NF-kappaB. J Cell Physiol 231, 1237-1248.

Quesseveur, G., David, D.J., Gaillard, M.C., Pla, P., Wu, M.V., Nguyen, H.T., Nicolas, V., Auregan, G., David, I., Dranovsky, A., Hantraye, P., Hen, R., Gardier, A.M., Deglon, N., Guiard, B.P., 2013. BDNF overexpression in mouse hippocampal astrocytes promotes local neurogenesis and elicits anxiolytic-like activities. Transl Psychiatry 3, e253.

Rahimi, F., Murakami, K., Summers, J.L., Chen, C.H., Bitan, G., 2009. RNA aptamers generated against oligomeric Abeta40 recognize common amyloid aptatopes with low specificity but high sensitivity. PLoS One 4, e7694.

Riazi, K., Galic, M.A., Kuzmiski, J.B., Ho, W., Sharkey, K.A., Pittman, Q.J., 2008. Microglial activation and TNFalpha production mediate altered CNS excitability following peripheral inflammation. Proceedings of the National Academy of Sciences of the United States of America 105, 17151-17156.

Rodriguez-Dorantes, M., Cerbon, M.A., Larralde, C., Morales-Montor, J., 2007. Modified progesterone receptor expression in the hypothalamus of cysticercotic male mice. Acta Trop 103, 123-132.

Roland, B.P., Zeccola, A.M., Larsen, S.B., Amrich, C.G., Talsma, A.D., Stuchul, K.A., Heroux, A., Levitan, E.S., VanDemark, A.P., Palladino, M.J., 2016. Structural and Genetic Studies Demonstrate Neurologic Dysfunction in Triosephosphate Isomerase Deficiency Is Associated with Impaired Synaptic Vesicle Dynamics. PLoS Genet 12, e1005941.

Russo, I., Caracciolo, L., Tweedie, D., Choi, S.H., Greig, N.H., Barlati, S., Bosetti, F., 2012. 3,6'-Dithiothalidomide, a new TNF-alpha synthesis inhibitor, attenuates the effect of Abeta1-42 intracerebroventricular injection on hippocampal neurogenesis and memory deficit. J Neurochem 122, 1181-1192.

Saarelainen, T., Hendolin, P., Lucas, G., Koponen, E., Sairanen, M., MacDonald, E., Agerman, K., Haapasalo, A., Nawa, H., Aloyz, R., Ernfors, P., Castren, E., 2003. Activation of the TrkB neurotrophin receptor is induced by antidepressant drugs and is required for antidepressant-induced behavioral effects. J Neurosci 23, 349-357.

Sairanen, M., Lucas, G., Ernfors, P., Castren, M., Castren, E., 2005. Brain-derived neurotrophic factor and antidepressant drugs have different but coordinated effects on neuronal turnover, proliferation, and survival in the adult dentate gyrus. J Neurosci 25, 1089-1094.

Saper, C.B., Romanovsky, A.A., Scammell, T.E., 2012. Neural circuitry engaged by prostaglandins during the sickness syndrome. Nat Neurosci 15, 1088-1095.

Sato, K., 2015. Effects of Microglia on Neurogenesis. Glia 63, 1394-1405.

Schafers, M., Sorkin, L., 2008. Effect of cytokines on neuronal excitability. Neurosci Lett 437, 188-193.

Schmidt-Hieber, C., Jonas, P., Bischofberger, J., 2004. Enhanced synaptic plasticity in newly generated granule cells of the adult hippocampus. Nature 429, 184-187.

Seguin, J.A., Brennan, J., Mangano, E., Hayley, S., 2009. Proinflammatory cytokines differentially influence adult hippocampal cell proliferation depending upon the route and chronicity of administration. Neuropsychiatr Dis Treat 5, 5-14.

Seitz, R.J., Heininger, K., Schwendemann, G., Toyka, K.V., Wechsler, W., 1985. The mouse blood-brain barrier and blood-nerve barrier for IgG: a tracer study by use of the avidin-biotin system. Acta Neuropathol 68, 15-21.

Semmler, A., Okulla, T., Sastre, M., Dumitrescu-Ozimek, L., Heneka, M.T., 2005. Systemic inflammation induces apoptosis with variable vulnerability of different brain regions. J Chem Neuroanat 30, 144-157.

Serrano Ocana, G., Ortiz Sablon, J.C., Ochoa Tamayo, I., Almaguer Arena, L., Serrano Ocana, L.M., Govender, S., 2009. Neurocysticercosis in patients presenting with epilepsy at St Elizabeth's Hospital, Lusikisiki. South African medical journal = Suid-Afrikaanse tydskrif vir geneeskunde 99, 588-591.

Sierra, A., Encinas, J.M., Deudero, J.J., Chancey, J.H., Enikolopov, G., Overstreet-Wadiche, L.S., Tsirka, S.E., Maletic-Savatic, M., 2010. Microglia shape adult hippocampal neurogenesis through apoptosis-coupled phagocytosis. Cell Stem Cell 7, 483-495.

Silverberg, J.I., 2017. Selected comorbidities of atopic dermatitis: Atopy, neuropsychiatric, and musculoskeletal associations. Clinics in Dermatology.

Soba, B., Beovic, B., Luznik, Z., Skvarc, M., Logar, J., 2014. Evidence of human neurocysticercosis in Slovenia. Parasitology 141, 547-553.

Sommer, A., Winner, B., Prots, I., 2017. The Trojan horse - neuroinflammatory impact of T cells in neurodegenerative diseases. Mol Neurodegener 12, 78.

Song, H., Stevens, C.F., Gage, F.H., 2002. Astroglia induce neurogenesis from adult neural stem cells. Nature 417, 39-44.

Stone, E.A., Lehmann, M.L., Lin, Y., Quartermain, D., 2006. Depressive behavior in mice due to immune stimulation is accompanied by reduced neural activity in brain regions involved in positively motivated behavior. Biol Psychiatry 60, 803-811.

Su, P., Zhang, J., Zhao, F., Aschner, M., Chen, J., Luo, W., 2014. The interaction between microglia and neural stem/precursor cells. Brain Res Bull 109, 32-38.

Sultan, S., Li, L., Moss, J., Petrelli, F., Casse, F., Gebara, E., Lopatar, J., Pfrieger, F.W., Bezzi, P., Bischofberger, J., Toni, N., 2015. Synaptic Integration of Adult-Born Hippocampal Neurons Is Locally Controlled by Astrocytes. Neuron 88, 957-972.

Tao, C., Zhang, G., Xiong, Y., Zhou, Y., 2015. Functional dissection of synaptic circuits: in vivo patch-clamp recording in neuroscience. Front Neural Circuits 9, 23.

Tarr, A.J., Chen, Q., Wang, Y., Sheridan, J.F., Quan, N., 2012. Neural and behavioral responses to low-grade inflammation. Behav Brain Res 235, 334-341.

Toth, C., 2014. Diabetes and neurodegeneration in the brain. Handb Clin Neurol 126, 489-511.

Tozuka, Y., Fukuda, S., Namba, T., Seki, T., Hisatsune, T., 2005. GABAergic excitation promotes neuronal differentiation in adult hippocampal progenitor cells. Neuron 47, 803-815.

Vallieres, L., Campbell, I.L., Gage, F.H., Sawchenko, P.E., 2002. Reduced hippocampal neurogenesis in adult transgenic mice with chronic astrocytic production of interleukin-6. J Neurosci 22, 486-492.

Vezzani, A., Viviani, B., 2015. Neuromodulatory properties of inflammatory cytokines and their impact on neuronal excitability. Neuropharmacology 96, 70-82.

Villeda, S.A., Luo, J., Mosher, K.I., Zou, B., Britschgi, M., Bieri, G., Stan, T.M., Fainberg, N., Ding, Z., Eggel, A., Lucin, K.M., Czirr, E., Park, J.S., Couillard-Despres, S., Aigner, L., Li, G., Peskind, E.R., Kaye, J.A.,

Quinn, J.F., Galasko, D.R., Xie, X.S., Rando, T.A., Wyss-Coray, T., 2011. The ageing systemic milieu negatively regulates neurogenesis and cognitive function. Nature 477, 90-94.

Wall, A.M., Mukandala, G., Greig, N.H., O'Connor, J.J., 2015. Tumor necrosis factor-alpha potentiates long-term potentiation in the rat dentate gyrus after acute hypoxia. J Neurosci Res 93, 815-829.

Watkins, W.E., Pollitt, E., 1997. "Stupidity or worms": do intestinal worms impair mental performance? Psychol Bull 121, 171-191.

Wilhelm, I., Nyul-Toth, A., Suciu, M., Hermenean, A., Krizbai, I.A., 2016. Heterogeneity of the blood-brain barrier. Tissue Barriers 4, e1143544.

Winland, C.D., Welsh, N., Sepulveda-Rodriguez, A., Vicini, S., Maguire-Zeiss, K.A., 2017. Inflammation alters AMPA-stimulated calcium responses in dorsal striatal D2 but not D1 spiny projection neurons. Eur J Neurosci.

Wlodkowic, D., Telford, W., Skommer, J., Darzynkiewicz, Z., 2011. Apoptosis and beyond: cytometry in studies of programmed cell death. Methods Cell Biol 103, 55-98.

Wolf, S.A., Boddeke, H.W., Kettenmann, H., 2017. Microglia in Physiology and Disease. Annu Rev Physiol 79, 619-643.

Xie, Z., Morgan, T.E., Rozovsky, I., Finch, C.E., 2003. Aging and glial responses to lipopolysaccharide in vitro: greater induction of IL-1 and IL-6, but smaller induction of neurotoxicity. Exp Neurol 182, 135-141.

Yirmiya, R., Goshen, I., 2011. Immune modulation of learning, memory, neural plasticity and neurogenesis. Brain Behav Immun 25, 181-213.

Zepeda, N., Solano, S., Copitin, N., Chavez, J.L., Fernandez, A.M., Garcia, F., Tato, P., Molinari, J.L., 2017. Apoptosis of mouse hippocampal cells induced by Taenia crassiceps metacestode factor. J Helminthol 91, 215-221.

Zhao, C., Deng, W., Gage, F.H., 2008. Mechanisms and functional implications of adult neurogenesis. Cell 132, 645-660.

Ziv, Y., Ron, N., Butovsky, O., Landa, G., Sudai, E., Greenberg, N., Cohen, H., Kipnis, J., Schwartz, M., 2006. Immune cells contribute to the maintenance of neurogenesis and spatial learning abilities in adulthood. Nat Neurosci 9, 268-275.

Zonis, S., Ljubimov, V.A., Mahgerefteh, M., Pechnick, R.N., Wawrowsky, K., Chesnokova, V., 2013. p21Cip restrains hippocampal neurogenesis and protects neuronal progenitors from apoptosis during acute systemic inflammation. Hippocampus 23, 1383-1394.

Zonis, S., Pechnick, R.N., Ljubimov, V.A., Mahgerefteh, M., Wawrowsky, K., Michelsen, K.S., Chesnokova, V., 2015. Chronic intestinal inflammation alters hippocampal neurogenesis. J Neuroinflammation 12, 65.

8 APPENDICES:

8.1 Appendix 1: Original proposal

Neuroinflammation and Neurogenesis in Helminth-Infected mice

Supervisor: Dr. Vinogran Naidoo; **Co-supervisor**: Dr. Joe. Raimondo
Neuroscience, Department of Human Biology
vinogran.naidoo@uct.ac.za

Background:

In developing countries, humans are susceptible to chronic infection by parasitic flatworms or tapeworms (Phylum: Platyhelminthes). The most important morbidities associated with helminth infection are under-nutrition, anaemia, slow physical growth and poor cognitive performance. Furthermore, the most common cause of epilepsy in the developing world is Neurocysticercosis, an infection of the central nervous system by parasitic tapeworm larvae following the oral ingestion of worm-eggs. Alterations to the gut-brain axis have been implicated in stress-related disorders such as depression and anxiety, in neurodevelopmental disorders such as autism, and in cognitive functioning, and there is also, albeit controversial, evidence that helminth infection is associated with cognitive impairment. Interestingly, in the gut, the ability of helminths to inhibit colonic inflammation suggests that they may have therapeutic potential for the treatment of immunologically-driven intestinal inflammation. In fact, the neural environment within the gut wall is strikingly similar to that of the brain, composed of neurons and glial cells. Neurogenesis, the birth of new neurones, in the hippocampus is thought to play an important role in learning and memory.

Objectives:

In the brain, one major factor of neuroinflammation is the activation of microglial cells but little is known about their role in the healthy brain and their reaction following a prolonged host-infection period with the parasitic tapeworm Taenia crassiceps. The overall goal of this project is to study, in mice infected with eggs from *T. crassiceps*, the relationship between neuroinflammation and neurogenesis in the brain and in the enteric (gut) nervous system.

Research plan:

We will characterize changes in the protein levels of cytokines and chemokines using a quantitative cytokine array, use immunohistochemistry and Western blotting to localize the expression of inflammation and neuronal markers as well as other markers of cellular injury, perform histological analyses of hematoxylin/eosin stained intestinal and brain sections, and conduct inflammation-activity assays.

8.2 Appendix : Further research

8.2.1 Helminthic and *T crassiceps* immune phenotypes

Anthony et al. (2007) and Gause et al. (2003) provide useful overviews of the host immune phenotype in response to helminth infection, commonly described as a type 2 response or T_H2-type response, characterised by its own set of cytokines and T cell lineage. Although both reviews recognise the heterogeneity of immune responses across organisms and the variable role of a T_H1 response, particularly in the initial phases of infection in many parasites, there does appear to be a common response characterised by activation of T_H2 cells, IgE secreting plasma cells, eosinophilia, mast cells and basophils (Anthony et al., 2007). Cytokines driving this response include IL-4, IL-5, IL-9, IL-13, IL-21, IL-17 (Anthony et al., 2007). The mechanisms by which this response is protective to the host have been less clearly elucidated, but resultant increased smooth-muscle gut contractility and luminal fluid flow appear to assist in helminth expulsion from the GIT. *Figure 15* shows a schematic of the roles of various cytokines and effector cells in the T_H2 response.

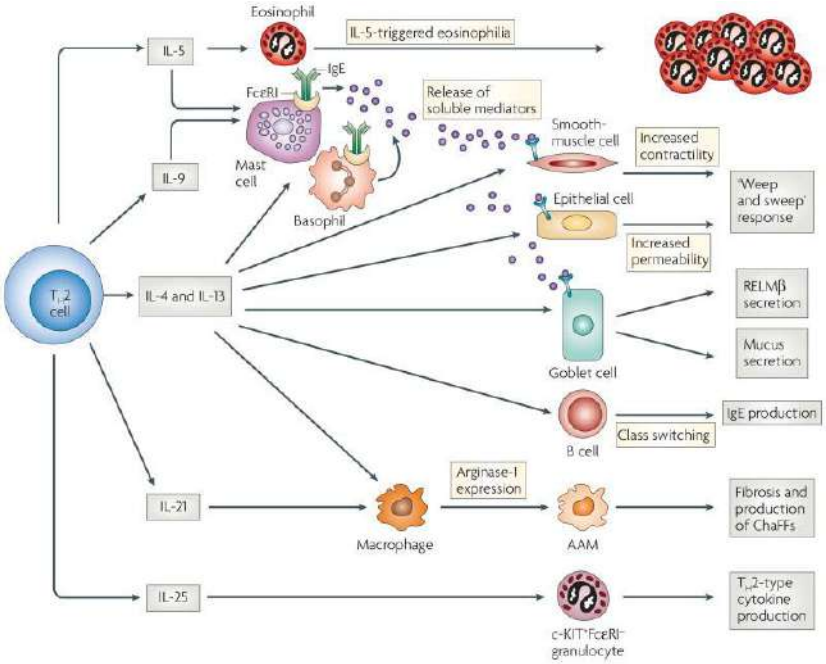

Figure 15 ***theoretic outline of a generic Th2 response****. Taken from Anthony et al. (2007).*

While there is naturally far less literature characterising the *T. crassiceps* immune phenotype, a thorough investigation by a group in Mexico have shown that *T. crassiceps* follow the classical pattern, inducing a transient Th1 proinflammatory response for two to three weeks followed by a strong, long-lasting Th2 response (Peon et al., 2013). The acute phase has typical high levels of IFNγ and NO which was protective against establishment of the infection. The Th2 response characterised by alternatively activated macrophages and myeloid-derived suppressor cells with low levels of lymphocytes, and LPS-

tolerant profile, as well as high levels of IL-4, IL-5, IL10, IL-13 and IgE antibodies, with low levels of NO, TNF-α, IL-1β, IL-12, IL-15, IL-18 and IL-23 systemically, but blocking this Th2 response had little effect on parasite loads, suggesting that it has little protective effect (Peon et al., 2013).

Finally, as mentioned previously, Morales-Montor et al. (2014) found that in the chronic phase of the infection, hippocampal levels of IL-6, IFN-γ and TNF-α mRNA were increased in both sexes and IL-4 expression was increased in females and decreased in males.

8.2.2 Apoptosis pathways

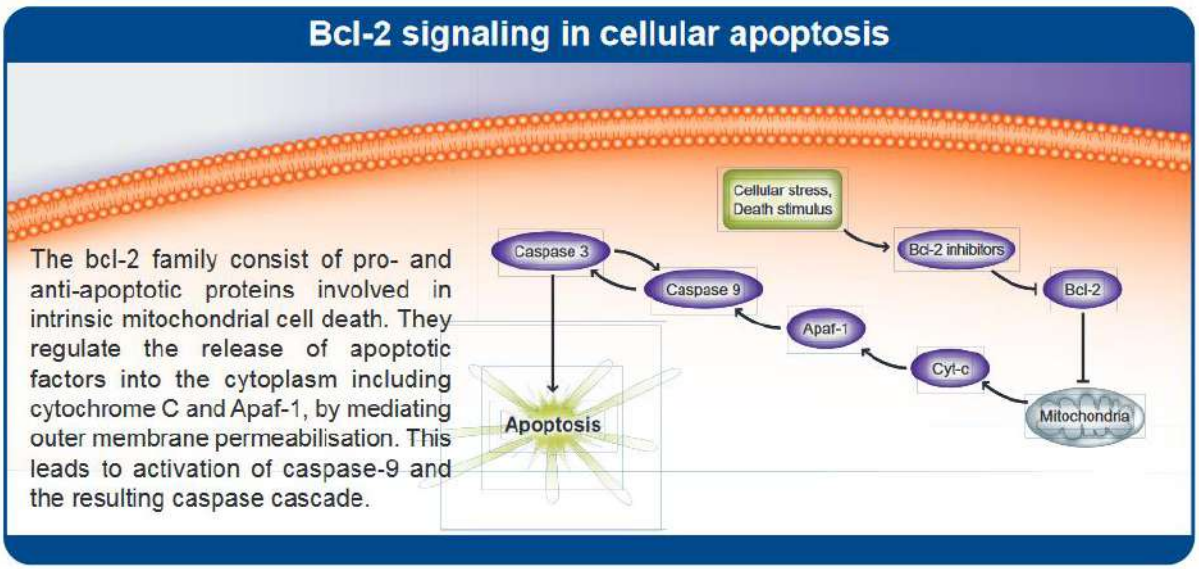

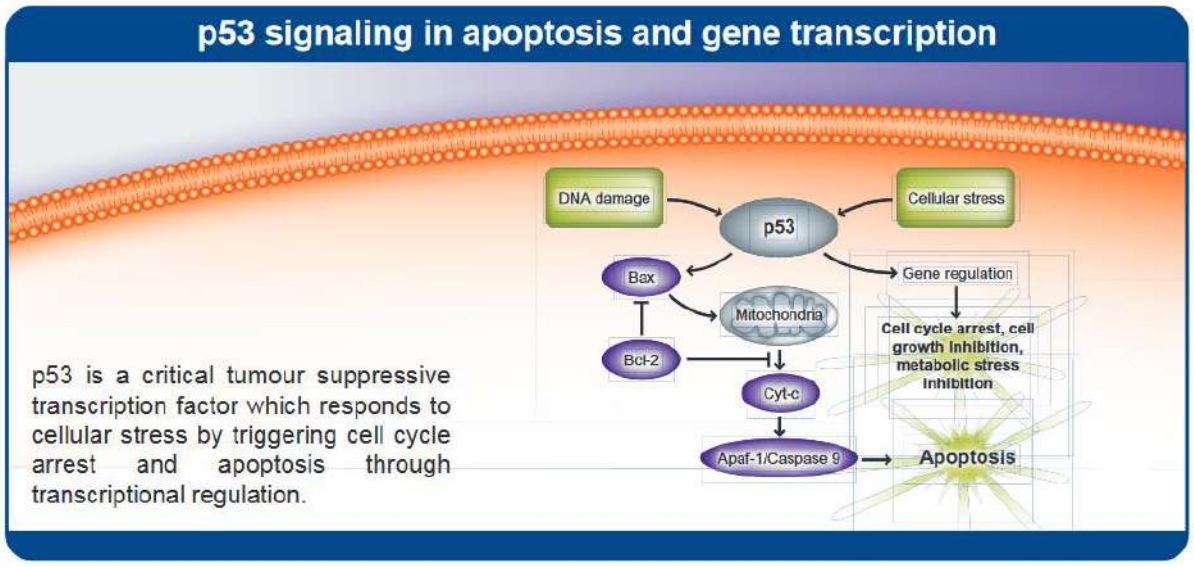

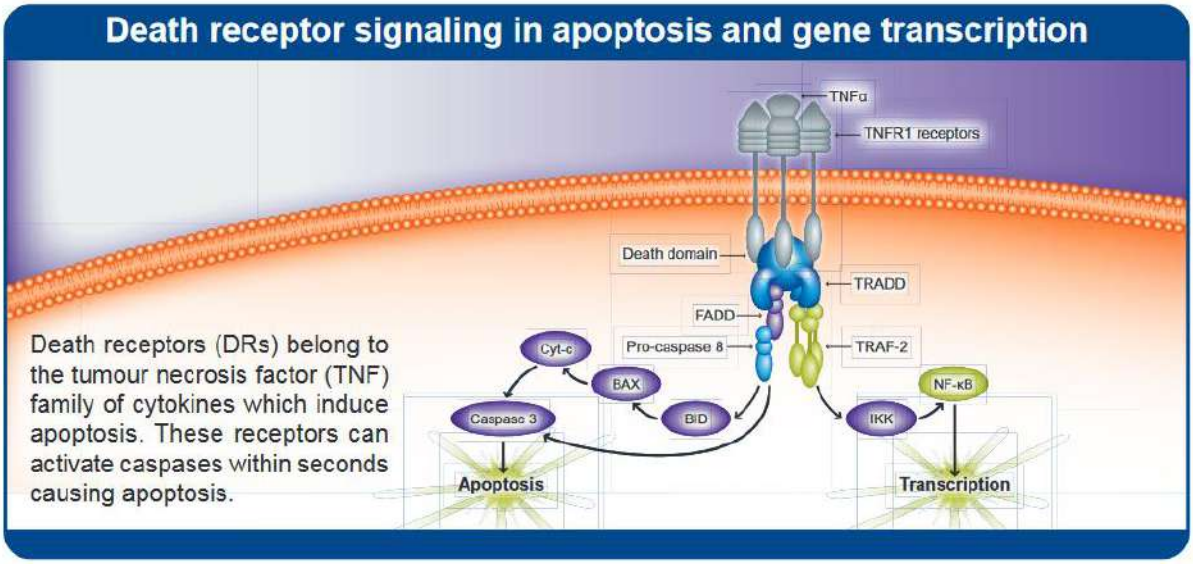

Figure 16: ***Apoptosis signalling pathways****, from abcam Biochemicals (2012) at http://docs.abcam.com/pdf/biochemicals/Apoptosis-Cancer-signaling-pathways.pdf*

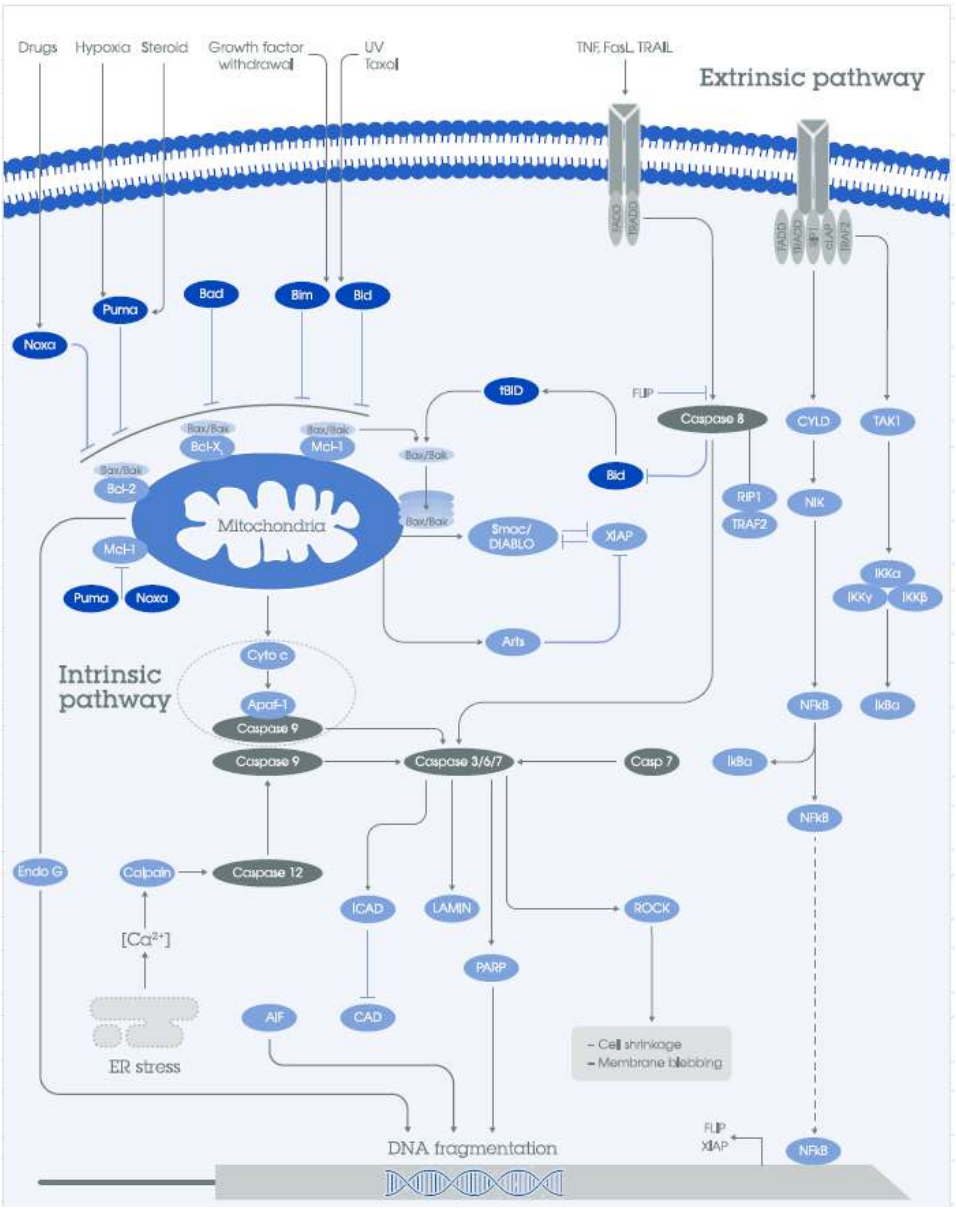

Figure 17: ***Apoptosis pathways****, from abcam's "Tools for cell death series 1" available at http://docs.abcam.com/pdf/kits/apoptosis-analysis-guide.pdf*

8.2.3 Neurogenesis

8.2.3.1 Mechanisms and stages of neurogenesis in the dentate gyrus

An understanding of the process of neurogenesis is vital if one is to attempt to study how external signals, such as cytokines, impact neurogenesis. Following on from the observations of Altman and Das (1965), studies have focused on the subgranular zone (SGZ) of the hippocampal dentate gyrus and the subventricular zone (SVZ) lining the lateral walls of the lateral ventricles in rodent models as areas housing neural progenitor cells (NPCs). In the SGZ, maturing cells migrate to the granular layer of the dentate gyrus, while in the SVZ, they have been observed to migrate a significant distance to the olfactory bulb (Zhao et al., 2008). Lately, however, studies in humans have called the SVZ-olfactory bulb migration dogma into question, showing instead migration to the striatum (Ernst et al., 2014). While new studies have implicated striatal neurogenesis in pathology, this line of research is still in its infancy (Apple et al., 2017). Furthermore, the signalling pathways and maturation patterns between the SGZ and SVZ vary considerably (Zhao et al., 2008). For these reasons, and for the sake of space constraints, this review focuses on neurogenesis as it relates to the hippocampus.

The neurogenic niche, the CNS equivalent of any stem cell niche, refers to the microenvironment surrounding differentiating and proliferating NPCs, which acts to provide stimulatory or inhibitory signals to the stem cells and their progeny (Bjornsson et al., 2015). Besides the differentiating and quiescent NPCs, the niche contains glial cells, adult neurones and synapses from distal neurones and extracellular matrix (ECM). Significantly, it also includes vascular clusters, which has led to some considering these areas to be “vascular niches” (Palmer et al., 2000). As Zhao et al. (2008) point out, any diffusible molecule produced by neighbouring cells, which has crossed the blood-brain barrier or is present in the ECM has the potential to impact neurogenesis. These molecules include neurotransmitters, growth factors, nutrients, and, particularly relevant to this review, cytokines.

However, one of the most significant proliferation signals is synaptic input – with neurogenesis being classified as an “activity-dependant process” (Crowther and Song, 2014; Kempermann et al., 2015). This means that neurogenesis is tightly regulated by overall brain functioning and is thus sensitive to external experiences. Although input predominantly comes from the entorhinal cortex, signals also come from other sources such as the septal nuclei the ventral tegmental area, using a diverse range of neurotransmitters (well laid-out in a supplementary table by Zhao et al. (2008)). To complicate matters further, neurotransmitters - particularly GABA – have different affects depending on the stage of stem cell differentiation.

A well-described set of differentiation phases has been generally accepted (Apple et al., 2017; Encinas et al., 2011; Kempermann et al., 2015; Zhao et al., 2008), roughly divided according to marker expression and morphology (). The phases comprise of a precursor phase which has proliferative capacity and sub-phases, a survival phase which no longer has proliferative capacity, a maturation phase and a late maturation phase.

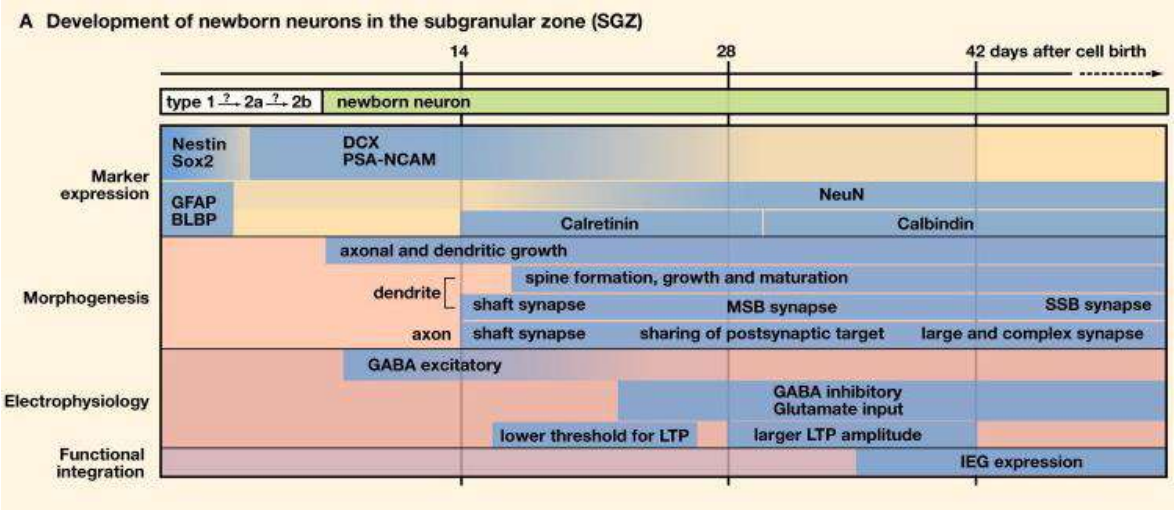

Figure 18 ***characteristics of developing neurones****, taken directly from (Zhao et al., 2008). MSB, multiple-synapse boutons; SSB, single-synapse boutons; LTP, long-term potentiation; IEG, immediate early gene*

The precursor phase is classically subdivided into type 1, type 2a and type 2b. Type 1, or radial glia-like cells, can divide symmetrically to self-renew or asymmetrically into astrocyte or neural progenitors. Their potential to self-renew has been shown to decrease in with electrical inactivity (Bonaguidi et al., 2012), reducing the stem cell pool. Type 2 cells carry the main proliferative burden. Type 2a cells continue to express glial markers, although they lack glial morphology, while Type 2b cells express neurone-specific transcription factors (Kempermann et al., 2015). A type 3 cell is also described by Kempermann et al. (2015) in the precursor phase with minimal proliferative capacity although other reviewers have not recognised this subtype.

After cell-cycle exit, the developing granule cell neurone enters the survival phase. Dendrites and axons begin developing, but the majority of cells are eliminated before target contact can be made. GABA receptors initially cause excitatory stimuli, but switch to inhibitory post-synaptic potentials when glutamate (Glu) receptors are expressed (Tozuka et al., 2005). During the brief maturation phase axons extend into the Ca3 region of the hippocampus, and during the late maturation phase the new neurones are electrophysiologically indistinguishable from mature neurones. A few markers (e.g. calretinin), however, remain different, and the neurones show increased plasticity that may have interesting functional implications (Schmidt-Hieber et al., 2004).

8.2.3.2 Regulation of neurogenesis

Although regulation of these stages is far less well-characterised, Kempermann et al. (2015) summarise some key findings. Several regulatory factors impact specific phases of the maturation process, whether proliferation, survival, differentiation, migration or integration, and it becomes critical to be able to differentiate at which stage progenitor cells are being impacted (Kempermann et al., 2004). Initial stimulation of NPCs to proliferate arises from GABAergic input from basket interneurones which means that relatively non-specific stimuli, such as seizures and physical activity, can stimulate proliferation. Survival, on the other hand, has been shown to be a critical and complex selection point, responding selectively to neurotransmitters, trophic factors such as BDNF, EGF and FGF2, p63, Hspb8 and activation of NFκB (Lee et al., 2002; Saarelainen et al., 2003; Sairanen et al., 2005).

Signalling mechanisms that induce astrocytic rather than neuronal differentiation also lack research, and astrogenesis is often ignored in reviews, although Encinas et al. (2011) provide a detailed model for identification of the stages of astrocytic versus neuronal differentiation (Figure 19). That said, preferential differentiation into astrocytes has been observed in several inflammatory models (Keohane et al., 2010; Zonis et al., 2015).

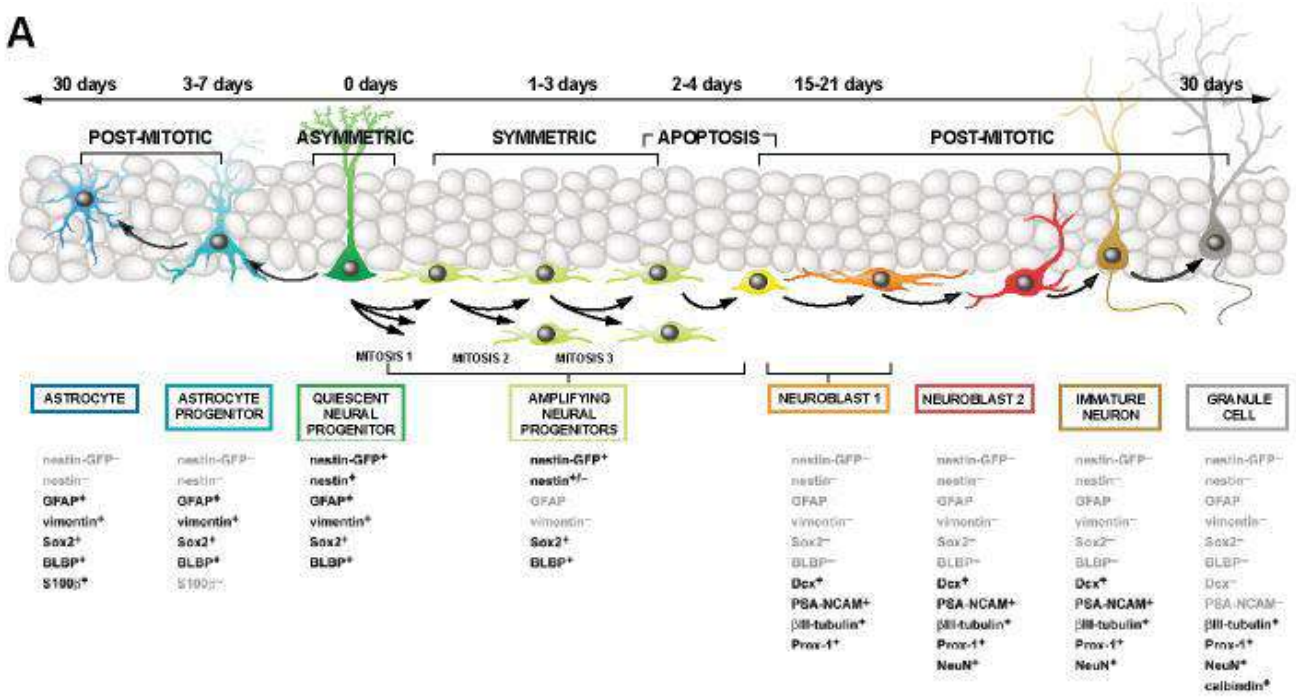

Figure 19: ***marker expression in across stages of NPC differentiation*** *into astrocytes and granule cells, taken directly from Encinas et al. (2011).*

8.2.3.3 Glia in neurogenesis and neuroinflammation

Vital to neurogenesis, glial cells sit at the heart of humoral signalling in the brain. Microglia, cells of monocyte origin, not only play a vital immunological role in infection, but also regulate basal neurological processes in the absence of immune activation (Kohman and Rhodes, 2013). Astrocytes, classically and exceptionally vaguely dubbed "support cells of the CNS", exist in a diverse range of phenotypes, suggesting an equally diverse range of function (Khakh and Sofroniew, 2015). The role of hippocampal oligodendrocytes in neurogenesis has been more or less ignored, despite interest in these cells in neurodegeneration and target finding in axonal repair (Lee et al., 2012), which may be translatable to axon growth in neurogenesis. Although interactions between these three types of glial cells are likely of vital importance, such signalling is beyond the scope of this review, and an overview of microglia and astrocytes will be examined individually. It is also important to note that interactions may not be unidirectional and that NPCs may have the capacity to signal to glia (Su et al., 2014).

Microglia have been broadly classified into two phenotypes when activated, the supposedly neurodegenerative M1 and neuroprotective M2 phenotypes (Kohman and Rhodes, 2013), although Sato (2015) warns against arbitrary subtyping. Even resting microglia have been shown to have an important role in the survival phase of neurogenesis by phagocytosing apoptotic cells (Sierra et al., 2010). Kettenmann et al. (2011) thus challenges the label "resting", noting that they also participate in active environmental surveillance.

At the core of the CNS's immune response, microglia have the potential to act as a kind of immune transmitter. Far more sensitive to peripheral cytokine signalling than other neural cells, microglia are able to sense and relay or amplify signals through cytokine production to neighbouring astrocytes and neurones (Kettenmann et al., 2011). When microglia are challenged, their processes retract, creating an amoeboid "reactive" phenotype.

As Wolf et al. (2017) note, the primary evidence for activated microglial involvement in neurogenesis is the observed inverse relationship between activated microglia and newborn neurones (Seguin et al., 2009; Xie et al., 2003; Ziv et al., 2006; Zonis et al., 2015) and similar behavioural outcomes (Ohgidani et al., 2016). However, data are conflicting, which may in part be due to the somewhat arbitrary classification of subtypes, or, conversely, by looking at microglia as a single entity (e.g. by quantifying total microglial populations).

That said, prominent cytokines known to "activate" microglia include TNFα, IL1β and IL-6 (Bowen et al., 2011; Seguin et al., 2009; Zonis et al., 2015), although distinction between factors that act on microglia versus astrocytes versus directly on NPCs, and activation of endogenous NPC pathways such as the NFκB, sonic hedgehog or p53/p21 systems (Lai et al., 2003; Pechnick et al., 2011; Zonis et al., 2013) is often difficult.

In their review on the interaction between microglia and NPCs, Su et al. (2014) provide a useful summary of regulatory factors of this interaction, including CD200 and its receptor, TGF-β, TNF-α, VEGF, CX3CL1, reactive oxygen species, KATP-channel, IGF-1 and TLR-9, however, even when looking at molecule-specific interactions, there is ambiguity due to activation of different receptors – as seen with TNF-α (Chesnokova et al., 2016; Dellarole et al., 2014; Pozniak et al., 2016).

Although astrocytes are often assessed and quantified in neurogenesis studies as part of determining differentiation outcome (Encinas et al., 2011; Keohane et al., 2010; Zonis et al., 2015), their role in altering neurogenesis has been less well characterised – although Song et al. (2002) demonstrated their vital role in inducing neurogenesis over a decade ago. From non-neurogenic studies, it is clear that they too are sensitive to inflammation, and are able to gain a so-called "reactive" phenotype. Again, this classification covers a broad range of responses, including hypertrophic reactive astrocytes and scar-forming reactive astrocytes (Khakh and Sofroniew, 2015).

The particular phenotype of astrocytes present in neurogenic niches is not well described, but emerging studies have shown a role for certain astrocytic factors such as BDNF (Quesseveur et al., 2013), connexin proteins (Liebmann et al., 2013) and ephrin signalling, as well as a role in controlling local synaptic integration (Sultan et al., 2015) in non-inflammatory models.

8.2.3.4 Studying neuroinflammation

Besides glia and cytokines, other effectors of the immune system – such as lymphocytes and immunoglobulins – are typically excluded from the brain by the blood-brain-barrier (Wilhelm et al., 2016). Although pathology is known to permeabilise this barrier, the extent to which there is penetration to and an impact on neurogenic niches has not been explored to the knowledge of the author. That said, complement has emerged as a potential modulator of neurogenesis in homeostasis and pathology, with NPCs expressing complement receptors (Moriyama et al., 2011).

When studying immune activation, a classical model involves lipopolysaccharide stimulation, a model of bacterial infection (Ekdahl et al., 2009; Monje et al., 2003; Xie et al., 2003; Zonis et al., 2013).It must be kept in mind that immune responses are multivariate and complex, particularly in chronic, autoimmune, or non-bacterial insults (i.e. viral, fungal, parasitic or neoplastic). There should also be a distinction between centrally versus peripherally administered immune-activating substrates, as systemic administration may result in confounding activation of other hormonal system. In order to study neurogenesis and neuroinflammatory interactions, specificity is far more beneficial – using transcription controlled genetic mutations or targeted administration of specific factors. That said, if the disease model is what is in question, broader models are pivotal, but then changes in neurogenesis can only form part of an hypothesis for observed changes.

8.2.3.5 *Variables in neurogenesis, neuroinflammation and behaviour*

Factor		Model	Effect (including measured outcome (see table 2)			Reference
Classification	**Variable**		**Neurogenesis**	**Other structural changes (Neuroinflammatory, glial and excitability)**	**Behaviour/pathology phenotype**	
Receptor	**TNF-R1** (TNFα) via TNFR1/p55	Chronic neuropathic pain induced by constriction of sciatic nerve in WT and TNFR1$^{-/-}$ mice	TNRFR1-/- mice: no changes in hippocampal neurogenesis and plasticity (Ki67, DCX, NeuN, BrdU). Impaired in WT mice		TNRFR1-/- mice: no development of depressive-like symptoms after injury (open field test), sucrose preference test. Development of anhedonia and weight loss in WT mice	(Dellarole et al., 2014)
		TNF-R1 KO mice. Induced status epilepticus (associated with elevated TNFα levels)	TNF KO mice showed elevated levels of new mature hippocampal neurones, as well as after status epilepticus, with increased proliferation			(Iosif et al., 2006)
		Intracolonic trinitrobenzene sulfonic acid model of IBD in rats. Administration of GABAergic agonist to evoke seizures to examine excitability		Rats with inflammation showed increased excitability. Antagonism of TNFα using antibodies or inhibition of microglia using minocycline prevented increased excitability Infusion of TNFα increased seizure susceptibility.		(Riazi et al., 2008)
Cytokines	**TNF** (see receptors TNF-R1 and TNF-R2)	Stressed mice: Water-immersion resistant stress in mic. Rescue experiment with TNFα inhibitor (etanercept)		Microglial cell numbers and cell morphology was not altered n acute stress Acute stress induced microglial TNFα production in the hippocampus	Working memory assessed with Y-maze test. Stress diminished working memory. TNFα inhibition after acute stress rescued working memory deficits	(Ohgidani et al., 2016)
		Induced TBI in rats and treated with etanercept (TNFα inhibitor)	Increased levels of DCX with TNF α inhibition		Neurological functional deficits improved on inhibition of TNFα	(Cheong et al., 2013)
		In vivo: Dextran sodium sulfate model of IBD in mice. *In vitro* NPC culture in presence of IL-1β, IL-6 or TNF α	*In vivo*: p21 protein and mRNA levels were increased Markers of progenitor cells were decreased. *In vivo*: increased GFAP (differentiation into astrocytes?), decreased numbers of new neurones *In vitro*: increased p21 expression in differentiating NPCs *In vitro*: IL-6 resulted in decreased neuroblasts and increase in GFAP positive cells	*In vivo*: Increased TNFα, IL1β and IL-6 (serum and hippocampal mRNA levels) *In vivo*: Increased expression of Iba1 (microglial activation		(Zonis et al., 2015)
		Systemic administration or repeated hippocampal infusions of TNFα, IL-1β or IL-6	Systemic administration of TNFα reduced proliferation (BrdU labelling). There was no effect consistent with IL-1β or IL-6. Repeated hippocampal infusion of IL-6 and IL-1β increased proliferation (BrdU) but not neurone numbers (DCX labelling) . Il-6 increased microglial staining. There was no change in BrdU labelling with TNFα			(Seguin et al., 2009)
		In vitro TNFα treatment on differentiating and proliferating neurospheres	TNFα treatment during proliferation had no effect on proliferation (BrdU) or differentiation. TNFα treatment during differentiation resulted in preferential astrocyte (GFAP+), rather than neurone (DCX+), differentiation, with neurones showing decreased branching			(Keohane et al., 2010)
		Intraventricular injection of β-amyloid followed by i.p. administration of 3,6' dithiothalidomide (TNFα synthesis inhibitor)	$A\beta_{1-42}$ resulted in proliferation of NPCs TNFα synthesis inhibitor attenuated increase in neurogenesis		$A\beta_{1-42}$ resulted in memory impairment (Morris water maze) TNFα synthesis inhibitor prevented memory deficits attenuated increase in neurogenesis	(Russo et al., 2012)

		TLR9 KO mice Seizure induction using i.p kaininc acid TLR7 KO for comparison i.p. Minocycline administration (inhibition of microglial activation)	TNFα microglial signalling attenuated aberrant neurogenesis following seizures Pharmacological inhibition of microglial activation or TNF α production exacerbated aberrant neurogenesis	TNFα expression is activated by TLR9 sensing of self-DNA TLR9 KO mice reduced seizure-mediated microglia activation TNFα production. TLR9 deficiency exacerbated recurrent seizure severity TLR9 activation resulted in TNFα secretion from microglia	TLR9 deficiency exacerbated seizure-induced cognitive decline	(Matsuda et al., 2015)
Intrinsic: Receptor	TNFR2/p77 (via NF-κB)					(Pozniak et al., 2016)
Extrinsic signalling molecule: Cytokine	IL-6	*In vivo*: Dextran sodium sulfate model of IBD in mice. *In vitro* NPC culture in presence of IL-1β, IL-6 or TNF α	*In vivo*: p21 protein and mRNA levels were increased Markers of progenitor cells were decreased. *In vivo*: increased GFAP (differentiation into astrocytes?), decreased numbers of new neurones *In vitro*: increased p21 expression in differentiating NPCs *In vitro*: IL-6 resulted in decreased neuroblasts and increase in GFAP positive cells	*In vivo*: Increased TNFα, IL1β and IL-6 (serum and hippocampal mRNA levels) *In vivo*: Increased expression of Iba1 (microglial activation		(Zonis et al., 2015)
		Systemic administration or repeated hippocampal infusions of TNFα, IL-1β or IL-6	Systemic administration of TNFα reduced proliferation (BrdU labelling). There was no effect consistent with IL-1β or IL-6. Repeated hippocampal infusion of IL-6 and IL-1β increased proliferation (BrdU) but not neurone numbers (DCX labelling) . Il-6 increased microglial staining. There was no change in BrdU labelling with TNFα			(Seguin et al., 2009)
		Transgenic production of IL-6 by astrocytes in mice (under control of GFAP)	Decreased neurogenesis by 63% (BrdU), although distribution and gliogenesis appeared normal			(Vallieres et al., 2002)
		IL-6 KO mice	Decrease in proliferation (BrdU), with significantly lower progenitor cell survival			(Bowen et al., 2011)
		In vivo: p21 KO mice, LPS treatment *In vitro* culturing of neuroblasts from p21 KO and WT mice in presence and absence if IL-6	*In vivo:* Increased proliferation of NPCs in KO mice. LPS treatment decreased number of neuroblasts due to apoptosis. *In vitro* p21 KO cells had increased proliferation rates. WT cells treated with IL-6 showed increased p21+ cells, with decreased proliferation. IL-6 treatment on p21 KO cell showed no effects			(Zonis et al., 2013)
Extrinsic signalling molecule: Cytokine	IL-1β	*In vivo*: Dextran sodium sulfate model of IBD in mice. *In vitro* NPC culture in presence of IL-1β, IL-6 or TNF α	*In vivo*: p21 protein and mRNA levels were increased Markers of progenitor cells were decreased. *In vivo*: increased GFAP (differentiation into astrocytes?), decreased numbers of new neurones *In vitro*: increased p21 expression in differentiating NPCs *In vitro*: IL-6 resulted in decreased neuroblasts and increase in GFAP positive cells	*In vivo*: Increased TNFα, IL1β and IL-6 (serum and hippocampal mRNA levels) *In vivo*: Increased expression of Iba1 (microglial activation		(Zonis et al., 2015)
		Systemic administration or repeated hippocampal infusions of TNFα, IL-1β or IL-6	Systemic administration of TNFα reduced proliferation (BrdU labelling). There was no effect consistent with IL-1β or IL-6. Repeated hippocampal infusion of IL-6 and IL-1β increased proliferation (BrdU) but not neurone numbers (DCX labelling) . Il-6 increased microglial staining. There was no change in BrdU labelling with TNFα			(Seguin et al., 2009)

Intrinsic	p21	p21 KO mice miRNA p21 suppression chronic treatment with antidepressants	*In vitro* NPC proliferation increased in p21 KO mice and miRNA suppressed mice. Antidepressants decreased p21 expression specifically and increased neurogenesis		P21 KO mice showed decreased immobility in forced swim test. Antidepressants did not improve functioning in KO mice (i.e. act through p21)	(Pechnick et al., 2011)
		In vivo: Dextran sodium sulfate model of IBD in mice. *In vitro* NPC culture in presence of IL-1β, IL-6 or TNF α	*In vivo*: p21 protein and mRNA levels were increased Markers of progenitor cells were decreased. *In vivo*: increased GFAP (differentiation into astrocytes?), decreased numbers of new neurones *In vitro*: increased p21 expression in differentiating NPCs *In vitro*: IL-6 resulted in decreased neuroblasts and increase in GFAP positive cells	*In vivo*: Increased TNFα, IL1β and IL-6 (serum and hippocampal mRNA levels) *In vivo*: Increased expression of Iba1 (microglial activation		(Zonis et al., 2015)
		In vivo: p21 KO mice, LPS treatment *In vitro* culturing of neuroblasts from p21 KO and WT mice in presence and absence if IL-6	*In vivo:* Increased proliferation of NPCs in KO mice. LPS treatment decreased number of neuroblasts due to apoptosis. *In vitro* p21 KO cells had increased proliferation rates. WT cells treated with IL-6 showed increased p21+ cells, with decreased proliferation. IL-6 treatment on p21 KO cell showed no effects			(Zonis et al., 2013)
	CX3CR1					
Extrinsic signalling molecule: neurotrophin	BDNF (see receptor TrkB)	Transgenic mice with reduced BDNF levels or impaired TrkB activation. Antidepressant (imipramine) treatment	Basal proliferation rate increased in transgenic mice. Survival was significantly reduced in transgenic mice No antidepressant-induced increase in surviving new neurones was seen with reduced BDNF signalling.			(Sairanen et al., 2005)
		BDNF KO (+/-) and WT mice on dietary restriction or ad libitum diets.	Decrease in proliferation (BrdU) in DG Increase in BDNF in dietary restriction			(Lee et al., 2002)
Intrinsic: receptor (neurotrophin)	TrkB	Transgenic mice with trkB.T1-overexpressing mice (reduced TrkB activation) and mice with reduced BDNF levels (+/-). Neurotrophin-3(+/-) transgenic mice		Antidepressant treatment induced phosphorylation and activation of TrkB, and was reduced in trekB.T1 overexpressing mice.	TrkB.T1 and BDNF (+/-) transgenic mice were resistant to effect of antidepressants in forced swim test. Neurotrophin-3 (+/-) mice showed a normal behavioural response.	(Saarelainen et al., 2003)
	CCL11					
	VEGF					
	Prox1					
Intrinsic: receptor	TLR4					
Intrinsic: receptor(DNA fragments)	TLR9	TLR9 KO mice Seizure induction using i.p kaininc acid TLR7 KO for comparison i.p. Minocycline administration (inhibition of microglial activation)	TNFα microglial signalling attenuated aberrant neurogenesis following seizures Pharmacological inhibition of microglial activation or TNF α production exacerbated aberrant neurogenesis	TNFα expression is activated by TLR9 sensing of self-DNA TLR9 KO mice reduced seizure-mediated microglia activation TNFα production. TLR9 deficiency exacerbated recurrent seizure severity TLR9 activation resulted in TNFα secretion from microglia	TLR9 deficiency exacerbated seizure-induced cognitive decline	(Matsuda et al., 2015)
Intrinsic	COX-pathway E2 receptor					
	TGFβ					
Extrinsic: signalling molecule Cytokine	IL-4					
Extrinsic: signalling molecule: Cytokine	IL-10					
Extrinsic: signalling molecule: Cytokine	INF-γ					
	IGF-4					

	HMGB1 (high mobility group box 1)					
Intrinsic - receptor	TLR (pathway = GSK3)					
Intrinsic – receptor	α_2-adrenoceptor	Receptor agonist (clonidine, guanabenz) Receptor antagonist (yohimbine) coadminsitration with antidepressants	Agonists decrease NPC proliferation but not survival or differentiation Coadministration of antagonist with antidepressants accelerates effects on NPC proliferation, maturation and expression of BDNF and VEGF.		Coadministration of antagonist with antidepressants accelerates effects on novelty suppressed feedin test	
Intrinsic – vesicle associated protein	Synapsin III	Synapsin III KO mice	30% decrease in proliferation, 55% increase in survival of NPCs. 6% increase in proportion of NPC differentiation in to neurones. No difference in volume of DG was observed.			(Kao et al., 2008)
Receptor	TAM receptor					
Hormone	corticosterone					
Neurotransmitter	5-HT					
Neurotransmitter	GABA					
Neurotransmitter	ACh					
Neurotransmitter	DA					
Neurotransmitter	NE					
Neurotransmitter	Glu					
Intrinsic	NF-κB		(+/)Survival & migration: dendritic development, axonal development (-) apoptosis		Involved in memory formation or neuro Involved in memory formation or neurogenesis	
Intrinsic	Hes1	*In vitro* TNFα treatment on differentiating and proliferating neurospheres	TNFα treatment during proliferation had no effect on Hes1 expression, with no alteration in numbers/proportion of DCX or GFAP-+ cells TNFα treatment during differentiation resulted in increased expression of Hes 1, with preferential astrocyte (GFAP+), rather than neurone (DCX+), differentiation , with neurones showing decreased branching			(Keohane et al., 2010)

8.3 Appendix 3: Mass spectrophotometry report

	Analytical Report
Report to	Vinogran Naidoo
Document Number	17102017-001_MASS
Version	1.0
Status	Completed
Date	17/10/2017
Project ID	1074MASS_A_NAIDOO_HEL
Author	Michelle du Plessis Proteomics Technician
Reviewer	Liam Bell Proteomics Manager

Table of Contents

1. Background and samples submitted

The goal of the project is to investigate the effect of helminth infection on signalling and inflammation in the brain of infected mice. Two in-gel samples were submitted for analysis by LC-MS and identification of proteins present.

2. Abbreviations

LCMS – Liquid chromatography mass spectrometry

AmBic – Ammonium bicarbonate

LCMS – Liquid chromatography mass spectrometry

TEAB - Triethylammonium bicarbonate

ACN – Acetonitrile

FA – Formic acid

TCEP - Tris(2-carboxyethyl)phosphine

IAA - Iodoacetamide

TFA - Trifluoroacetic

3. Analysis synopsis

Gel slice samples, totalling 2 samples, were submitted to the CPGR. Gel-resolved protein was subjected to trypsin digestion. Peptides were then analysed by LC-MS and protein ID results sent back to the client.

Proteins containing at least two unique peptides and that were above the first false positive protein identified for each sample were reported. The raw data was searched against a mouse reference proteome database (Mus_musculus_10090_23112016_ref.fasta) of reviewed proteins downloaded from UniprotKB on 23/11/2016.

4. Detailed analysis

4.1. LCMS

LCMS analysis was conducted with a Q-Exactive quadrupole-Orbitrap mass spectrometer (Thermo Fisher Scientific, USA) coupled with a Dionex Ultimate 3000 nano-HPLC system. Peptides were dissolved in 0.1% Formic Acid (FA; Sigma 56302), 2% Acetonitrile (ACN; Burdick & Jackson BJLC015CS) and loaded on a C18 trap column (300 µm × 5 mm × 5 µm) at

3.5% solvent B and a flow rate of 5µl/min and washed for four minutes. Chromatographic separation was performed with a PepAcclaim C18 column (75 µm × 25 cm × 1.7 µm). The solvent system employed was solvent A: LC water (Burdick and Jackson BJLC365); 0.1% FA and solvent B: ACN, 0.1% FA. The multi-step gradient for peptide separation was generated at 300 nL/min as follows: time change 6.2 min, gradient change: 3.5 – 11.4% Solvent B, time change 45.3 min, gradient change 11.4 – 24.6% Solvent B, time change 2 min, gradient change 24.6 – 38.7%, time change 2.1 min, gradient change 38.7 – 52.8% Solvent B, time change 0.4 min, gradient change 52.8 – 85.4%. The gradient was then held at 85.4% solvent B for 10 minutes before returning it to 3.5% solvent B for 15 minutes to condition the column. The mass spectrometer was operated in positive ion mode with a capillary temperature of 320°C. The applied electrospray voltage was 1.95 kV. Details of data acquisition are shown in the table below.

Full Scan	
Resolution	70,000 (@ *m/z* 200)
AGC target value	1e6
Scan range	350-2000 m/z
Maximal injection time (ms)	250
Data-dependent MS/MS	
Inclusion	Off
Resolution	17,500 (@ *m/z* 200)
AGC target value	1e5
Maximal injection time (ms)	50
Loop Count	5
Isolation window width (Da)	2
NCE (%)	27
Data-dependent Settings	
Underfill ratio (%)	1
Charge exclusion	1, 7,8, >8
Peptide match	preferred
Exclusion isotopes	on

27	Score version	2
28	precursor_assignment_flags	2
29	po_NumberMonosReturn	2
30	Recalibration option	No recalibration
31	Precursor recalibration coefficient m00	-0.762000561
32	Precursor recalibration coefficient m11	0.002844529
33	Precursor recalibration coefficient m22	-2.46E-06
34	Fragment recalibration coefficient m00	-0.000627184
35	Fragment recalibration coefficient m11	5.45E-06
36	Fragment recalibration coefficient m22	-4.53E-09
37	%Modification searches:	
38	common_modifications_max	1
39	rare_modifications_max	1
40	%Fixed and variable modifications:	
41	Oxidation / +15.994915 @ M | common2	
42	Deamidated / +0.984016 @ N, Q | common2	
43	Carbamidomethyl / +57.021464 @ C | fixed	
44	% Custom modification text below	
45	%Glycan modifications:	
46	Show all N-glycopeptides	0
47	%Addition parameters:	
48	Product Version	PMI-Byonic-Com:v2.6.46

6. Experimental procedures

6.1. In-gel trypsin digestion

All reagents were analytical grade or equivalent. Gel pieces were destained twice with 100mM ammonium bicarbonate (AmBic; Sigma 40867), 50% ACN for 45 minutes with agitation at room temperature. Excess liquid was removed and the gel pieces were dehydrated with ACN and subjected to vacuum centrifugation for five minutes. Protein was then reduced by rehydrating the gel pieces in 2mM tris-carboxyethyl phosphine (TCEP; Sigma 646547), made up in 25mM AmBic, and agitating at room temperature for 15 minutes. Excess liquid was removed and protein alkylated by covering the gel pieces in 20mM iodoacetamide (IAA; Sigma I6125), made up in 25mM AmBic, and incubating in the dark at room temperature for 30 minutes. After alkylation gel pieces were washed three times with 25mM AmBic at room temperature for 15 minutes with agitation. Excess liquid was removed and gel pieces were dehydrated as before. Protein was digested by

rehydrating the gel pieces in 0.02mg/ml trypsin (Promega PRV5111) made up in 50mM Ambic. Gel pieces were incubated on ice for 1 hour and excess liquid was removed. Gel pieces were then covered with 50mM AmBic and digested overnight at 37˚C. After digestion excess liquid was transferred to a new tube and the gel pieces were soaked in 0.1% trifluoroacetic acid (TFA; Sigma T6508) for 1 hour at 37 ˚C. Excess liquid was removed and added to the first extract. Samples were then dried down by vacuum centrifugation and the buffer replaced by Millipore water. Samples were dried down again and resuspended in 0.1 % FA, 2 % ACN made up in analytical grade water for LCMS analysis.

7. Deviations

None

8. Enquiries

Your application specialist on this project is Liam Bell; do not hesitate to contact him on 021 447 5669 or liam.bell@cpgr.org.za for additional discussion or information on this report.

9. Appendices

The following data files have been sent to the client:

1074_PBS2.raw_20171010_Byonic
1074_TC3.raw_20171010_Byonic

8.4 Appendix 4: Raw data

8.4.1 Western blots

8.4.1.1 p53

Unable to distinguish from nonspecific band

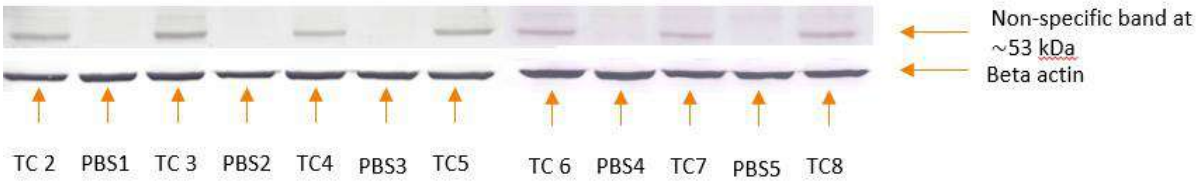

*Figure 20: **Western blot of cell death marker p53**. Showing no signal besides non-specific binding*

8.4.1.2 p21

No signal

8.4.1.3 c-fos

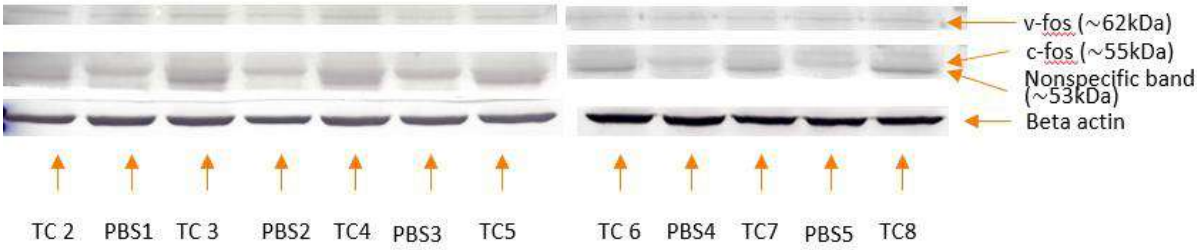

*Figure 21 **Western blot of IEG c-fos/v-fos.**. Sample TC2 excluded from analysis due to uneven background. Linear separation of non-specific band and c-fos was used.*

Table 1: ***Quantification and analysis of western blot of IEG c-fos/v-fos.***

	c-fos pixel total	actin pixel total	Normalised
TC2			
PBS1	51636	676701	0.410444
TC3	82011	644318	0.684652
PBS2	23356	509658	0.246501
TC4	80484	623958	0.693829
PBS3	38305	555881	0.370657
TC5	70954	642613	0.593917
TC6	123469	1071471	0.783284
PBS4	56716	992603	0.388393
TC7	71916	924372	0.528835
PBS5	39689	884166	0.305125
TC8	86619	909173	0.647602

Table Analyzed	c-fos
Column B	PBS
vs.	vs.
Column A	T.C
Mann Whitney test	
P value	0.0043
Exact or approximate P value?	Exact
P value summary	**
Significantly different? (P < 0.05)	Yes
One- or two-tailed P value?	Two-tailed
Sum of ranks in column A,B	51.00 , 15.00
Mann-Whitney U	0
Difference between medians	
Median of column A	0.6661
Median of column B	0.3707
Difference: Actual	-0.2955
Difference: Hodges-Lehmann	-0.3008

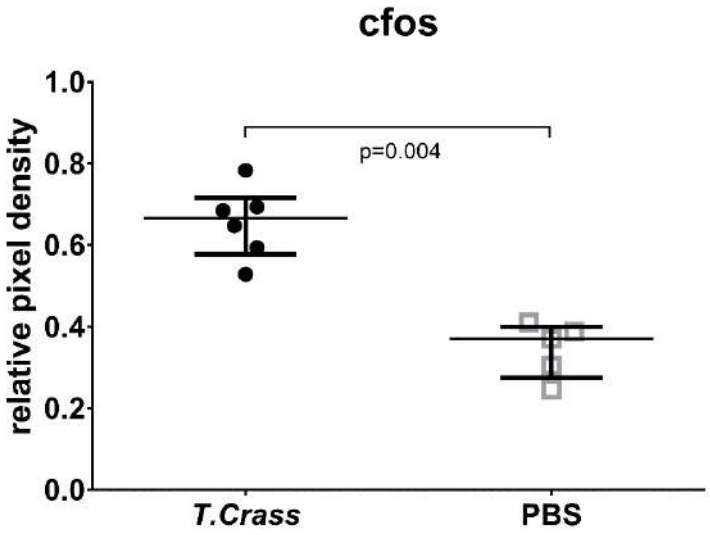

Figure 22: ***Anlysis of western blot for IEG c-fos (interquartile range and median used)***

8.4.1.4 *synaptophysin*

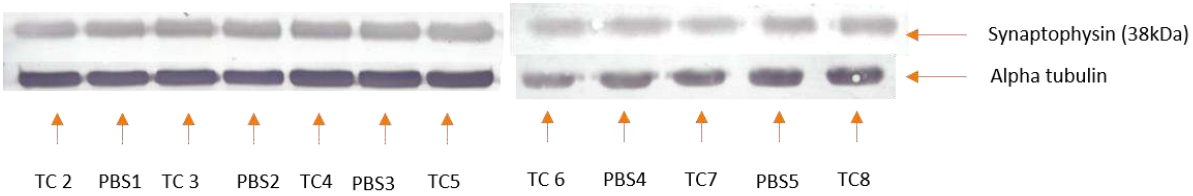

Figure 23 ***Western blot of snaptic marker synaptophysin.*** *Primary: mouse anti-synaptophysin 1:5000; anti-alpha tubulin 1:5000, secondary DAM-AP 1:2000. Sample TC8 excluded from analysis due to artefact.*

Table 2 ***Quantification and analysis of w estern blot of synaptic marker synaptophysin***

	Synapto pixel total	tubulin pixel total	Normalised
TC2	617582	1076473	0.446356
PBS1	637144	948156	0.522814
TC3	704367	1001656	0.547104
PBS2	659108	875662	0.585612
TC4	686256	1123306	0.475311
PBS3	636677	1120564	0.442051
TC5	702046	1177354	0.463926
TC6	272256	426586	0.646299
PBS4	270595	535738	0.511481
TC7	213456	530125	0.407749
PBS5	294273	685885	0.434472
TC8	312120		

Table Analyzed	synapto
Column B	PBS
vs.	vs.
Column A	T.C
Mann Whitney test	
P value	> 0.9999
Exact or approximate P value?	Exact
P value summary	ns
Significantly different? (P < 0.05)	No
One- or two-tailed P value?	Two-tailed
Sum of ranks in column A,B	36.00 , 30.00
Mann-Whitney U	15
Difference between medians	
Median of column A	0.4696
Median of column B	0.5115
Difference: Actual	0.04186
Difference: Hodges-Lehmann	0.01121

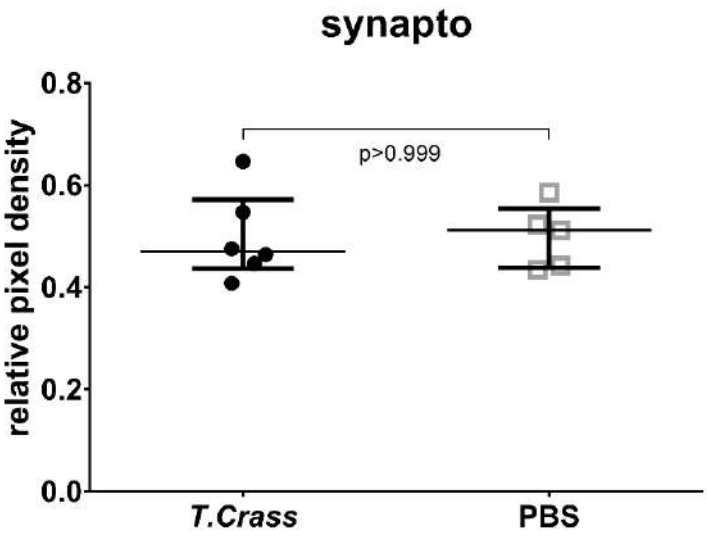

Figure 24 ***Anlysis of western blot for synaptic marker synaptophysin (interquartile range and median used)***

8.4.1.5 Tyrosine hydroxylase

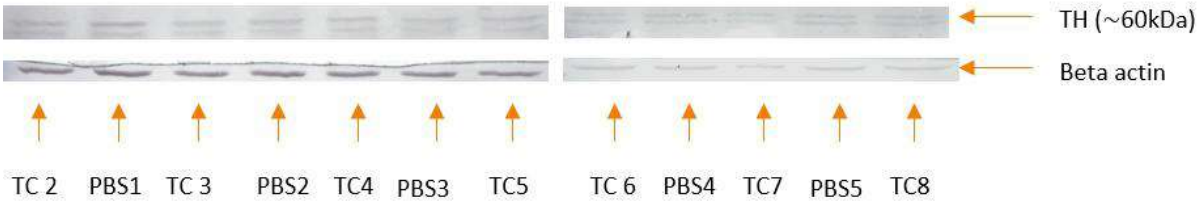

Figure 25: ***Western blot of neurotransmitter synthesis enzyme TH.*** *Primary: Mouse anti-TH 1:3000; mouse anti-beta actin 1:2000. Secondary DAM-AP 1:2000.*

Table 3: ***Quantification and analysis of western blot of neurotransmitter synthesis enzyme TH***

	TH pixel total	actin pixel total	Normalised
TC2	11081	341374	1.129677
PBS1	8640	360612	0.833834
TC3	9711	315463	1.071325
PBS2	811	233707	0.120769
TC4	1689	312253	0.188247
PBS3	615	268075	0.079841
TC5	1803	271060	0.231492
TC6	11752	40085	0.45127
PBS4	7097		
TC7	677	9287	0.112207
PBS5	7782	23167	0.517045
TC8	18424	32030	0.885388

Table Analyzed	TH
Column B	PBS
vs.	vs.
Column A	T.C
Mann Whitney test	
P value	0.3818
Exact or approximate P value?	Exact
P value summary	ns
Significantly different? (P < 0.05)	No
One- or two-tailed P value?	Two-tailed
Sum of ranks in column A,B	47.00 , 19.00
Mann-Whitney U	9
Difference between medians	
Median of column A	0.4513
Median of column B	0.3189
Difference: Actual	-0.1324
Difference: Hodges-Lehmann	-0.1312

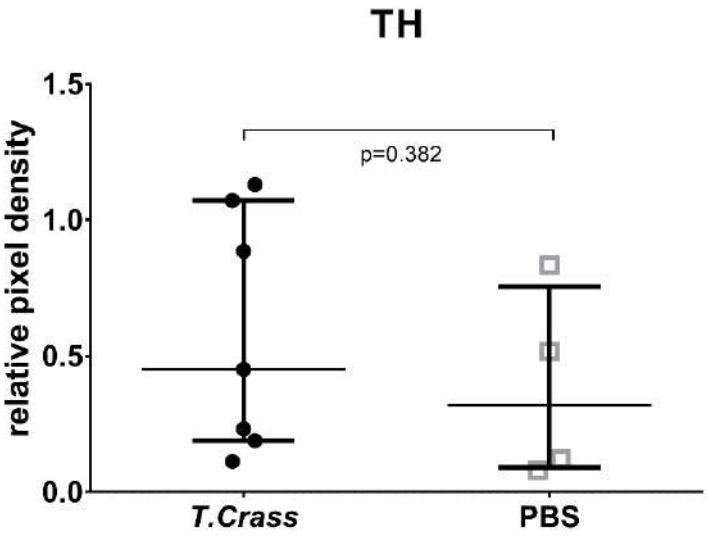

Figure 26: ***Anlysis of western blot for neurotransmitter synthesis enzyme TH. (interquartile range and median used)***

8.4.1.6 DARP-32

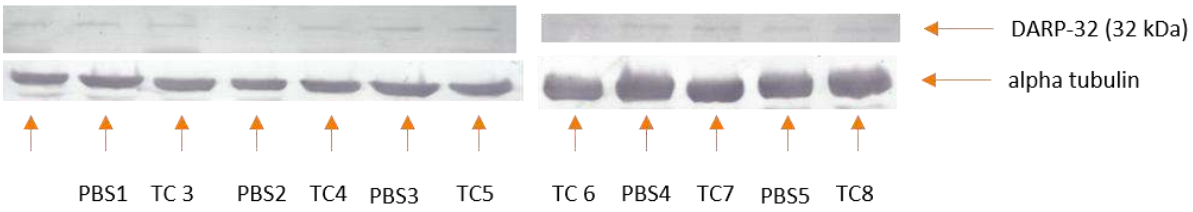

Figure 27. ***Western blot of dopamine-related proten DARP-32.*** *Primary: mouse anti-DARP32 1:500; mouse anti-alpha tubulin 1:5000. Secondary: DAM 1:2000*

Table 4 ***Quantification and analysis of w estern blot of dopamine related protein DARP-32***

	Darp-32 pixel total	tubulin pixel total	Normalised
TC2	40179	582128	0.54651
PBS1	24652	615739	0.31701
TC3	19288	575564	0.265345
PBS2	8992	475648	0.149688
TC4		612249	
PBS3	62158	702893	0.700206
TC5	90281	699981	1.02124
TC6	4500	1193746	0.753824
PBS4	1770	1480100	0.23914
TC7	4185	1315695	0.636077
PBS5	39	1275973	0.006112
TC8	9390	1511598	1.242221

Table Analyzed	Darp32
Column B	PBS
vs.	vs.
Column A	T.C
Mann Whitney test	
P value	0.0519
Exact or approximate P value?	Exact
P value summary	ns
Significantly different? (P < 0.05)	No
One- or two-tailed P value?	Two-tailed
Sum of ranks in column A,B	47.00 , 19.00
Mann-Whitney U	4
Difference between medians	
Median of column A	0.695
Median of column B	0.2391
Difference: Actual	-0.4558
Difference: Hodges-Lehmann	-0.4616

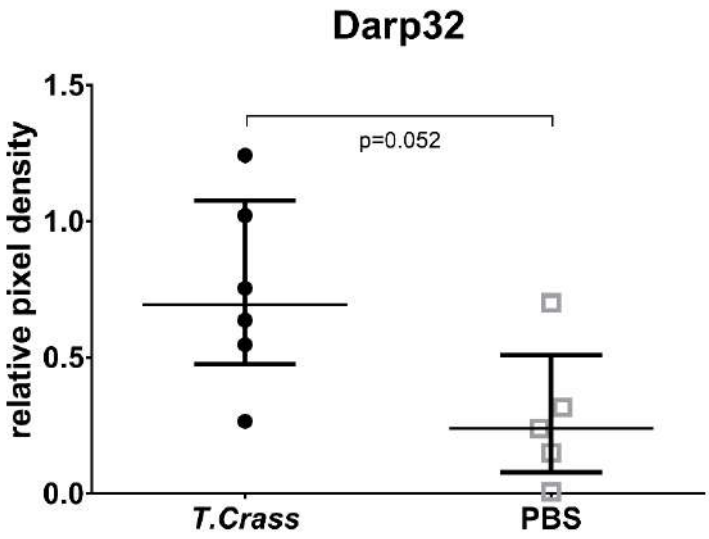

Figure 28: ***Anlysis of western blot for dopamine-related protein DARP-32 (interquartile range and median used)***

8.4.1.7 Iba-1

No signal

8.4.1.8 NeuN

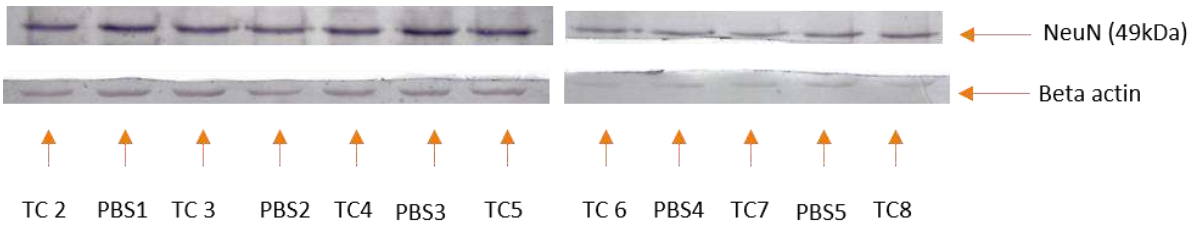

Figure 29 ***Western blot of mature neurone marker NeuN****, using beta actin as a loading control*

Table 5 ***Quantification and analysis of w estern blot of mature neurone marker NeuN***

	NeuN pixel total	actin pixel total	Normalised
TC2	114719	67111	0.379578
PBS1	157474	68790	0.508326
TC3	114485	66751	0.380846
PBS2	74656	39318	0.421631
TC4	106529	51306	0.461061
PBS3	162448	51839	0.695852
TC5	133228	55579	0.532284
TC6	130645	16151	0.275732
PBS4	104360	7660	0.464407
TC7	73882	3157	0.797734
PBS5	112402	8291	0.462127
TC8	130889		

Table Analyzed	**NeuN**
Column B	PBS
vs.	vs.
Column A	T.C
Mann Whitney test	
P value	0.4242
Exact or approximate P value?	Exact
P value summary	ns
Significantly different? (P < 0.05)	No
One- or two-tailed P value?	Two-tailed
Sum of ranks in column A,B	31.00 , 35.00
Mann-Whitney U	10
Difference between medians	
Median of column A	0.421
Median of column B	0.4644
Difference: Actual	0.04345
Difference: Hodges-Lehmann	0.06427

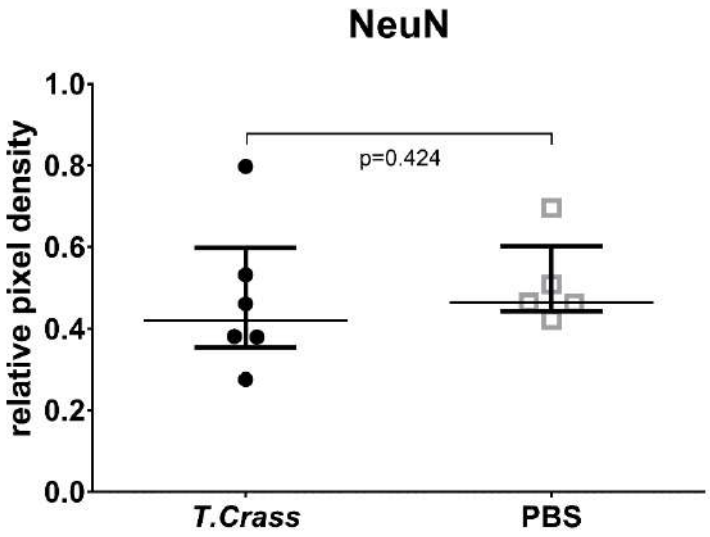

Figure 30: ***Anlysis of western blot for mature neruone marker NeuN (interquartile range and median used)***

8.4.1.9 CD86

No anti-rat secondary available

8.4.1.10 CD206

No signal

8.4.1.11 S100B

No signal

8.4.1.12 DCX

No signal

8.4.1.13 Nestin

No signal

8.4.1.14 Non-specific binding

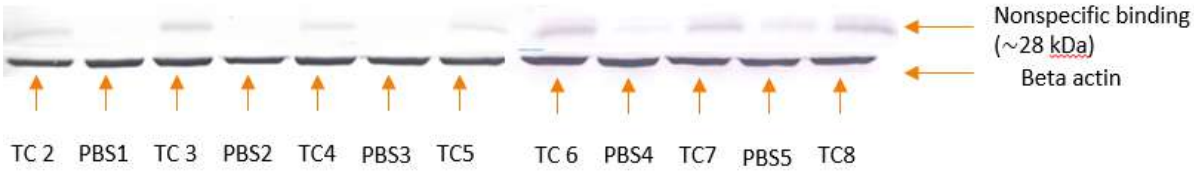

Figure 31: ***Western blot showing unkown band at ~28 kDa.*** *Primary: mouse anti- p53 1:500, secondary: DAM-AP 1:2 000. Blot for p53, which gave no specific signal, used for quantification*

Table 6: ***Quantification and analysis of western blot of uknown band at ~28 kDa***

	Nonspecific28 pixel total	actin pixel total	Normalised
TC2	131773	649007	1.324119
PBS1	6758	637833	0.069097
TC3	112104	647817	1.128545
PBS2	6518	541928	0.078437
TC4	64271	647846	0.646984
PBS3	4558	628273	0.047313
TC5	62853	639910	0.640556
TC6	312929	1071471	0.844759
PBS4	20719	992603	0.060375
TC7	198905	924372	0.622395
PBS5	82142	884166	0.268719
TC8	326648	909173	1.039204

Table Analyzed	Nonspecific28
Column B	PBS
vs.	vs.
Column A	T.C
Mann Whitney test	
P value	0.0025
Exact or approximate P value?	Exact
P value summary	**
Significantly different? (P < 0.05)	Yes
One- or two-tailed P value?	Two-tailed
Sum of ranks in column A,B	63.00 , 15.00
Mann-Whitney U	0
Difference between medians	
Median of column A	0.8448
Median of column B	0.0691
Difference: Actual	-0.7757
Difference: Hodges-Lehmann	-0.7705

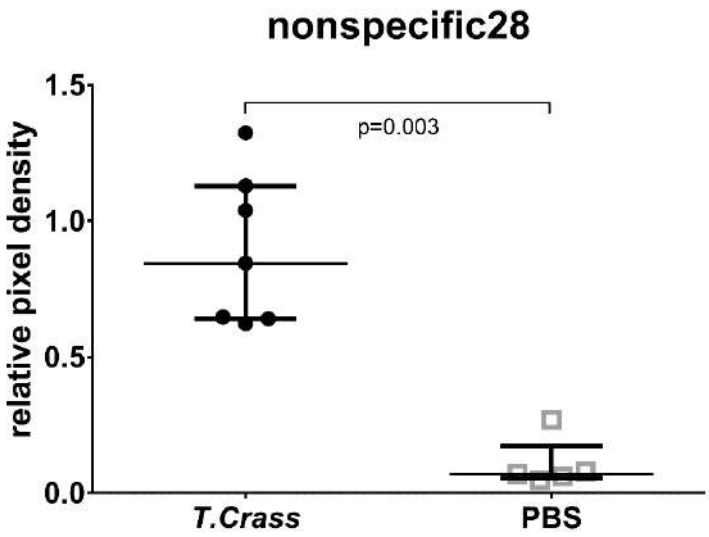

Figure 32 ***Anlysis of western blot for unknown band at ~28 kDa. (interquartile range and median used)***

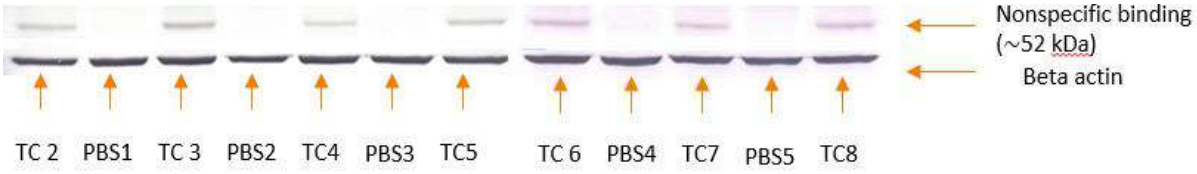

Figure 33: ***Western blot showing unkown band at ~52 kDa.*** *Primary: p53 1:500, secondary: DAM-AP 1:2 000. Blot for p53, which gave no specific signal, used for quantification*

Table 7: ***Quantification and analysis of western blot of uknown band at ~52 kDa***

	Nonspecific52 pixel total	actin pixel total	Normalised
TC2	95896	641248	1.084713
PBS1	0	622237	0
TC3	117533	630783	1.351513
PBS2	0	530197	0
TC4	49565	633430	0.567567
PBS3	13	612074	0.000154
TC5	85108	619798	0.996003
TC6	149349	1192378	1.097936
PBS4	0	1097375	0
TC7	92385	1022595	0.791929
PBS5	0	975436	0
TC8	129292	1020903	

Table Analyzed	Nonspecific52
Column B	PBS
vs.	vs.
Column A	T.C
Mann Whitney test	
P value	0.0025
Exact or approximate P value?	Exact
P value summary	**
Significantly different? (P < 0.05)	Yes
One- or two-tailed P value?	Two-tailed
Sum of ranks in column A,B	63.00 , 15.00
Mann-Whitney U	0
Difference between medians	
Median of column A	1.085
Median of column B	0
Difference: Actual	-1.085
Difference: Hodges-Lehmann	-1.085

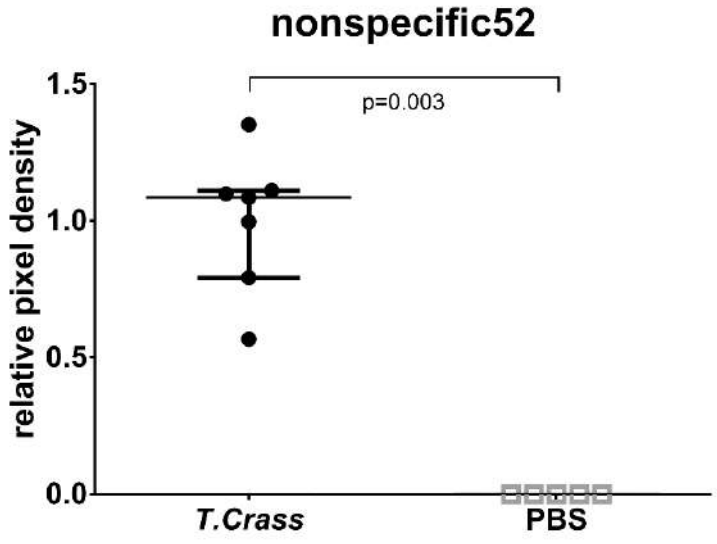

Figure 34 ***Anlysis of western blot for unknown band at ~52 kDa. (interquartile range and median used)***

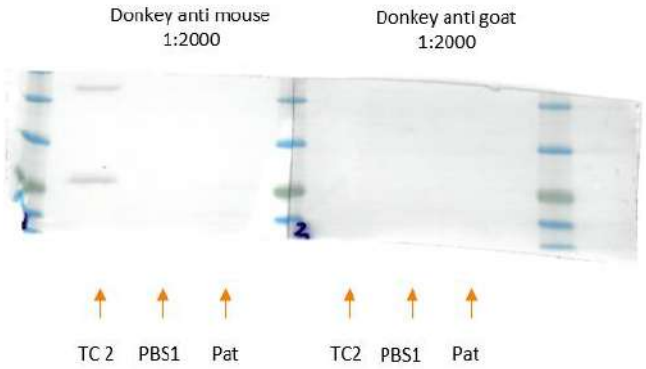

Figure 35: ***Western blot showing specificity of unknown band to anti-mouse secondaries*** *incubation with secondary antibodies against mouse and goat. "Pat" refers to a negative control of rat hippocampal homogenate from an unrelated study*

Figure 36: ***Western blot showing specificity of unknown band to a different anti-mouse secondary.*** *c-fos primary antibody, Goat-anti-mouse HRP-conjugate secondary antibody, chemiluminescent detection, showing that non-specific binding occurs independent of anti-mouse secondary antibody used,*

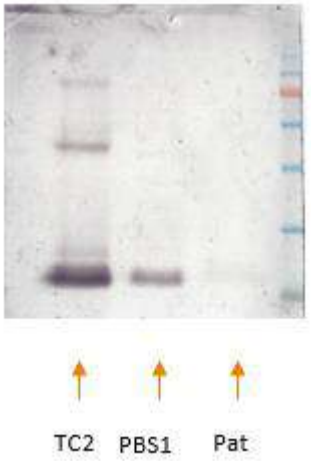

Figure 37 ***Western blot showing similar staining patterns to unknown band using an antibody against IgG.*** *Primary: goat anti-IgG 1:100, Secondary, DAG 1:2000. "Pat" refers to a negative control of rat hippocampal homogenate from an unrelated study*

8.4.2 Cytokine Array

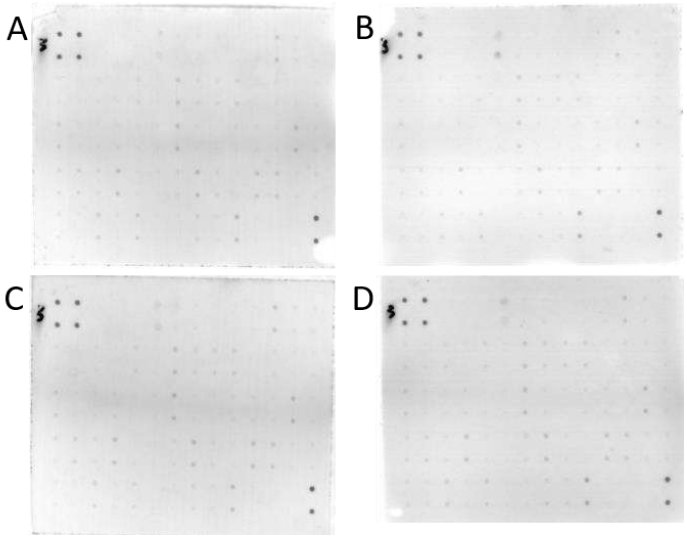

*Figure 38: **Scans of cytokine arrays.** A: sample PBS1. B sample PBS5. C sample TC3. D: sample TC8. A and C: loaded with 160ug protein. B and D: loaded with 220ug protein*

*Table 8: **Array map provided by RayBiotech**. Each antibody is spotted in duplicate vertically. A1,B1, A2 and B2 were used as internal references and L9, M9, L10 and m10 were used as negative controls during normalisation*

	A	B	C	D	E	F	G	H	I	J	K	L	M	N
1	POS	POS	NEG	NEG	BLANK	Axl	BLC (CXCL13)	CD30 Ligand (TNFSF8)	CD30 (TNFRSF 8)	CD40 (TNFRSF 5)	CRG-2	CTACK (CCL27)	CXCL1 6	Eotaxi n-1 (CCL11)
2	POS	POS	NEG	NEG	BLANK	Axl	BLC (CXCL13)	CD30 Ligand (TNFSF8)	CD30 (TNFRSF 8)	CD40 (TNFRSF 5)	CRG-2	CTACK (CCL27)	CXCL1 6	Eotaxi n-1 (CCL11)
3	Eotaxi n-2 (CCL24)	Fas Ligand (TNFSF 6)	Fractalkin e (CX3CL1)	GCSF	GM-CSF	IFN-gama	IGFBP-3	IGFBP-5	IGFBP-6	IL-1 alpha (IL-1 F1)	IL-1 beta IL-1 F2)	IL-2	IL-3	IL-3 R beta
4	Eotaxi n-2 (CCL24)	Fas Ligand (TNFSF 6)	Fractalkin e (CX2CL1)	GCSF	GM-CSF	IFN-gama	IGFBP-3	IGFBP-5	IGFBP-6	IL-1 alpha (IL-1 F1)	IL-1 beta IL-1 F2)	IL-2	IL-3	IL-3 R beta
5	IL-4	IL-5	IL-6	IL-9	IL-10	IL-12 p40/p7 0	IL-12 p70	IL13	IL-17A	KC (CXCL1)	Leptin R	Leptin	LIX	L-selecti n
6	IL-4	IL-5	IL-6	IL-9	IL-10	IL-12 p40/p7 0	IL-12 p70	IL13	IL-17A	KC (CXCL1)	Leptin R	Leptin	LIX	L-selecti n
7	Ltn (XCL1)	MCP-1 (CCL2)	MCP-5	M-CSF	MIG (CXCL 9)	MIP-1 alpha (CCL3)	MIP-1 gamma	MIP-2	MIP-3 beta (CCL19)	MIP-3 alpha (CCL20)	PF-4 (CXCL 4)	P-selecti n	RANTE S (CCL5)	SCF
8	Ltn (XCL1)	MCP-1 (CCL2)	MCP-5	M-CSF	MIG (CXCL 9)	MIP-1 alpha (CCL3)	MIP-1 gamma	MIP-2	MIP-3 beta (CCL19)	MIP-3 alpha (CCL20)	PF-4 (CXCL 4)	P-selecti n	RANTE S (CCL5)	SCF
9	SDF-1 alpha	TARC (CCL17)	I-309 (TCA-3/CCL1)	TECK CCL25)	TIMP-1	TNFalph a	TNF RI (TNFRSF1 A)	TNF RII (TNFRSF1 B)	TPO	VCAM-1 (CD106)	VEGF-A	BLANK	BLANK	POS
1 0	SDF-1 alpha	TARC (CCL17)	I-309 (TCA-3/CCL1)	TECK CCL25)	TIMP-1	TNFalph a	TNF RI (TNFRSF1 A)	TNF RII (TNFRSF1 B)	TPO	VCAM-1 (CD106)	VEGF-A	BLANK	BLANK	POS

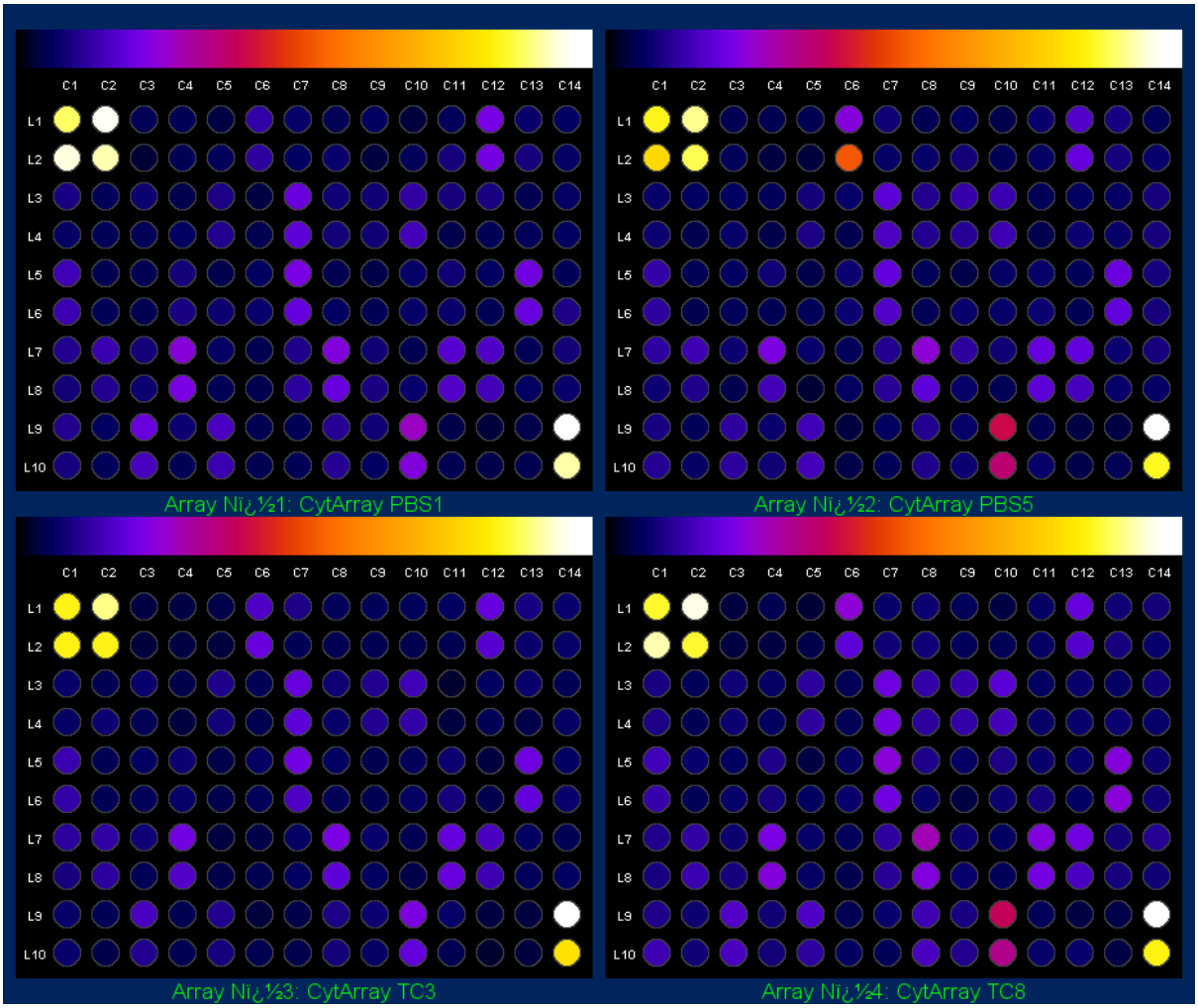

Figure 39: ***Cytokine array intensity map prior to normalisation****. Arrays PBS1 and TC3 were performed using 160ug protein, while Arrays PBS5 and TC8 were performed using 220ug. Generated in ImageJ using the Protein Array Analyzer plugin.*

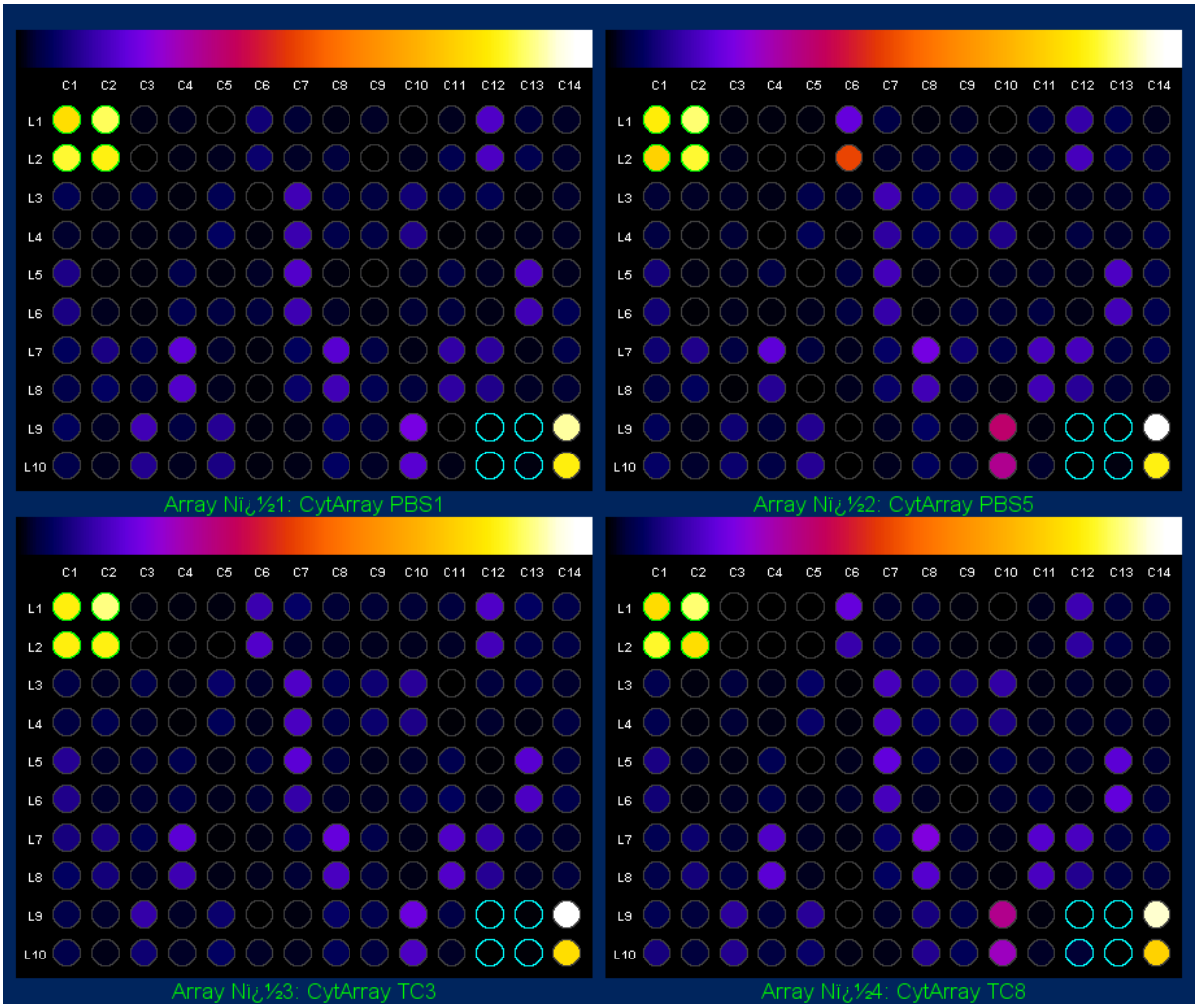

Figure 40: ***Cytokine array normalised intensity map.*** *Uses C1L1, C2L1, C1L2, C2L2 as internal references and C12L9, C13L9, C12L10 and C13L10 as internal controls. Arrays PBS1 and TC3 were performed using 160ug protein, while Arrays PBS5 and TC8 were performed using 220ug. Generated in ImageJ using the Protein Array Analyzer plugin.*

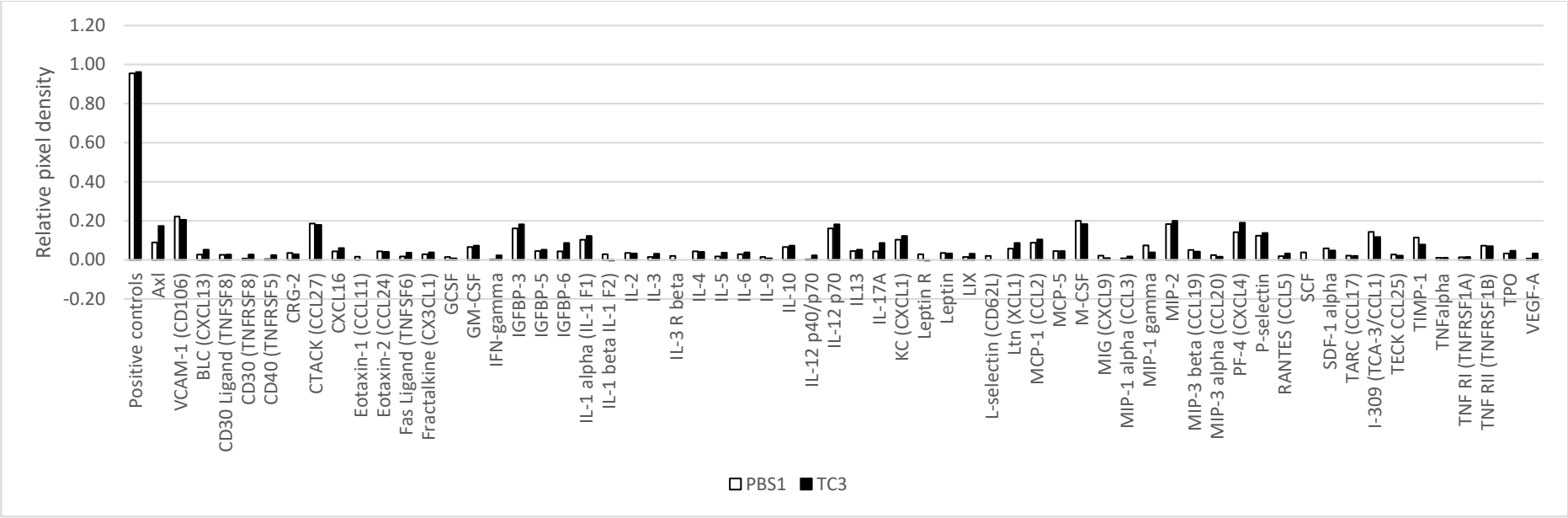

Figure 41 ***Normalised values for the first set of cytokine arrays*** *(using 160ug protein)*

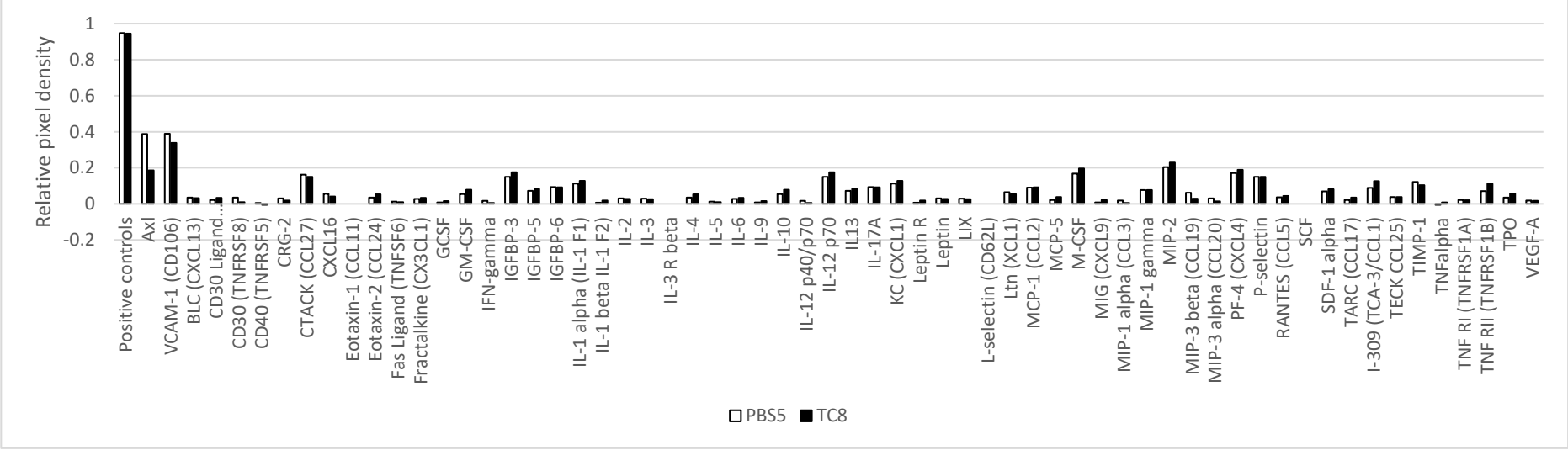

Figure 42 ***Normalised values for the second set of cytokine arrays*** *(using 220ug protein)*

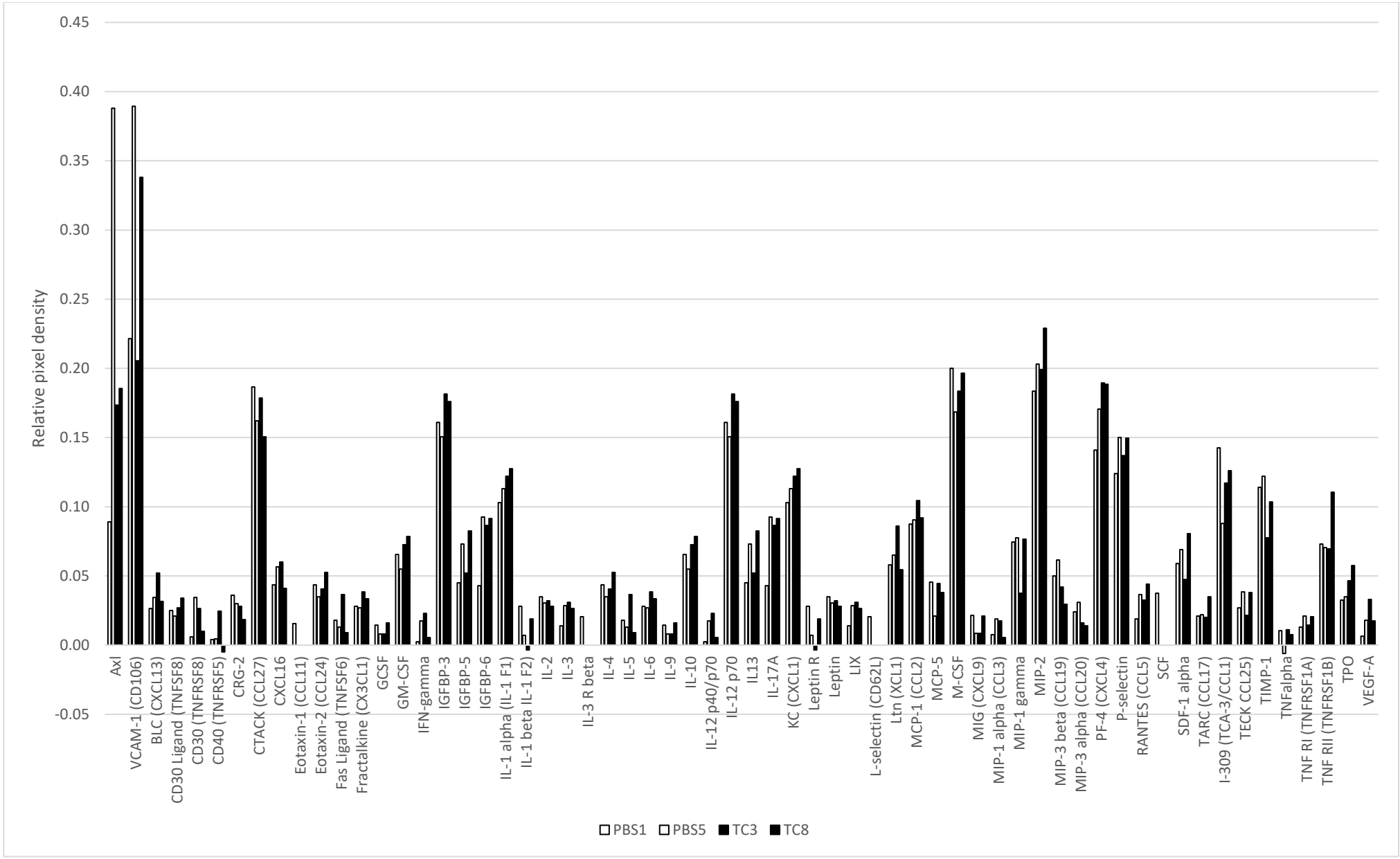

Figure 43 ***Combined normalised values for cytokine arrays***

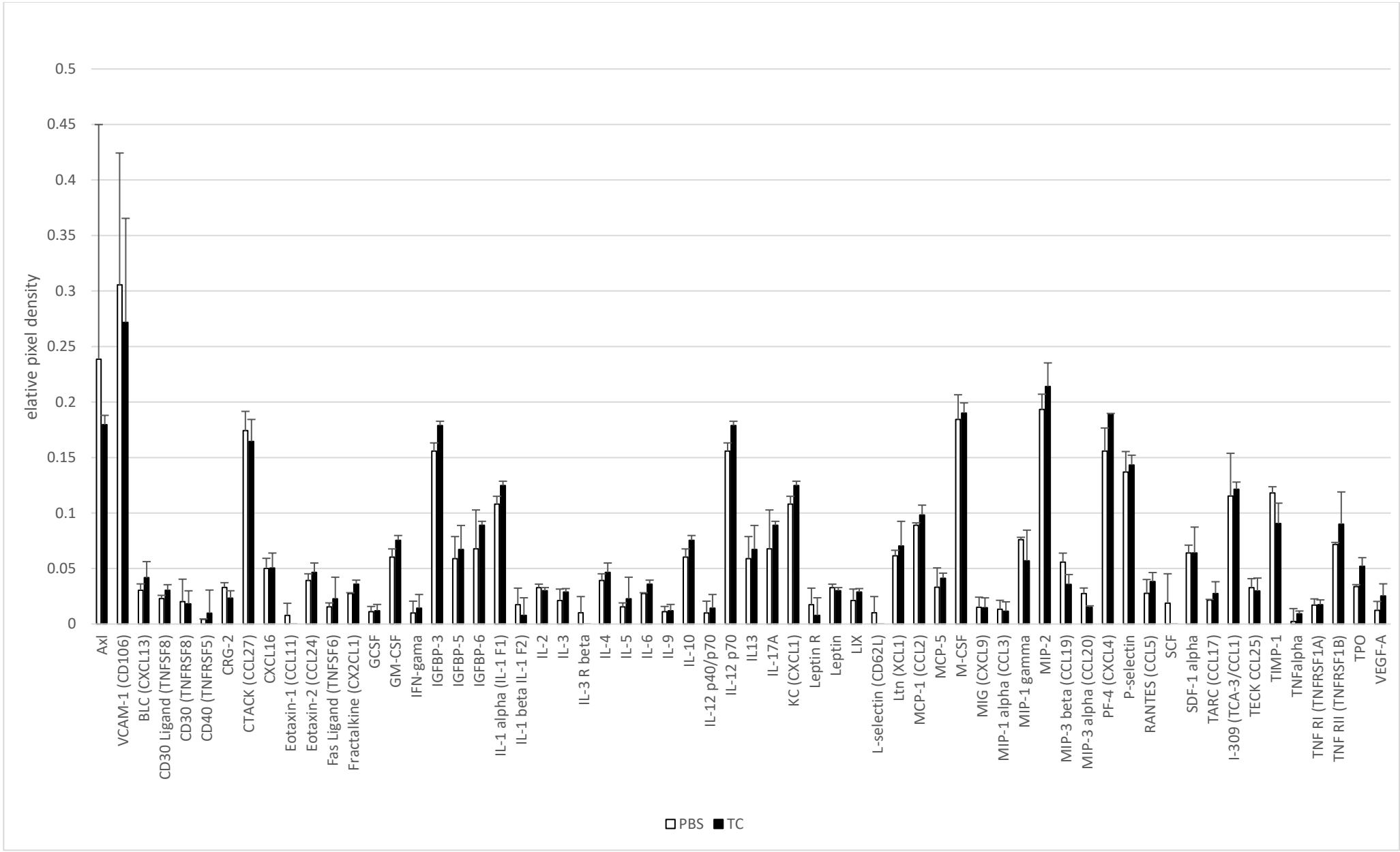

Figure 44 ***Graph of analysied cytokine arrays****. combined mean values and variation is shown as 95% confidence intervals (Axl and VCAM-1 have been excluded to retain scale)*

Table 9 ***Cytokine Array analysis****. Normalised values (relative pixel density) for each cytokine on each array, and non-parametric t-test performed between the PBS and TC groups*

Antibody	***PBS1***	***PBS5***	***TC3***	***TC8***	***T-test***
Positive controls	0.95	0.948	0.96	0.9445	0.868
Axl	0.09	0.39	0.17	0.1855	0.761
BLC (CXCL13)	0.03	0.03	0.05	0.0315	0.460
CD30 Ligand (TNFSF8)	0.03	0.02	0.03	0.034	0.235
CD30 (TNFRSF8)	0.01	0.03	0.03	0.01	0.917
CD40 (TNFRSF5)	0.00	0.00	0.02	-0.005	0.773
CRG-2	0.04	0.03	0.03	0.0185	0.247
CTACK (CCL27)	0.19	0.16	0.18	0.1505	0.653
CXCL16	0.04	0.06	0.06	0.041	0.970
Eotaxin-1 (CCL11)	0.02	0.00	0.00	0	0.500
Eotaxin-2 (CCL24)	0.04	0.04	0.04	0.0525	0.438
Fas Ligand (TNFSF6)	0.02	0.01	0.04	0.009	0.691
Fractalkine (CX2CL1)	0.03	0.03	0.04	0.0335	0.171
GCSF	0.01	0.01	0.01	0.016	0.898
GM-CSF	0.07	0.06	0.07	0.0785	0.159
IFN-gama	0.00	0.02	0.02	0.0055	0.748
IGFBP-3	0.16	0.15	0.18	0.176	0.093
IGFBP-5	0.05	0.07	0.05	0.0825	0.729
IGFBP-6	0.04	0.09	0.09	0.0915	0.548
IL-1 alpha (IL-1 F1)	0.10	0.11	0.12	0.1275	0.132
IL-1 beta IL-1 F2)	0.03	0.01	0.00	0.019	0.591
IL-2	0.04	0.03	0.03	0.028	0.459
IL-3	0.01	0.03	0.03	0.0265	0.482
IL-3 R beta	0.02	0.00	0.00	0	0.500
IL-4	0.04	0.04	0.04	0.0525	0.438
IL-5	0.02	0.01	0.04	0.009	0.691
IL-6	0.03	0.03	0.04	0.0335	0.171
IL-9	0.01	0.01	0.01	0.016	0.898
IL-10	0.07	0.06	0.07	0.0785	0.159
IL-12 p40/p70	0.00	0.02	0.02	0.0055	0.748
IL-12 p70	0.16	0.15	0.18	0.176	0.093
IL13	0.05	0.07	0.05	0.0825	0.729
IL-17A	0.04	0.09	0.09	0.0915	0.548
KC (CXCL1)	0.10	0.11	0.12	0.1275	0.132
Leptin R	0.03	0.01	0.00	0.019	0.591
Leptin	0.04	0.03	0.03	0.028	0.459
LIX	0.01	0.03	0.03	0.0265	0.482
L-selectin (CD62L)	0.02	0.00	0.00	0	0.500
Ltn (XCL1)	0.06	0.07	0.09	0.0545	0.677
MCP-1 (CCL2)	0.09	0.09	0.10	0.092	0.369
MCP-5	0.05	0.02	0.04	0.038	0.631
M-CSF	0.20	0.17	0.18	0.1965	0.781
MIG (CXCL9)	0.02	0.01	0.01	0.021	0.980
MIP-1 alpha (CCL3)	0.01	0.02	0.02	0.0055	0.853
MIP-1 gamma	0.07	0.08	0.04	0.0765	0.508
MIP-2	0.18	0.20	0.20	0.229	0.382
MIP-3 beta (CCL19)	0.05	0.06	0.04	0.0295	0.144
MIP-3 alpha (CCL20)	0.02	0.03	0.02	0.014	0.152
PF-4 (CXCL4)	0.14	0.17	0.19	0.1885	0.265
P-selectin	0.12	0.15	0.14	0.1495	0.721
RANTES (CCL5)	0.02	0.04	0.03	0.044	0.435
SCF	0.04	0.00	0.00	0	0.500
SDF-1 alpha	0.06	0.07	0.05	0.0805	1.000
TARC (CCL17)	0.02	0.02	0.02	0.035	0.570
I-309 (TCA-3/CCL1)	0.14	0.09	0.12	0.126	0.857
TECK CCL25)	0.03	0.04	0.02	0.038	0.797
TIMP-1	0.11	0.12	0.08	0.1035	0.260
TNF-alpha	0.01	-0.01	0.01	0.0075	0.550
TNF RI (TNFRSF1A)	0.01	0.02	0.01	0.0205	0.930
TNF RII (TNFRSF1B)	0.07	0.07	0.07	0.1105	0.537
TPO	0.03	0.04	0.05	0.0575	0.172
VCAM-1 (CD106)	0.22	0.39	0.21	0.338	0.784
VEGF-A	0.01	0.02	0.03	0.0175	0.320

Table 10: ***Selected cytokines showing promising trends (p<0.25) and their known functions as described by Uniprot****. The arrows refer to direction of change in cytokine levels in T. crassiceps mice compared to PBS*

	Cytokine	Function	Uniprot accession no
↑	CD30 ligand	Membrane-associated glycoprotein belonging to TNF superfamily CD8-positive, alpha-beta T cell differentiation, defence response to Gram positive bacterium. Induces proliferation of T cells	P32972
↓	CRG-2/ CXCL10/ IP10	Binds to CXCR3. **Cellular response** to heat/cold, LPS, viruses, gamma radiation, auditory stimulus, vitamin D; **positive regulation** of cAMP-mediated signalling and metabolic processes, release of sequestered calcium ions into cytosol cell proliferation, leukocyte and monocyte chemotaxis, T cell migration **negative regulation:** angiogenesis, myoblast differentiation and fusion	P17515
↑	Fractalkine /CX3CL1	Binds to CX3CR1 and integrins. Soluble form chemotactic for T-cells and monocytes by not neutrophils. Membrane-bound form promotes adhesion of leukocytes to endothelial cells **Role in** angiogenesis in wound healing, cell adhesion, cellular response to IFNγ/IL-1/TNF, lymphocyte/macrophage /monocyte/neutrophil chemotaxis, integrin activation, leukocyte adhesive activation, **Negative regulation:** cell migration, extrinsic apoptotic signalling pathway in absence of ligand **Positive regulation** angiogenesis, calcium-independen cell-cell adhesion, ERK1 and ERK2 cascade, GTPase activity, inflammatory response, TGFβ1 production	O35188
↑	GM-CSF	**Cellular response** to LPS **Role in** dendritic cell and monocyte differentiation, epithelial fluid transport, histamine secretion, macrophage, activation, regulation of circadian rhythm, fluid shear stress and silicon dioxide **Negative regulation:** cytolysis, extrinsic apoptotic signalling pathway in absence of ligand **Positive regulation:** cell proliferation, DNA replication, gene expression, IL-23 production, macrophage derived foam cell differentiation, podosome assembly, tyrosine phosphorylation of STAT protein.	P04141
↑	IGFBP-3	Alters interaction of IGFs with cell surface receptors, prolong the half-life of IGFs and exhibit IGF-independent effects mediated by IGFBP-3R **Negative regulation:** cell proliferation, protein phosphorylation, smooth muscle cell migration, smooth muscle cell proliferation, **Positive regulation:** apoptotic processes, IGF receptor signalling pathway, MAPK cascade, myoblast differentiation	P47878
↑	IL-1 alpha	Produced by activated macrophages, induces IL-2 release, B cell maturation and proliferation, fibroblast growth factor activity. Act as endogenous pyrogens. Bin to IL-1R **Role in:** cellular response to heat, connective tissue replacement, ectopic germ cell programmed cell death, extrinsic apoptotic signalling pathway in absence of ligand, fever generation, response to copper ion **Negative regulation:** cell proliferation **Positive regulation**: angiogenesis, cell division, cytokine secretion, gene expression, IL-2 biosynthetic process, IL-6 production, mitotic nuclear division, monocyte chemotactic protein-1 production, neutrophil extravasation, protein secretion, VEGF production	P01582
↑	IL-6	Inducer of acute phase response, role in differentiation of B-cells into plasma cells. Required for generation of Th17 cells, induces nerve cell differentiation. **Role in**: acute phase response, aging, bone remodelling, cell growth, response to dexamethasone stimulus, oestradiol stimulus, hydrogen peroxide, IL-1, LPS, nutrient levels, prolactin, TNF; defense response to protozoan and viruses; glucose homeostasis, neurone projection development. Neutrophil apoptotic processes, circadiane rhythm. **Response to:** antibiotics, auditory stimulus, codeine, cold, drugs, electrical stimulus, calcium ion, glucocorticoid, heat, insulin, wounding, yease **Negative regulation:** apoptotic process, bone resorption, cell proliferation, chemokine biosynthetic processes, collagen biosynthetic processes, cytokine secretion, gluconeogenesis, hormone secretion, Il-1 mediated signalling pathway, membrane potetntial, muscle organ development, neurone death, protein kinase activity **Positive regulation:** acute inflammatory response, apoptotic processes, B cell activation, cell proliferation, chemokine production, epithelial cell proliferation, ERK1 and ERK2 cascade, JAK-STAT cascade, MAPK cascade, neurone projection development, nitric oxide synthesis, T cell proliferation, Th2 cytokine production and differentiation, transmission of nerve impulse,	P08505
↑	IL-10	Inhibits synthesis of cytokines – IFNγ, IL-2, IL-3, TNF, GM-CSF **Role in cellular response to**: oestradiol, LPS, bacteria and protozoa, activity carbon monoxide, drugs, glucocorticoids, inactivity, insulin, **Negative regulation:** B cell proliferation, cell proliferation, chronic inflammatory response to antigenic stimulus, cytokine activity, endothelial cell apoptotic process, growth of symbiont in host, IFNγ production, IL-12 production, IL6 production, dendritic cell activation, NO biosynthetic process, TNF production, **Positive regulation:** B cell apoptotic process, cell cycle, cytokine secretion, endothelial cell proliferation, MHC clas II biosynthetic process	P18893
↑	IL-12 p70	Act as a growth factor for activated T and NK cells, enhance lytic activity of NK/stimulate production of IFN-gamma **Role in** cell cycle arrest, cell migration, response to LPS/ viruses/Gram-pos bacteria/protozoa/UV-B, IL-12 mediated signaliing pathway Negative regulation of IL-17 production, smooth muscle cell proliferation Positive regulation of cell adhesion, dendritic cell chemotaxis, IFNγ production, lymphocyte proliferation, mononuclear cell proliferation, NK cell activation, smooth muscle cell apoptosis, T cell differentiation, T cell mediated cytotoxicity, t cell proliferation	P43431
↑	KC	Binds to CXCR **Cellular response** to LPS/molecules of bacterial origin **Positive regulation** of haematopoietic stem cell proliferation, superoxide anion generation, neutrophil chemotaxis, neutrophil mediated killing of fungus,	P12850
↓	MIP-3 alpha CCL20	Ligand for CCR6, induces strong chemotactic response of dendritic cells, effector/memory T cells and B cells. Lymphocytes and nuetrophills (slightly) but not monocytes. mobilisation of intracellular calcium ions. Recruitment of Th17 cells and Tregs to inflammation sites.	O89093

		Role in cellular response to IFNγ, IL-1, LPS, lipoteichoic acid, TNF **Role in** lymphocyte/monocyte/neutrophil chemotaxis, G-protein coupled receptor signalling pathway, T cell migration, thymocyte migration, wound healing. **Positive regulation**: ERK1 and ERK2 cascade, GTPase activity, IL-1 biosynthetic process, NO synthase biosynthetic process, T cell migration.	
↓	MIP-3 beta CCL19	Chemotactic for naïve CD4 and CD8 T cells and weakly attractive for resting B cells and memory CD4 T cells. Binds to chemokine receptor CR7 and atypical chemokine receptor ACKR4. Mediates recruitment of beta arresetin to ACKR4. **Role in:** activation of JUN kinase, cell maturation, dendritic cell/lymphocyte/monocyte/dendritic cell/neutrophil chemotaxis, establishment of T cll polarity, immunological synapse formation, IL-12 secretion, dendritic cell differentiation, regulation of cell projection assembly, release of sequestered calcium ions inot cytosol, response to NO and prostaglandin E	O70460

		Negative regulation of leukocyte apoptotic process Positive regulaton of cell motilit, chemotaxis, dendritic cell antigen processing and presentation, dendritic cell dendrite assembly, endocytosis, ERK1 and ERK2 cascade, glycoprotein biosynthetic process, GTPase activity, IL-12 production, IL-1 secretion, JNK cascade, neutrophil chemotaxis, NFkB import into nucleus, , T cell proliferation, TNF production, Th1 differentiation **Cellular response to** IFNγ, IL-1, TNF, viruses	
↑	Thrombopoietin	Affects proliferation and maturation of megakaryocytes from committed progenitor cells. Role in cell proliferation, myeloid cell differentiation, thrombopoietin-mediated signalling pathway Positive regulation of ERK1and ERK2 cascade, haematopoietic stem cell proliferation, megakaryocyte differentiation, protein kinase B signalling, protein phosphorylation	P40226

8.4.3 Mass spectrophotometry

Table 11 ***Proteins of interest from mass spectrometry****. Highlighted values indicate that they have fallen below the false discovery rate (their identity is relatively uncertain) Relative intensity is the intensity divided by that of actin. "Difference" refers to the absolute difference between the relative intensities, and the table is ordered according to this variable. Only proteins where the difference is greater than 1 were included. Repeat samples are not included.*

	Total intensity PBS	Relative intensity PBS	Total intensity TC	Relative intensity TC	Difference
>sp|P63101|1433Z_MOUSE 14-3-3 protein zeta/delta OS=Mus musculus GN=Ywhaz PE=1 SV=1	1295165.6	0.159659033	1612173238	172.5412325	172.3816
>sp|P17751|TPIS_MOUSE Triosephosphate isomerase OS=Mus musculus GN=Tpi1 PE=1 SV=4	132333880.2	16.31320296	269849210.4	28.88034254	12.56714
>sp|O08709|PRDX6_MOUSE Peroxiredoxin-6 OS=Mus musculus GN=Prdx6 PE=1 SV=3	81377367.8	10.03163751	150019688.3	16.05570748	6.02407
>sp|Q9DBJ1|PGAM1_MOUSE Phosphoglycerate mutase 1 OS=Mus musculus GN=Pgam1 PE=1 SV=3	21265135.5	2.621418421	76141032.7	8.148918067	5.5275
>sp|O55126|NIPS2_MOUSE Protein NipSnap homolog 2 OS=Mus musculus GN=Gbas PE=1 SV=1	16337562.6	2.013981409	66333873.5	7.099316637	5.085335
>tr|Q7TMG8|Q7TMG8_MOUSE Glioblastoma amplified sequence OS=Mus musculus GN=Gbas PE=1 SV=1	16337562.6	2.013981409	66333873.5	7.099316637	5.085335
>sp|P10649|GSTM1_MOUSE Glutathione S-transferase Mu 1 OS=Mus musculus GN=Gstm1 PE=1 SV=2	81428658.3	10.03796025	136939096.6	14.6557702	4.61781
>sp|P35276|RAB3D_MOUSE Ras-related protein Rab-3D OS=Mus musculus GN=Rab3d PE=1 SV=1		0	39437699.6	4.220780457	4.22078
>sp|P08730|K1C13_MOUSE Keratin, type I cytoskeletal 13 OS=Mus musculus GN=Krt13 PE=1 SV=2	4292265.1	0.529120673	38223275.1	4.090807886	3.561687
>sp|P63011|RAB3A_MOUSE Ras-related protein Rab-3A OS=Mus musculus GN=Rab3a PE=1 SV=1	28725743.7	3.541110458		0	3.54111
>Reverse >sp|Q8CFI7|RPB2_MOUSE DNA-directed RNA polymerase II subunit RPB2 OS=Mus musculus GN=Polr2b PE=1 SV=2		0	32922443.5	3.523491672	3.523492
>sp|P62823|RAB3C_MOUSE Ras-related protein Rab-3C OS=Mus musculus GN=Rab3c PE=1 SV=1	9387044.0	1.157169681	39437699.6	4.220780457	3.063611
>Reverse >sp|Q6A078|CE290_MOUSE Centrosomal protein of 290 kDa OS=Mus musculus GN=Cep290 PE=1 SV=2	24621191.9	3.035129779	694497.5	0.074327902	2.960802
>sp|Q9DCW4|ETFB_MOUSE Electron transfer flavoprotein subunit beta OS=Mus musculus GN=Etfb PE=1 SV=3	12440017.6	1.533519093	40941873.2	4.381763136	2.848244
>sp|Q6IFZ6|K2C1B_MOUSE Keratin, type II cytoskeletal 1b OS=Mus musculus GN=Krt77 PE=1 SV=1		0	24045582.5	2.573454479	2.573454
>sp|P48962|ADT1_MOUSE ADP/ATP translocase 1 OS=Mus musculus GN=Slc25a4 PE=1 SV=4	3917562.6	0.482929947	26886153.2	2.877463725	2.394534
>sp|Q61885|MOG_MOUSE Myelin-oligodendrocyte glycoprotein OS=Mus musculus GN=Mog PE=1 SV=1	20719791.6	2.554192208	45146101.0	4.831716422	2.277524
>sp|Q9CQA3|SDHB_MOUSE Succinate dehydrogenase [ubiquinone] iron-sulfur subunit, mitochondrial OS=Mus musculus GN=Sdhb PE=1 SV=1	15314025.4	1.887806842	36639341.9	3.921289015	2.033482
>sp|P00920|CAH2_MOUSE Carbonic anhydrase 2 OS=Mus musculus GN=Ca2 PE=1 SV=4	3423880.7	0.422072267	22846094.8	2.445080505	2.023008
>sp|Q9CY00|TT30B_MOUSE Tetratricopeptide repeat protein 30B OS=Mus musculus GN=Ttc30b PE=2 SV=1	1894383.7	0.233526484	20843827.4	2.230789834	1.997263
>sp|Q9R0P9|UCHL1_MOUSE Ubiquitin carboxyl-terminal hydrolase isozyme L1 OS=Mus musculus GN=Uchl1 PE=1 SV=1	67264105.2	8.291852383	95910006.4	10.26467276	1.97282
>sp|P67871|CSK2B_MOUSE Casein kinase II subunit beta OS=Mus musculus GN=Csnk2b PE=1 SV=1		0	18315958.4	1.960247176	1.960247
>sp|Q9WV55|VAPA_MOUSE Vesicle-associated membrane protein-associated protein A OS=Mus musculus GN=Vapa PE=1 SV=2		0	15584113.1	1.667874158	1.667874
>sp|O55022|PGRC1_MOUSE Membrane-associated progesterone receptor component 1 OS=Mus musculus GN=Pgrmc1 PE=1 SV=4	13777455.0	1.6983891	31259913.9	3.3455611	1.647172
>sp|Q9R0H0|ACOX1_MOUSE Peroxisomal acyl-coenzyme A oxidase 1 OS=Mus musculus GN=Acox1 PE=1 SV=5		0	15008901.0	1.606312657	1.606313
>Reverse >sp|Q9DBS4|ACOXL_MOUSE Acyl-coenzyme A oxidase-like protein OS=Mus musculus GN=Acoxl PE=1 SV=1	12883923.0	1.588240672		0	1.588241

>sp|P46638|RB11B_MOUSE Ras-related protein Rab-11B OS=Mus musculus GN=Rab11b PE=1 SV=3	30143854.0	3.71592526	19935530.7	2.133580286	1.582345
>sp|O70435|PSA3_MOUSE Proteasome subunit alpha type-3 OS=Mus musculus GN=Psma3 PE=1 SV=3	6263951.7	0.772176522	21250447.2	2.274307912	1.502131
>sp|P48774|GSTM5_MOUSE Glutathione S-transferase Mu 5 OS=Mus musculus GN=Gstm5 PE=1 SV=1	14630426.5	1.80353751	30830355.0	3.299587988	1.49605
>tr|A8DUK4|A8DUK4_MOUSE Beta-globin OS=Mus musculus GN=Hbbt1 PE=1 SV=1	5459624.9	0.673024693	20248346.3	2.167059063	1.494034
>sp|Q9WUR9|KAD4_MOUSE Adenylate kinase 4, mitochondrial OS=Mus musculus GN=Ak4 PE=1 SV=1	10611320.4	1.308089985	25854300.8	2.767030751	1.458941
>sp|Q9QXS1|PLEC_MOUSE Plectin OS=Mus musculus GN=Plec PE=1 SV=3		0	13615928.5	1.457231164	1.457231
>sp|P01831|THY1_MOUSE Thy-1 membrane glycoprotein OS=Mus musculus GN=Thy1 PE=1 SV=1	25948364.7	3.198734437	43249899.1	4.628777305	1.430043
>sp|P50446|K2C6A_MOUSE Keratin, type II cytoskeletal 6A OS=Mus musculus GN=Krt6a PE=1 SV=3	13358584.8	1.646753686	2330594.5	0.249429551	1.397324
>sp|Q64105|SPRE_MOUSE Sepiapterin reductase OS=Mus musculus GN=Spr PE=1 SV=1		0	12697707.5	1.358959478	1.358959
>sp|Q9D172|ES1_MOUSE ES1 protein homolog, mitochondrial OS=Mus musculus GN=D10Jhu81e PE=1 SV=1	20086626.6	2.476140018	35266075.1	3.774316506	1.298176
>sp|Q6ZWN5|RS9_MOUSE 40S ribosomal protein S9 OS=Mus musculus GN=Rps9 PE=1 SV=3		0	12004998.0	1.284822935	1.284823
>sp|Q9CQD1|RAB5A_MOUSE Ras-related protein Rab-5A OS=Mus musculus GN=Rab5a PE=1 SV=1	10102709.1	1.245391911	23022299.1	2.463938594	1.218547
>sp|P60879|SNP25_MOUSE Synaptosomal-associated protein 25 OS=Mus musculus GN=Snap25 PE=1 SV=1	10724144.1	1.321998108	23584891.2	2.524149452	1.202151
>sp|O08756|HCD2_MOUSE 3-hydroxyacyl-CoA dehydrogenase type-2 OS=Mus musculus GN=Hsd17b10 PE=1 SV=4		0	10334437.4	1.106032853	1.106033
>sp|Q9R1P0|PSA4_MOUSE Proteasome subunit alpha type-4 OS=Mus musculus GN=Psma4 PE=1 SV=1	5246447.2	0.646745624	16333057.3	1.748029164	1.101284
>sp|Q9DCT2|NDUS3_MOUSE NADH dehydrogenase [ubiquinone] iron-sulfur protein 3, mitochondrial OS=Mus musculus GN=Ndufs3 PE=1 SV=2	13071062.5	1.611309931	25080082.1	2.684170767	1.072861
>sp|O35381|AN32A_MOUSE Acidic leucine-rich nuclear phosphoprotein 32 family member A OS=Mus musculus GN=Anp32a PE=1 SV=1		0	9703657.6	1.038524274	1.038524
>sp|Q8BH95|ECHM_MOUSE Enoyl-CoA hydratase, mitochondrial OS=Mus musculus GN=Echs1 PE=1 SV=1	11049305.7	1.362081775	22140349.9	2.369548861	1.007467
>sp|P63260|ACTG_MOUSE Actin, cytoplasmic 2 OS=Mus musculus GN=Actg1 PE=1 SV=1	8112072.2	1	9343698.4	1	0